NORTH PACIFIC RESEARCH BOARD PROJECT FINAL REPORT

Life history and population dynamics of Alaskan skates: providing essential biological information for effective management of bycatch and target species

NPRB Project 510 Final Report

David A. Ebert[1, 3], Wade D. Smith[1, 2], Diane L. Haas[1], Shaara M. Ainsley[1], Gregor M. Cailliet[1, 3]

[1]Pacific Shark Research Center, Moss Landing Marine Laboratories, 8272 Moss Landing Road, Moss Landing, CA 95039. (831) 771-4427, debert@mlml.calstate.edu

[2]*Present address*: Department of Fisheries and Wildlife, Oregon State University

[3]Principal investigator and co-principal investigator

August 2007

Abstract In the Gulf of Alaska and Bering Sea, skates (*Raja* and *Bathyraja* spp.) are among the most common bycatch species taken in groundfish fisheries. Additionally, directed fisheries recently developed for *Raja binoculata* and *R. rhina* in the Gulf of Alaska. The susceptibility of skates to fishing pressure has been well documented, however, life history information required for stock assessments and implementation of sustainable management plans is largely unknown for species occurring in Alaskan waters. To address this knowledge gap, the age, growth, longevity, reproductive biology, and demography of two common bathyrajid species (*Bathyraja aleutica* and *B. interrupta*) and reproductive biology and demography of two currently targeted rajid species (*R. rhina* and *R. binoculata*) were examined. Maximum age estimates for *B. aleutica* and *B. interrupta* were 17 and 13 years, respectively. Multiple growth models were applied to evaluate growth characteristics. No significant differences were detected between the growth of females and males for either species. Three parameter von Bertalanffy growth functions generated estimates of $k = 0.11$ yr^{-1} $L_\infty = 172.6$ cm TL for *B. aleutica* and $k = 0.08$ yr^{-1} $L_\infty = 126.4$ cm TL for *B. interrupta*. Median size at maturity was estimated to be 124.4, 70.2, 148.6, and 113.1 cm TL for female *B. aleutica*, *B. interrupta, R. binoculata,* and *R. rhina*, respectively. Demographic models incorporating uncertainty in vital rates projected annual population growth rates of 25% for *B. aleutica*, 36% for *B. interrupta*, 33% for *R. binoculata,* and 20% for *R. rhina*.

Keywords: Aleutian skate, Bering skate, big skate, longnose skate, age, growth, maturity, reproduction, Gulf of Alaska, eastern Bering Sea

Citation: Ebert, D.A., W.D. Smith, D.L. Haas, S.M. Ainsley, and G.M. Cailliet. Life history and population dynamics of Alaskan skates: providing essential biological information for effective management of bycatch and target species. North Pacific Research Board Final Report 510, 124 p.

Table of Contents

Study chronology

June-August 2004: Pacific Shark Research Center researchers participate in NMFS – Alaska Fisheries Science Center Eastern Bering Sea Continental Slope survey to collect vertebral and caudal thorn samples for future skate age, growth, and reproductive biology studies.

September 2004-June 2005: Vertebral samples were collected by Jerry Hoff (NMFS-AFSC) working under NPRB Project 415.

March 2005: NPRB grant proposal approved.

June-September 2005: Field studies were initiated in the Gulf of Alaska. PSRC researchers participated in NMFS-AFSC Gulf of Alaska survey. Samples for future diet studies on Gulf of Alaska skates (NPRB #621) were collected during this survey.

September 2005: Presentation at the American Fisheries Society meetings in Anchorage, AK.

August 2005: Port sampling conducted in Kodiak.

October 2005: Vertebrae and caudal thorns for the big and longnose skates and sent to NMFS-AFSC for processing and Aleutian and Bering skates collected by NMFS-AFSC were sent to PSRC collaborators for ageing studies.

November 2005-April 2006: Special collection request approved. Vertebral samples were collected by NMFS-AFSC Fisheries Observer Program from the eastern Bering Sea.

January 2006: Poster presentation of preliminary results to date presented at Alaska Marine Science Symposium.

April 2006: Port sampling conducted in Kodiak.

June-September 2006: Ageing and reproductive sampling continued throughout the summer as PSRC researchers participate in Alaska Department of Fish and Game survey cruises in the Gulf of Alaska.

July 2006: A poster presentation on NPRB Project #510 was given at the American Elasmobranch Society (AES) meetings as part of a symposium on the "Biology of Skates". This symposium was co-organized by PI David Ebert.

January 2007: Alaska skate identification brochure, the outreach component for the project is completed and distributed. Poster presentation of preliminary results presented at Alaska Marine Science Symposium.

May 2007: Gonad samples sent to Louisiana State University for histological processing were received.

July 2007: Poster presentation on NPRB #510 presented at AES meeting.

August 2007: Submission of NPRB #510 final report.

Introduction

The susceptibility of skates to direct and indirect fishing pressure has been well documented. In the North Atlantic, populations of two once abundant species, the barndoor skate (*Dipturus laevis*) and the common skate (*D. batis*) have been fished to small fractions of their historical population levels (Brander 1981, Casey and Myers 1998). Fishing mortality has also dramatically altered the relative abundance and population structure of North Sea skates (Walker and Hislop 1998, Dulvy et al. 2000, Frisk et al. 2002). Mortality of discarded skates and rays from trawl fisheries may range between 41-65% with survival rates being greater among shelf species (Stobutzki et al. 2002, Laptikhovsky 2004). Because skates are often discretely distributed, vary widely in length and age at maturity, and generally have low fecundity, populations may be differentially susceptible to exploitation and the potential for altering abundance and populations structure may be great (Walker and Hislop 1998, Dulvy and Reynolds 2002).

In the U.S. Pacific, Alaskan skate landings greatly exceed those of all other states combined. During 2005, approximately 620,000 tons of skates were caught as bycatch in Alaskan groundfish fisheries in the Bering Sea and Aleutian Islands, of which most was discarded (Gaichas et al. 2005). Recently, directed fisheries for big (*Raja binoculata*) and longnose (*R. rhina*) skates have emerged in the Gulf of Alaska. The deleterious effects of fishing on North Atlantic skate populations emphasize the need for detailed biological information and effective management strategies for this vulnerable group. However, life history information available for skates from Alaskan waters is extremely limited (Ebert 2005).

In Alaska, skates are among the most common bycatch species taken in commercial fisheries (Camhi 1999, Gaichas and Ianelli 1999). Little, however, is known about the life histories of the local fauna or the impact of fishery exploitation on these species. Of the estimated 47.8 million pounds of skates caught in Alaskan waters during 1997, less than 10 million pounds were landed (Camhi 1999, North Pacific Fisheries Management Council (NPMFC) 1999). Until 2005, only two skate species were recognized in National Marine Fisheries Service (NMFS), Alaska Fisheries Science Center (AFSC) taxonomic categories for landings statistics, and fishery observers had only identified skates to gross taxa ("skate unidentified") (Gaichas et al. 2005, Matta et al. 2006). Current and historic species composition and relative abundance of skate landings are therefore essentially unknown. Incidental capture and landings of skates have increased in recent years and in 2003, a directed fishery for big (*Raja binoculata*) and longnose (*R. rhina*) skates was developed in the Gulf of Alaska (GOA) off Kodiak Island (NPFMC 1999, Gaichas et al. 2003). Despite precautionary management of this incipient fishery (Matta et al. 2006), it is highly likely that, given the relatively large take and amount of currently unutilized biomass, directed fisheries for skates are likely to expand in other areas of Alaska.

Skates are generally managed as part of the "other species" category and are attributed an aggregate quota along with taxonomically and biologically dissimilar groups (i.e. sharks, sculpins, squids, and octopi) (Gaichas et al. 2005). As directed fisheries for species in this category develop, the potential for overfishing is a primary concern of fisheries managers (Gaichas et al. 1999, 2005). Skates are common components of demersal fish assemblages in Alaska where they occupy high trophic positions and can cause physical modifications and disturbance to benthic environments (Probert 1984, Orlov 1998, 1999). A decline in abundance or shift in species composition could therefore have unpredictable cascading impacts on the benthic community (Parsons 1992, Carpenter and Kitchell 1992). To protect skate stocks, species-level quotas were established for *R. binoculata* and *R. rhina* soon after the Kodiak fishery was initiated (Gaichas et al. 2003, Matta et al. 2006). Similar measures will be necessary as species-specific contributions of skates among bycatch are better known and new skate species, including bathyrajids, are targeted. However, before effective management of any species can be undertaken, life history characteristics, especially age, growth, and reproduction, must be understood and incorporated into management strategies. Yet the lack of detailed biological information for this group greatly impedes the development of species-specific management strategies (or refined multi-species approaches) and restricts a broader understanding of ecosystem-level interactions and processes. Because many elasmobranchs, including skates, are reported to possess life history characteristics (e.g. slow growth, late maturity, low fecundity) that make them especially vulnerable to fisheries exploitation, details on these species-specific traits are imperative for developing realistic stock assessments and establishing sustainable skate management in Alaskan waters.

Objectives

The objectives of this study were to determine the age, growth, and reproductive characteristics of four common skate species that are caught either as bycatch or directly targeted in Alaskan groundfish fisheries in the EBS and GOA. Age and growth studies were conducted for the Aleutian (*B. aleutica*) and Bering (*B. interrupta*) skates and aspects of the reproductive biology were investigated for *B. aleutica*, *B. interrupta*, big skates (*R. binoculata*), and longnose skates (*R. rhina*). The use of caudal thorns as an alternative, non-lethal ageing structure was evaluated for *B. aleutica* and *B. interrupta*. Based on the resulting life history parameters, age-based demographic models were developed for each species to evaluate and compare their population growth potential and resilience.

Specific research questions addressed in this study include:

1) What is the age and size of 50% and 100% maturity?
2) What is the size at birth?
3) Do seasonal spawning peaks occur for these skates?
4) What are the estimated fecundity rates?
5) Are caudal thorns useful ageing structures?
6) Do growth parameters of females differ from males?
7) What are the maximum observed and theoretical longevities of selected study species?
8) What are the projected annual rates of population growth and how do these compare among species?

Methods

Skates were collected intermittently from June 2004 to October 2006 in the eastern Bering Sea (EBS) and Gulf of Alaska (GOA; Fig. 1). Specimens of *Bathyraja aleutica* were obtained in 2004 during trawl surveys conducted by the National Marine Fisheries Service Alaska Fisheries Science Center (NMFS-AFSC) along the EBS upper continental slope and shelf from Unalaska and Akutan Island to the U.S.-Russia border. Additional *B. aleutica* samples were collected during 2004-05 by Jerry Hoff (NMFS-AFSC) working under NPRB Project 415 and in 2005 and 2006 in the EBS by the NMFS-AFSC Fisheries Observer Program. Specimens of *B. interrupta*, *Raja binoculata*, and *R. rhina* were obtained during 2005 and 2006 in the GOA from surveys conducted by the Alaska Department of Fish and Game (ADF&G) and the NMFS-AFSC along the Alaskan Peninsula to Kamishak Bay and Kodiak. Samples were also obtained from direct and indirect fishery landings in Kodiak for *B. interrupta*, *R. binoculata*, and *R. rhina* taken from the northern GOA.

Biological measurements taken at the time of collection included total length (TL), disc width (DW), inner clasper length, testes length, testes width, oviducal gland width, uterus width, and total weight (nearest gram) whenever possible. TL was measured to the nearest mm from the tip of the snout to the tip of the tail and inner clasper length was measured from the point of insertion of the clasper shaft to the tip. Sex and maturity status were also determined for each specimen. Additionally, the number of mature ova per ovary and maximum ovum diameter were recorded from mature females if the gonads were not damaged.

Ageing structures and reproductive tracts were collected from sampled skates. Sections of at least eight vertebrae, excised from the region posterior to the cranium between the 5th and 20th vertebral elements, along with five or more of the anterior most caudal thorns, were stored frozen until further processing. For a subset of samples, segments were taken from the posterior portion of the vertebral column as well, to allow for comparison in age structures along the vertebral column. Those vertebrae retained from *R. binoculata* and *R. rhina* were sent to fishery biologists at the NMFS-AFSC for age and growth studies. A subsample of whole reproductive tracts from both sexes was preserved in 10% buffered formalin for histological analysis.

Age and growth

Vertebrae were thawed, tissue was removed using a scalpel, and three to four individual centra were separated and dried. Caudal thorns were cleaned by removing excess tissue with a scalpel, followed either by soaking in 1% trypsin solution for 10+ hours, or boiling in fresh water until remaining tissue was easily removed. Thorns were further cleaned, rinsed in fresh water, and stored dry.

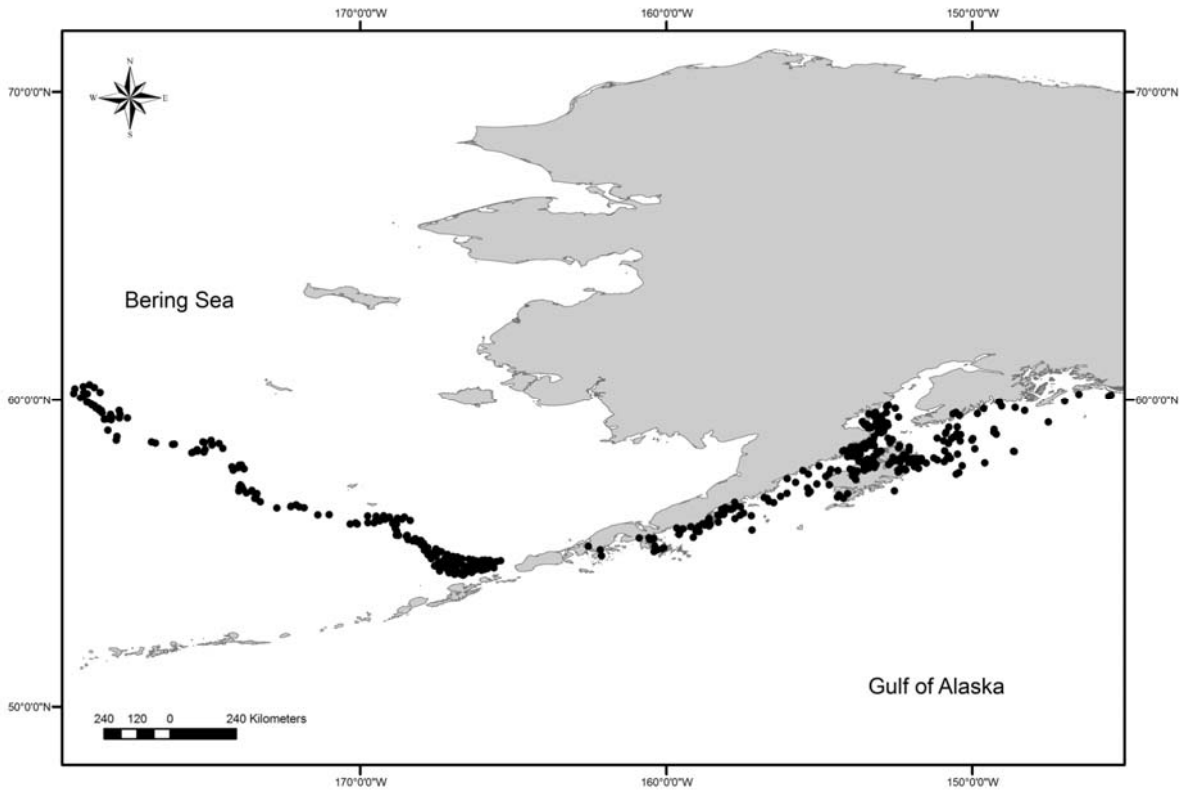

Fig. 1. Trawl survey sampling locations.

Centra were mounted in polyester casting resin on waxed paper tags prior to sectioning. Using a low speed precision saw (Buehler Isomet, Lake Bluff, IL, USA) with diamond edged blades, a section between 0.3 and 0.4 mm thick containing the focus was extracted along the sagittal plane of the vertebral centrum (Fig. 2a). Thin-sectioned centra were adhered to a microscope slide, and polished with wet sandpaper of successive grits (grades 600, 800, and 1200), to provide optimal thickness for viewing banding patterns (0.2-0.3mm).

Several techniques were applied to enhance the clarity of banding patterns in structures for age estimation. Alizarin red (LaMarca 1966), crystal violet (Johnson 1979), and oil enhancement (Cailliet et al. 1983) methods were assessed for vertebral thin sections and whole caudal thorns. In addition, lead microtopography (Neer and Cailliet 2001) techniques were tested on caudal thorns. Vertebral sections were best viewed using oil enhancement in both species. A combination of oil enhancement and lead microtopography best improved the clarity of bands in *B. aleutica* caudal thorns (Fig. 2b). Banding patterns in *B. interrupta* caudal thorns were best visualized after staining with 1% crystal violet (15 minutes) using a method adapted from Carlson et al. (2003) and Johnson (1979) (Fig. 3).

The vertebral column was assessed to determine if centra grow in proportion to TL. Centrum diameter was measured to the nearest 0.1 mm at two perpendicular axes. A simple linear regression of TL and mean centrum diameter (MCD) was calculated, and relationships between sexes were compared using Analysis of Covariance (ANCOVA). Similarly, to determine if caudal thorns were appropriate for estimating growth rate, thorn height, width, and base length were measured and plotted against TL. Because curves were nonlinear, sexes were compared using Analysis of Residual Sums of Squares (ARSS; Chen et al. 1992). To determine whether centrum banding patterns differed throughout the vertebral column, mean age estimates from anterior and posterior regions were compared using a paired sample t-test (Zar 1999).

Age determination

Vertebral sections and caudal thorns were examined for the birthmark (age 0) and the number of band pairs. The birthmark was defined as the first distinct mark distal to the focus that coincides with an angle change in the corpus calcareum in vertebrae (Walmsley-Hart et al. 1999, Sulikowski et al. 2003), and band counts began from that point. The base of the protothorn at the apex of the caudal thorn was considered the birthmark on that structure (Gallagher and Nolan 1999, Matta 2006). In vertebral centra, a band pair was defined as one opaque and one translucent band that extended across the intermedialia to the arms of the corpus calcareum (Cailliet et al. 2006). Ages were estimated by counting the number of band pairs, which typically have been assumed to represent annual growth in skates (Zeiner and Wolf 1993, Sulikowski et al. 2005a, Frisk and Miller 2006). Thin ‘bands’ that did not span the width of the

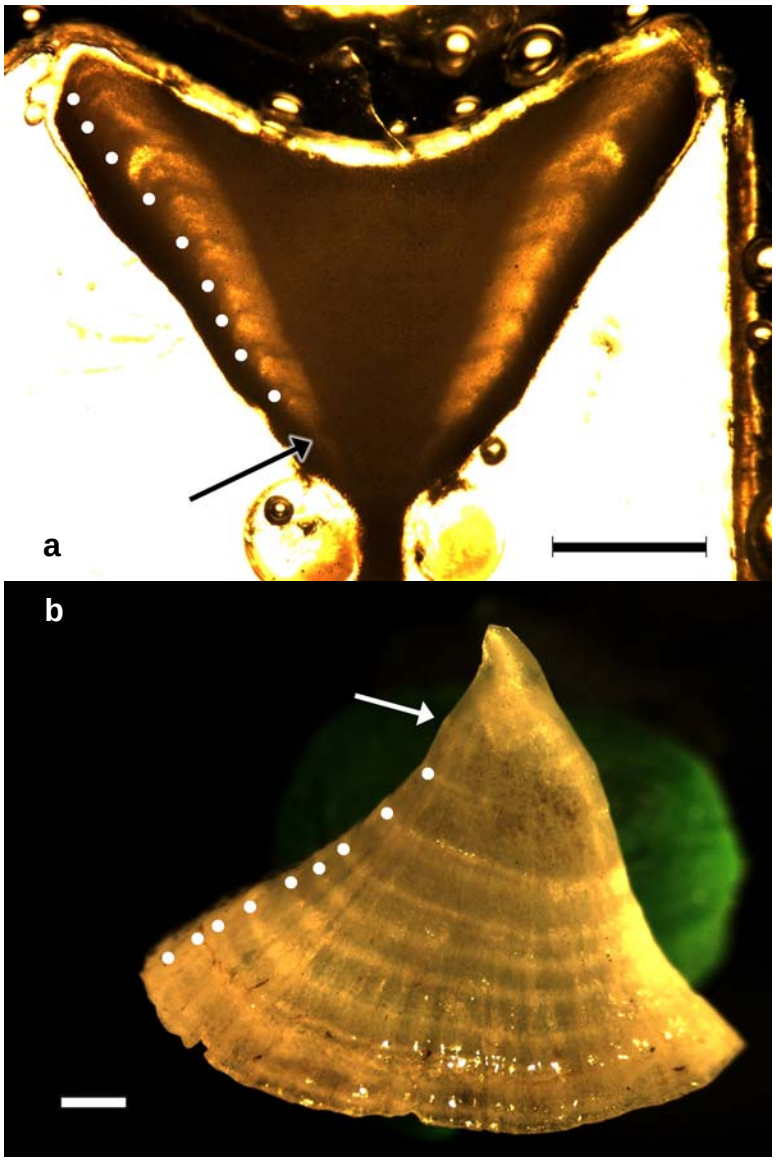

Fig. 2. Vertebral thin section (**a**) and caudal thorn (**b**) from a 9 year old, 100 cm total length *Bathyraja aleutica*. Arrows identify the birthmark, signified by an angle change of the corpus calcareum on the vertebral thin section, and a ridge associated with the protothorn on the caudal thorn. Band pairs (i.e. one opaque and one translucent band) are indicated by white dots. Bar = 1 mm.

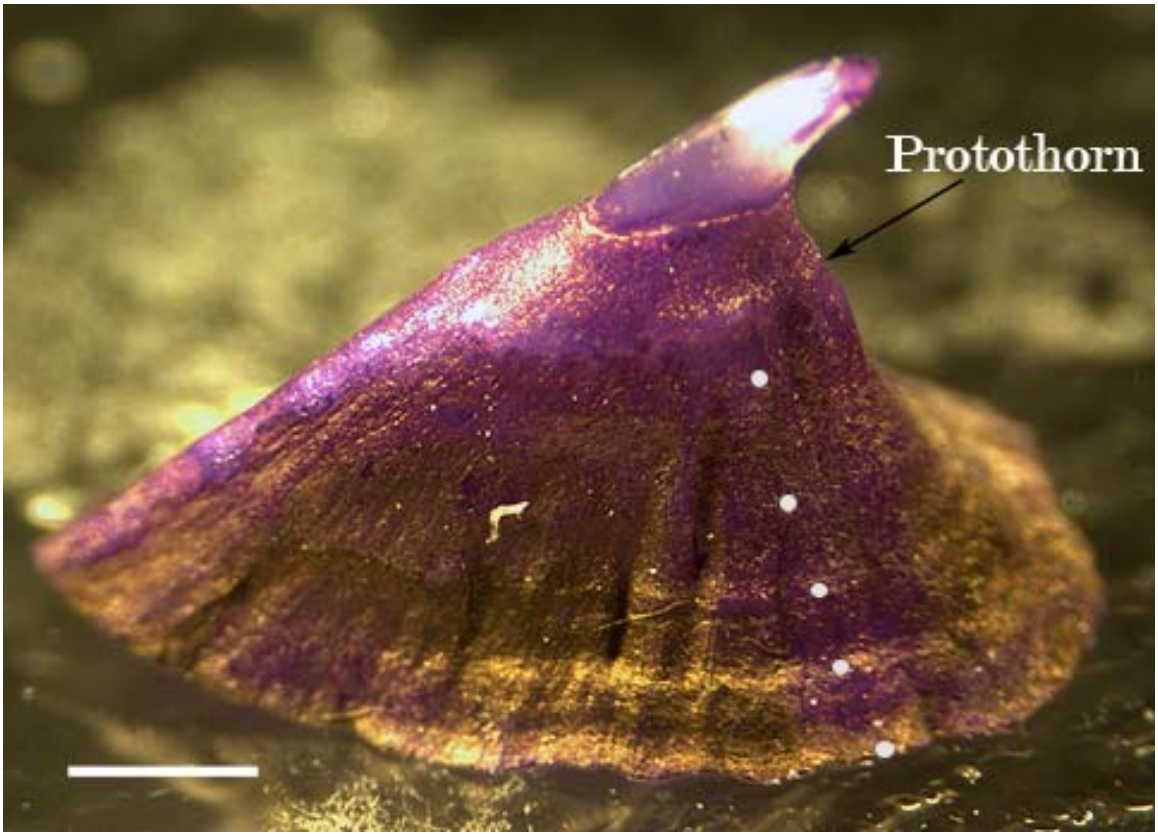

Fig. 3. A caudal thorn from *Bathyraja interrupta* with an estimated age of 5 years. The caudal thorn was dyed with crystal violet and viewed under reflected light. White dots represent the ridges (band pairs) counted to obtain age estimates. The prototthorn is marked by the arrow. Scale bar = 1 mm.

corpus calcareum and were not visible in the intermedialia were considered check marks and were not counted. For ageing of whole caudal thorns, a band pair was defined as a concentric ridge and an associated broad growth zone on the surface of the thorn (Gallagher et al. 2006).

Age estimates of each structure were determined in three randomized trials, with a minimum of one week between successive reads, and no knowledge of sex, length, or previous counts, when ageing the structure. One centrum from each individual was read three times by the same reader. For a subsample of the specimens, one caudal thorn was also read three times. Vertebral sections were examined with a dissecting microscope under transmitted light, while caudal thorns were examined using the same microscope under reflected light. Final age estimates for both structures were assigned based on the agreement of two or more reads. If there was not an agreement between two of the first three reads, a fourth read was conducted to clarify the disagreement among age estimates (Neer and Thompson 2005). If no agreement was reached after the fourth read, the sample was not included in further analyses. Vertebral centra and caudal thorn age estimates were compared using age bias plots (Campana et al. 1995) and a paired sample t-test (Zar 1999).

Readability was assessed using the categories from Smith (2005), with grade 1 being the lowest readability and grade 5 being the highest (Table 1). Individuals given a grade of 2 or 1 were re-sectioned and examined again. For *B. interrupta* samples, if the readability was still 2 or 1, then the individuals were excluded from statistical tests. For samples of *B. aleutica*, those with a readability of 1 were excluded.

Precision and error analyses

Precision and error analyses were used to assess reader consistency and reproducibility among reads of the same centrum or thorn, as well as facilitate comparison between age estimates from centra and thorn reads. To examine for possible biases between reads and between structures, pair-wise age difference plots were used (Campana et al. 1995). Several measures were used to assess reader precision. Average percent error (APE) is a common tool that provides a relatively good indication of precision (Beamish and Fournier 1981), however, APE values are not independent of age estimates (Cailliet and Goldman 2004). For comparability, the index of average percent error (IAPE) is generally reported and was calculated as:

$$IAPE_j = 100\% * \frac{1}{N}\sum_{j=1}^{N}\left[\frac{1}{R}\sum_{i=1}^{R}\frac{\left|X_{ij} - X_j\right|}{X_j}\right]$$

where N is the total number of samples, R is the number of reads per ageing structure, X_{ij} is the i^{th} age determination of the j^{th} ageing structure, and X_j is the mean age determination for the j^{th} ageing structure

Table 1. Categories applied for assessing the readability and clarity of vertebral centra.

Grade	Criteria
1	Banding pattern vague; increments irregular or cloudy; limited confidence distinguishing band count; sample may be damaged
2	More than two band counts possible; indefinite banding pattern in one or more sample locations; best estimate recorded
3	Two band counts possible; recorded estimate is the most probable
4	Band count unambiguous but increment/s are not of exceptional clarity
5	Band count unambiguous; all increments are distinct and readily distinguished

(Beamish and Fournier 1981). Because age 0 samples can distort APE estimates (Officer et al. 1996), they were excluded from precision calculations.

In addition, the coefficient of variation (CV) and index of precision (D) were estimated to facilitate comparisons with other studies (Chang 1982). CV uses the standard deviation instead of the absolute deviation from the mean, making it less biased and more consistent (Campana et al. 1995, Panfili 2002). The index of precision (D) assesses the percent error of each observation. These were calculated as:

$$CV_j = 100\% * \frac{\sqrt{\sum_{i=1}^{R} \frac{(X_{ij} - X_j)^2}{R-1}}}{X_j}$$

and

$$D_j = \frac{CV_j}{\sqrt{R}}$$

where CV_j and D_j each represent a precision estimate for the j^{th} ageing structure (Chang 1982), which were then averaged among individuals to produce mean CV and D values (Matta 2006).

Age validation

Validation of age estimates is necessary to ensure the accuracy of the assumption that growth zones being counted represent some temporal unit, such as year (Cailliet et al. 2006). To assess whether the timing of the band pairs reflected annual deposition, two types of indirect age validation were conducted: marginal increment ratio (quantitative) and edge analysis (qualitative). As the first band pair is not completely formed in age zero individuals, they were not included in validation assessments. Only individuals with final age estimates of three years or more were used in studying these analyses.

Marginal increment analysis was performed on a sub-sample of vertebral thin sections following Conrath et al. (2002). The marginal increment ratio (MIR) was calculated as:

$$MIR = MW/PBW$$

where the margin width (MW), or the distance from the last opaque band to the edge of the margin, is divided by previous (penultimate) band pair width (PBW). Digital photographs taken of each sectioned centra were used to measure the ultimate and penultimate bandwidths along the corpus calcareum using Image Pro Plus software (Media Cybernetics, Silver Springs, MD, USA). To reveal differences in band deposition over time, mean MIRs were plotted by month. A non-parametric Kruskal-Wallis one-way ANOVA by ranks was employed to test for potential differences among months (Simpfendorfer et al. 2000).

Edge analysis compares the optical characteristics of the ultimate band (edge) of each centrum

through time to discern seasonal changes in growth (Tanaka and Mizue 1979, Cailliet et al. 2006). The centrum marginal edge was categorized as either: 1) narrow opaque band forming, 2) broad opaque band well-formed, 3) narrow translucent band forming, or 4) broad translucent band well-formed (Natanson and Cailliet 1990, Smith et al. 2007). A narrow band was defined as a band that was less than one half the width of the previous narrow band and conversely, a broad band was defined as a band that was greater than or equal to half the width of the previous broad band. The proportion of edge types per month was used to detect seasonal differences in edge type.

Growth models

Total length-at-age data were used to generate separate growth curves for males and females using six different growth functions. Growth model parameters were estimated using a non-linear least-squares regression and SigmaPlot graphical software (SPSS Inc., 2002).

The three parameter von Bertalanffy growth function (VBGF; Beverton and Holt 1957) was used to estimate demographic parameters as it is the most common growth model used in elasmobranch age and growth studies (Cailliet et al. 2006). The model was fitted to the data with the following equation:

$$L_t = L_\infty\left(1 - e^{(k\,t - t_o))}\right),$$

where L_t = length at age t; L_∞ = asymptotic or maximum length; k = growth coefficient; and t_o = age at theoretical length zero (Ricker 1979). Length at birth (L_0) was then calculated as:

$$L_0 = L_\infty(1 - e^{kt_0}),$$

in order to check whether the resulting value falls within the range of observed length at birth (Cailliet et al. 2006). Alternatively, a two parameter VBGF (von Bertalanffy 1960) was fitted to the data, which uses an estimate of L_0 in lieu of t_o as it is more biologically meaningful (Cailliet and Goldman 2004):

$$L_t = L_\infty - \left(L_\infty - L_0\right)\left(e^{(-k+t)}\right)$$

where parameters are as previously defined.

Size-at-age models also were obtained based on the Gompertz growth function, which has provided the best fit for some batoids (Mollet et al. 2002, Neer and Thompson 2005). Because of the limited weight-at-age data collected TL-at-age data were substituted for weight variables. The Gompertz parameters were estimated using:

$$L_t = L_\infty\left(e^{\left(-ke^{(-gt)}\right)}\right)$$

where L_t, L_∞, and t are as previously defined; k = a constant such that kg is the instantaneous growth rate when $t = 0$ and, and $L_t = L_0$; and g = instantaneous rate of growth when $t = t_o$ (Ricker 1979). Predicted L_o

was also estimated from this equation.

A Logistic model (modified from Ricker 1979) was also fit to TL-at-age data. Logistic parameters were estimated using:

$$L_t = \frac{L_\infty}{1 + e^{-g(t-t_0)}}$$

where g = instantaneous rate of growth, t_o the inflection point, and other parameters as previously defined.

A four parameter Richards growth model (Richards 1959, Neer and Thompson 2005) was fitted to TL-at-age data in the form:

$$L_t = L_\infty \left[\left(1 - L_0\left(e^{-k*t}\right)\right)\right]^P$$

where P is a shape parameter and others are as previously defined.

Finally, the following three parameter polynomial function was applied to TL-at-age data:

$$L_t = a + b*t + c*t^2$$

where L_t is as previously defined and a, b, and c are constants. Polynomial functions were considered because of potential mathematical advantages over the traditional VBGF and do not assume asymptotic growth (Roff 1980).

Growth model goodness-of-fit was assessed by comparisons of several values. The coefficient of determination (r^2), significance level ($p < 0.05$), and residual mean square error (MSE) were compared to determine which model best fit the TL-at-age estimates (Carlson and Baremore 2005, Neer and Thompson 2005). Growth curves were tested for differences between sexes using a nonlinear Analysis of Residual Sums of Squares (ARSS; Chen et al. 1992).

Maturity and reproduction

Maturity status was assessed in the field by visual inspection of the reproductive organs following Ebert (2005) (Table 2). Three reproductive classifications (juvenile, adolescent, adult) were determined for both sexes. Specimens identified as adult were considered to be mature.

Changes in reproductive organ sizes were used to further assess the onset of maturity. Oviducal gland width, uterus width and inner clasper length were plotted against TL. A sharp increase in growth of each structure relative to TL was assumed to correspond with the onset of maturity, followed by a slowing of growth, which was assumed to correspond with full maturation of the individual.

Histological assays of reproductive tracts were conducted to examine potential seasonal changes in the reproductive cycle and to verify macroscopic maturity assessments of each skate species. Sections (3-4 mm thick) of fixed testes were removed from preserved reproductive tracts, placed in tissue cassettes

Table 2. Maturity classifications of female and male skates as determined by macroscopic inspection of reproductive organs.

Stage	Female	Male
Juvenile	Ovaries white and undifferentiated; oviducal glands undeveloped and not distinct from uteri	Testes white and undifferentiated; epididymides thin and filamentous; claspers short and flexible and do not extend past pelvic fins
Adolescent	Ova small and clear; oviducal glands poorly developed; uteri narrow and constricted	Testes becoming lobular; epididymides thickening and loosely coiled; claspers extend past pelvic fins but terminal cartilage elements not calcified
Adult	Ova large, yellow, and vascularized; oviducal glands distinct from uteri; uteri thick and pendulous	Testes lobular; epididymides highly coiled; claspers fully calcified and elongate
Gravid	Egg cases present *in utero*	

for sectioning, and stored in 70% ethanol. Gonad sections were shipped to the University of New Hampshire and Louisiana State University veterinary laboratories for processing using standard hematoxylin and eosin staining (e.g. Maruska et al. 1996). Maturity stages of sperm in the testes were evaluated for samples from each available month. Prepared slides were then examined under a compound microscope. The developmental stages of spermatogenesis have been well described for several elasmobranch groups, including skates, and hormonal analysis have confirmed that spermatocyst and spermatid stages are associated with reproductive readiness (Heupel et al. 1999, Sulikowski et al. 2004). Therefore, we concentrated on these specific stages; stage III, spermatocytes; stage IV, spermatids; stage V, immature spermatozoa; stage VI, mature spermatocysts (Fig. 4) (Maruska et al. 1996, Conrath and Musick 2002). Stage VII, consisted of empty spermatocysts and free spermatogonia, were considered mature and included with stage VI estimates. Mean proportion of mature spermatocysts was estimated along a transect crossing a full, representative section of testis lobe. The tightness and organization of sperm packets in the spermatocysts were used to determine maturity (Sulikowski et al. 2005a, b). The mean proportion of testes occupied by each stage per month was compared to discern any seasonal pattern in testis development.

Size and age at maturity were determined using maturity ogives. Median TL and age at maturity were estimated by fitting to binomial maturity data (0 = immature; 1 = mature) (Mollet et al. 2000). Maturity data were binned into 5 cm TL size classes for *B*. *aleutica*, *R*. *binoculata*, and *R*. *rhina* and assessed using 1.5 cm TL size classes for *B. interrupta*. Males and females were analyzed separately for each species. A logistic equation was fitted using least squares non-linear regression and SigmaPlot graphical software (SPSS Inc., vers. 8.0, Chicago, IL) in the following form:

$$Y = \frac{1}{\left(1 + e^{-(a+bx)}\right)}$$

where Y = maturity status and x = TL in cm or age in years. Median TL at maturity (TL_{50}) was calculated as $-a/b$. Additional logistic ogives were developed to determine median age at maturity for *B. aleutica* and *B. interrupta* using resulting age estimates. Median age at maturity estimates for *R*. *binoculata*, and *R*. *rhina* were determined by relating TL_{50} to observed size-at-age estimates (present study, Gburski et al. 2007).

Ovulation cycles may be detected by comparing ova size among months in mature females (Conrath 2004). In females, all mature ova visible on the surface of each ovary were enumerated, and the diameter of the largest ovum was measured to the nearest mm. Mature ova were characterized by their yolky appearance and size, typically exceeding 10 mm in diameter (Ebert 2005). The number of mature ova in left and right ovaries was compared for significant differences using a paired sample *t*-test (Zar

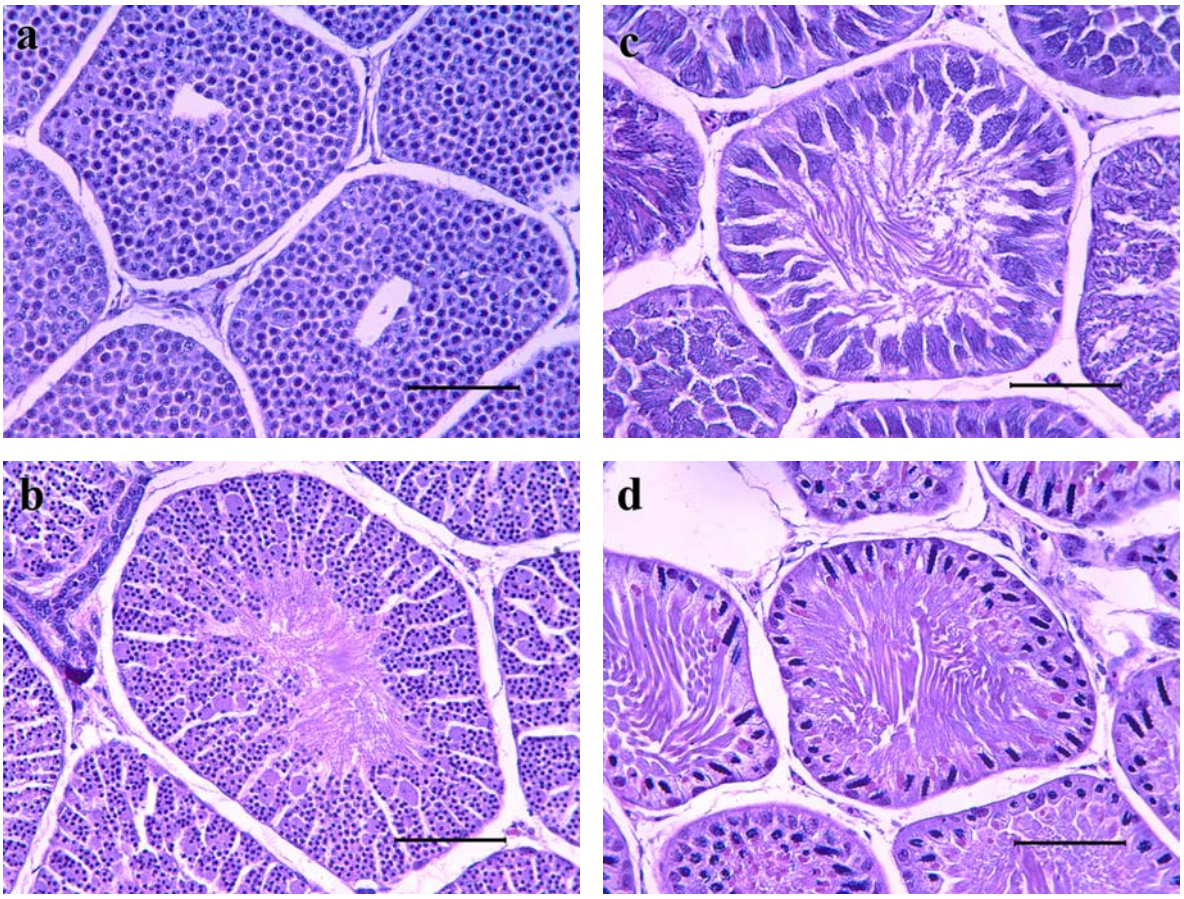

Fig. 4. Stages III through VI of spermatogenesis used to classify spermatocysts in skate testes at 200× magnification. Classification follows Maruska et al. (1996): **a**) stage III spermatocytes; **b**) stage IV spermatids; **c**) stage V immature spermatozoa; and **d**) stage VI mature spermatocysts. Bar = 100 μm.

1999). To discern any peaks in reproductive activity, mean maximum ova diameter and number of mature ova were plotted against month of capture. Differences between months in maximum ova diameter and number of mature ova were each tested using one-way ANOVA or non-parametric Kruskal-Wallis tests (Matta 2006). The percentage of mature females with developing egg cases *in utero* also was plotted against each month, and differences in proportion were assessed using a Chi-square (χ^2) test for homogeneity (Zar 1999).

The effects of maternal size and age on reproduction in *B. aleutica* and *B. interrupta* were assessed using multiple regression analysis of ova size and number of mature ova on maternal size and age. Maximum ova diameter and number of mature ova each were regressed against length and age to determine if these factors contribute significantly to variation of ova size and number (Matta 2006).

Demography

Density-independent, age-structured models were developed using empirical age, growth, and maturity estimates for *B. aleutica*, *B. interrupta*, *R. binoculata*, and *R. rhina* from the GOA. Population projections were estimated from probabilistic life tables that incorporated uncertainty in life history parameters by varying age-specific vital rates and longevity using Monte Carlo simulations (n = 1500) (Caswell 2001, Cortés 2002). Simulations were conducted with Microsoft Excel® spreadsheet software equipped with Crystal Ball add-in risk-assessment software (Decisioneering Inc. 2000) and Microsoft Visual Basic for Applications macros. All models were female-specific and structured using one-year projection intervals assuming a closed population.

The instantaneous rate of population increase (r) was iteratively solved for using the discrete form of the Euler-Lotka equation (Ebert 1999):

$$1 = \sum_{x=1}^{\omega} l_x m_x e^{-rx}$$

where l_x is the probability of an individual being alive at the beginning of age x, m_x is the number of offspring produced annually by individuals at age x, and ω is the maximum age. Initial values of l_x (age 0) were set at 1.0. Estimates of r provided a foundation for calculating additional demographic parameters, including the finite annual population growth rate (λ), net reproductive rate (R_o), rate of increase per generation (rT, Fowler 1988), and theoretical population doubling time (t_{x2}, Krebs 2001). However, values of r are not reported in this study, as λ (where $\lambda = e^r$) is presented as the basis for population growth rate. Additionally, two measures of generation time were calculated: mean age of the parents of the offspring produced by a population at the stable age distribution ($\bar{A}$) and mean age of mothers of offspring produced by a cohort over its life span (μ_1) (Caswell 2001). Estimates of μ_1 were incorporated as generation time when determining rT (Fowler 1988). The range and mean of

demographic parameters were calculated and 95% confidence intervals calculated as the values bounded by the 97.5th and upper and 2.5th lower percentiles for each probabilistic model. Additionally, the intrinsic rate of increase (r) was used as a surrogate of λ to estimate the value of fishing mortality at which a stationary population growth rate would be attained (λ=1.0 or r=0) (Mollet and Cailliet 2002).

Survival and fecundity/fertility are interrelated life history traits that are measured on different scales. Elasticity analysis relates the proportional contribution of these differing matrix or life table elements in relation to the population λ, providing an assessment of the contribution of changes in survival and reproduction to the population growth rate (Caswell 2001). A large elasticity value would indicate a relatively greater change in λ resulting from an alteration to the associated rate of fertility or survivorship. Life tables were expanded to incorporate the elements necessary to obtain individual elasticities (e_{ij}) and calculated following de Kroon *et al*. (1986) and Ebert (1999):

$$e_{ij} = \frac{a_{ij}}{\lambda} \frac{v_i w_j}{\langle w, v \rangle}$$

where a_{ij} is the element corresponding to row i of column j (in both matrix and life table notation), λ is the finite rate of increase, v_i is the value of row i in the reproductive value (V_x) column, w_j is the value of row j in the stable age distribution (c_x) column, and $\langle w, v \rangle$ is the scalar product of row elements in the c_x and v_x distributions. Fertility elasticity values were calculated as the sum of fertility columns (which also corresponds to a single row in life table notation). Because a pre-breeding census was used, this sum is the product the age-specific fecundity and age 0 survivorship terms (Caswell 2001). Juvenile and adult survival elasticities were summed across age classes and adjusted to reflect that both life stages are present within the same age class at the median (i.e. 50%) age at first reproduction. Adult survival to fertility, juvenile survival to fertility, and adult survival to juvenile survival elasticity ratios were determined from each scenario (Heppell et al. 1999, Cortés 2002). An adult survival to fertility ratio of 2.5, for example, indicates that a 10% reduction in adult survival would necessitate a 25% increase in fertility to maintain the observed annual λ.

Given the preliminary nature of the ageing results for *B. aleutica* (D. Haas, unpublished data) and *B. interrupta* (S. Ainsley, unpublished data) and the relatively small sample size for published *R. binoculata* and *R. rhina* age and growth results from Alaskan waters (Gburski et al. 2007), estimates of longevity (ω) were randomly varied in each model to account for uncertainty in the life span of these species. The maximum observed ages are 13 (*B. interrupta*; this study), 17 (*B. aleutica*; this study), 24 (*R. rhina*; Gburski et al. 2007), and 26 years (*R. binoculata*; McFarlane and King 2006). Triangular probability density functions were developed for each species (Table 3). Because maximum observed age may be considered to be an initial underestimate of ω (Beukema 1989), maximum ω values were

Table 3. Probability density functions developed to incorporate uncertainty in longevity (ω), median age at first reproduction (α), and fecundity (m_x) in demographic models for *Bathyraja aleutica*, *B. interrupta*, *Raja binoculata*, and *R. rhina*.

Species	Parameter	Probability Distribution	Min.	Max.	Mean/ Likeliest	SD
Bathyraja aleutica	ω	Triangular	18	24	21	
	α	Normal	9	11	10	0.80
	m_x	Uniform	50	85		
Bathyraja interrupta	ω	Triangular	15	25	18	
	α	Normal	6	9	7.5	1.20
	m_x	Uniform	30	75		
Raja binoculata	ω	Triangular	18	31	26	
	α	Uniform	8	11	9	
	m_x	Uniform	50	100		
Raja rhina	ω	Triangular	21	36	25	
	α	Uniform	13	16	15	
	m_x	Uniform	50	85		

arbitrarily projected based on increases of approximately 40-50% of the maximum observed ages. Probability distributions for skates with greater variability in reported size-at-age estimates (*B. interrupta* and *R. binoculata*) were expanded to account for a greater potential for uncertainty in these estimates.

Probabilities of age-specific annual survivorship (S_x) were determined from six indirect methods for estimating natural mortality (M), where $S_x = e^{-M}$ (Ebert 1999). These approaches included those of Hoenig (1983; two methods), Jensen (1996; three methods), and Campana et al. (2001; one method) and are derived from correlative relationships between M and specific life history parameters. Individual formulas for these equations are presented along with the results for each species (Table 6). Values applied to these equations were determined from female life history traits and drawn from the results of this NPRB funded study, McFarlane and King (2006), and Gburski et al. (2007). These parameters included median age at maturity (α), maximum observed age, and the von Bertalanffy growth coefficient (k).

Published empirical studies have not provided evidence that one indirect approach of estimating M (and therefore S_x) produces more accurate estimates than another. Additionally, extensive variability in survivorship among years and age classes has been reported within fish populations (Vetter 1988). Therefore, S_x values based on these six indirect methods were drawn from uniform distributions specific for each age class, wherein the lowest and highest calculated values were set as the lower and upper bounds. Survivorship estimates for egg cases (age 0) were derived from published estimates of hatching success and mortality and ranged from 0.54-0.91 yr^{-1} for all species (Cox and Koob 1991, Smith and Griffiths 1997, Cox et al. 1999, Lucifora and Garcia 2004, Koop 2005). Survivorship of age classes 1 (young of the year) and 2 were reduced by 50% and 25% of the overall estimates, respectively, to account for increased mortality during these early life history stages (Hoenig and Gruber 1990, Heupel and Simpfendorfer 2002).

Median age at maturity estimates were assumed to provide a proxy for the median age at first reproduction in this study. We developed truncated probability distributions based on minimum, median, and maximum observed ages at maturity to reflect uncertainty in the age at first reproduction (Table 3). Estimates of age at 50% (median) maturity are presented elsewhere in this study for *B. aleutica* and *B. interrupta*. Because median age at maturity estimates for *B. aleutica* and *B. interrupta* were directly calculated from empirical data, normal probability distributions of age at first reproduction were used in Monte Carlo simulations. In contrast, median age at maturity for *R. binoculata* and *R. rhina* were indirectly estimated using correlative size at maturity size estimates determined in this study with size at age estimates reported by McFarlane and King (2006) and Gburski et al. (2007). On this basis, probability distributions were not assumed to be normally distributed and triangular median age at maturity distributions were applied to *R. binoculata* and *R. rhina* demographic models. The proportional

contribution of the first reproductive age class (median age at first reproduction) was adjusted to reflect that only half of this group was likely to reproduce in each model. All females were assumed to be reproductively active in successive years.

Information on the annual fecundity (m_x) of skates remains sparse, particularly for species from the Pacific. With the exception of two species, *R. binoculata* and *R. pulchra*, one embryo is typically contained in each egg case (Ebert and Davis 2007). However, as many as eight embryos have been recorded to occur in individual egg cases of *R. binoculata* (Ford 1971), with 3-4 being most common (Hitz 1964). Although the potential for multiple embryos being deposited within individual egg cases has only been observed in two species, egg deposition frequently occurs over many months (Templeman 1987, Sulikowski et al. 2004), further complicating estimates of fecundity. We estimated annual fecundity of *B. aleutica*, *B. interrupta*, *R. binoculata*, and *R. rhina* from the best available biological information for five Atlantic skates (Holden 1975, Koop 2005). These overall estimates of fecundity were reduced by half to represent the annual number of female offspring produced per adult female. It was assumed that larger species have a greater potential for reproductive output, however it is unknown if reproductive output within a population increases with female size or age. The sex ratio at birth is not reported to differ significantly from 1:1 in *R. binoculata* (Hitz 1964), and this relationship was assumed to apply to all species in these analyses. Age-specific values of fecundity were randomly drawn from uniform probability distributions and applied separately to each adult age class (Table 3). Gestation (the egg case period) was assumed to be one year for each species.

Results

Age and growth

Coordinated sampling efforts provided a total of 743 *B. aleutica* from nine months, although samples were not obtained from all months within each sampling year. Males (n = 332) ranged in size from 23.9 to 149.9 cm TL, and females (n = 441) ranged from 20.6 to 153.4 cm TL (Fig. 5).

Overall, 606 specimens of *B. interrupta* were caught in the GOA during various ADF&G and NMFS-AFSC surveys in 2005 and 2006. Port sampling in Kodiak, Alaska provided an additional 108 samples. Total length ranged from 20.3 to 87.1 cm for females (n = 402) and 18.9 to 82.4 cm for males (n = 312) (Fig. 6).

The fewest samples were obtained for *R. binoculata*. A total of 445 were collected from fishery independent surveys and fishery landings, ranging from 19.5 to 183.3 cm TL (Fig. 7). The majority of specimens consisted of females, which were observed to attain greater sizes. Few of the males examined exceeded 140 cm TL.

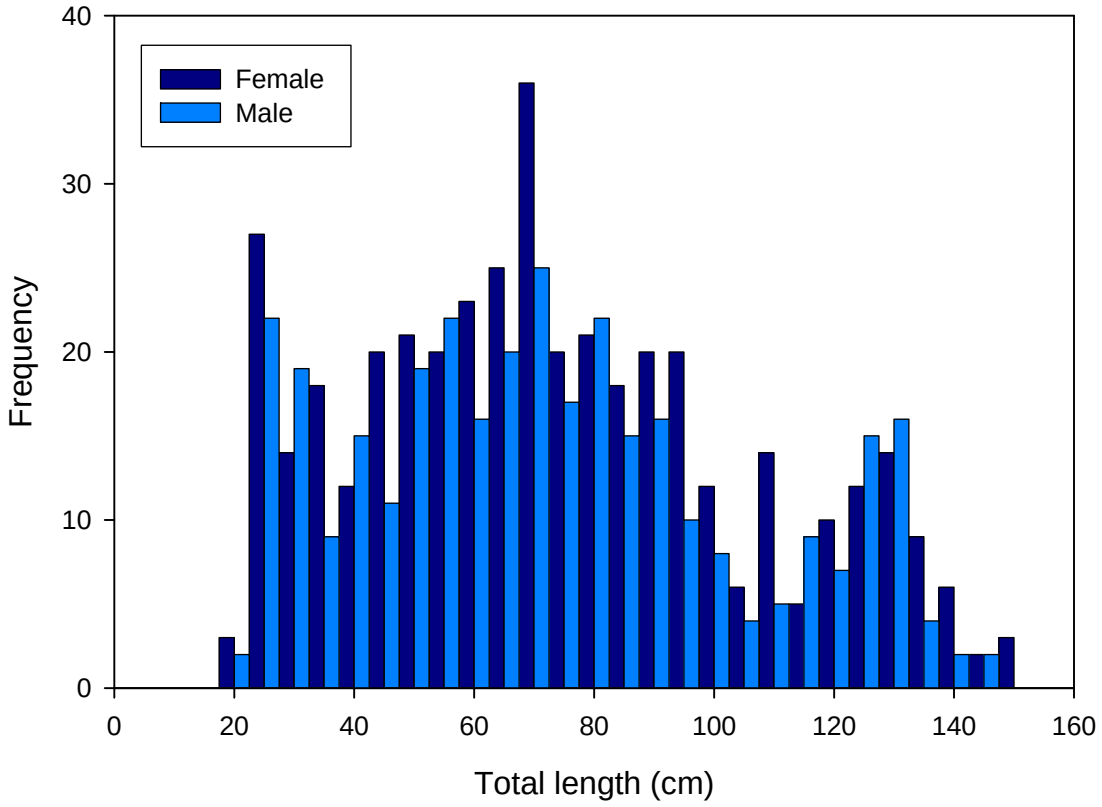

Fig. 5. Length frequencies of female (*n*=411) and male (*n*=332) *Bathyraja aleutica* examined from fisheries observers samples and fishery independent surveys, 2004-2006.

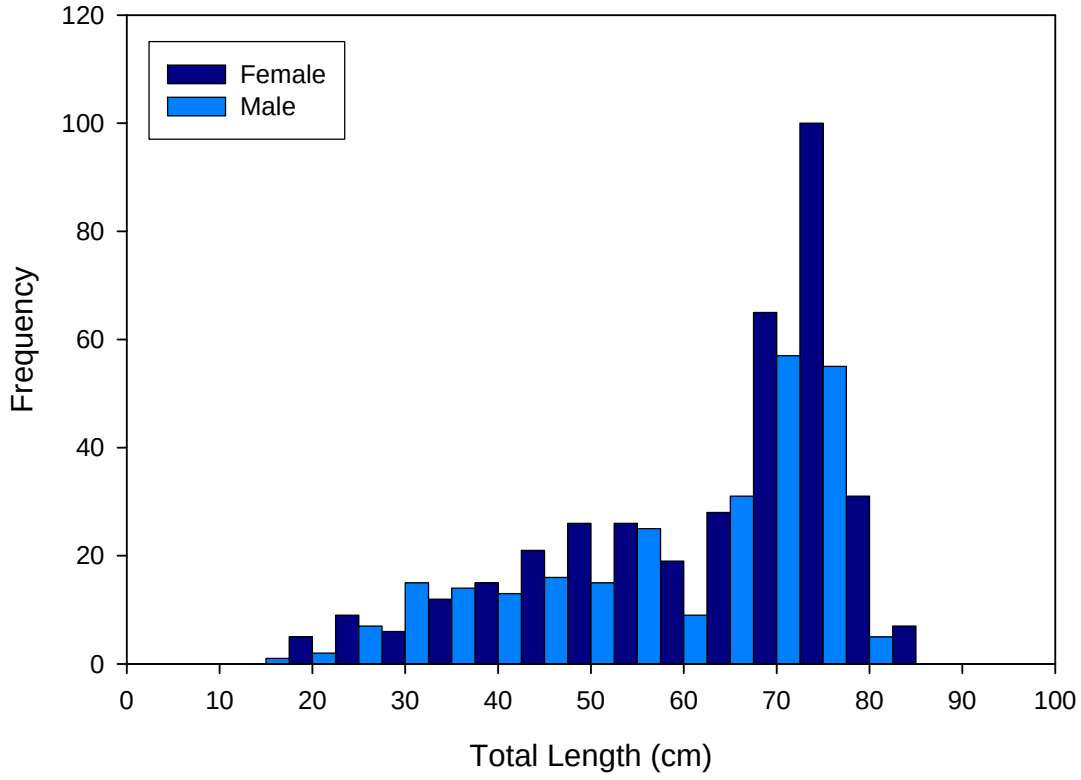

Fig. 6. Length frequencies of female (*n*=370) and male (*n*=265) *Bathyraja interrupta* examined from port sampling and fishery independent surveys, 2005-2006.

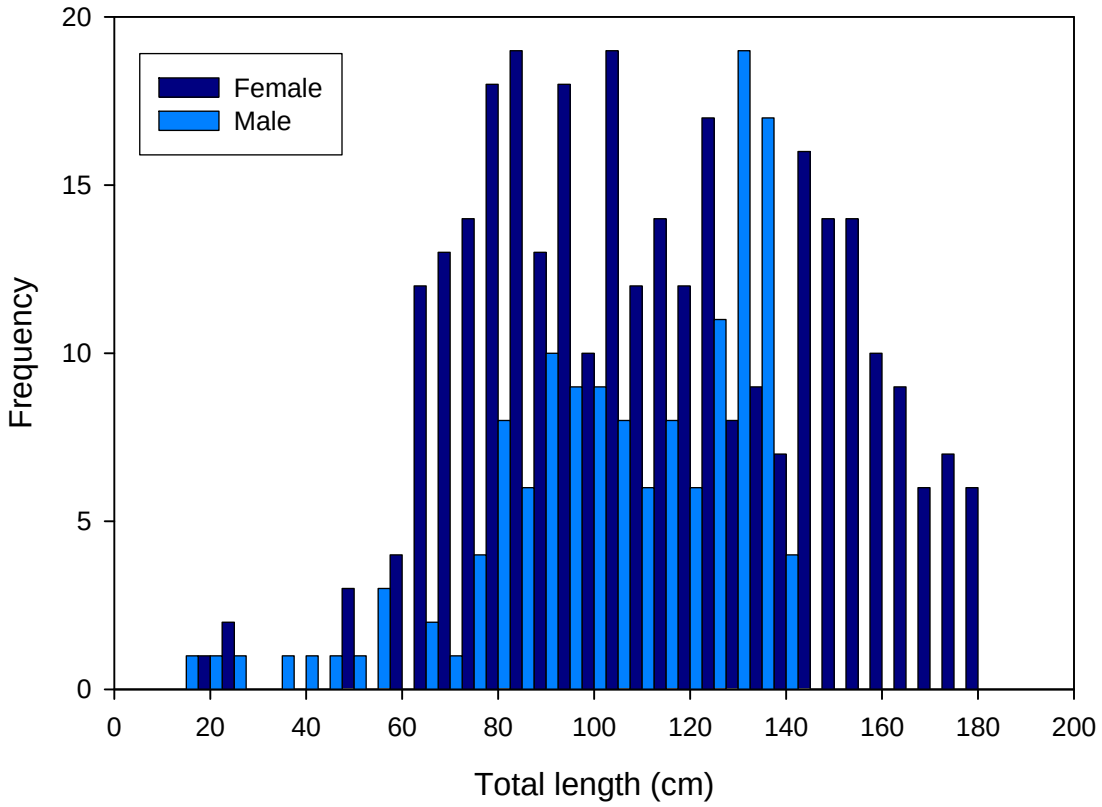

Fig. 7. Length frequencies of female (*n*=307) and male (*n*=138) *Raja binoculata* examined from port sampling and fishery independent surveys, 2004-2006.

A total of 672 *R. rhina* were sampled from fishery independent surveys and port sampling. These ranged in size from 18.1 to 145.0 cm TL (Fig. 8). The largest female and male specimens measured were 145.0 and 135.8 cm TL, respectively.

Age determination

Bathyraja aleutica. Measurements of centrum diameter taken over the observed size range revealed a linear and significant relationship between TL and MCD. No significant difference in TL (cm) and MCD (mm) was detected between males and females, so these data were combined (ANCOVA, $F = 0.60$, $p = 0.44$, $n = 157$), resulting in a positive linear relationship (TL = 6.593 + 14.671 x MCD, $r^2 = 0.98$; Fig 9).

There was no detectable bias in centrum banding patterns from anterior and posterior regions of the vertebral column (Fig. 10). Differences between age estimates were not significant ($t = -1.564$, $p = 0.13$), therefore all age estimates were based on counts of anterior vertebral centra.

Relationships of caudal thorn measurements to TL were best described by power functions. Differences between TL (cm) and thorn base length (TBL) (mm) for males and females were not significant, so these data were combined (ARSS, $F = 0.83$, $p = 0.48$, $n = 68$), and were described by the following power function: TBL = 0.2493 x $TL^{.7581}$ ($r^2 = 0.81$). The relationship of TL to TBL resulted in the best fit when compared to thorn width to TL ($r^2 = 0.78$) and thorn height to TL ($r^2 = 0.64$) regressions (Fig. 11).

Vertebral centra from 410 *B. aleutica* were processed for ageing. Examination of ageing structures showed that banding patterns were highly variable within each structure. Of these, 325 (80%) had suitable quality (grade 2 or greater) and agreement among age estimates for further analysis. A subset of caudal thorns from 75 specimens was prepared for age analysis. Poor quality and lack of agreement resulted in a 28% loss; therefore age estimates from 54 caudal thorns were compared with vertebral thin sections from the same specimens. Caudal thorn and vertebral thin section age estimates were positively correlated ($r = 0.87$), however a paired t test revealed significant differences between age estimates ($t = 4.517$, $p < 0.001$). Comparison between ageing structures indicated thorn estimates were biased towards older ages (Fig. 12).

Bathyraja interrupta. Both sexes demonstrated a strong linear relationship between TL and MCD, indicating that centra grow in proportion to total length (Males: TL = 12.45 x MCD + 6.82, $r^2 = 0.95$, $n = 43$; Females: TL = 10.7 x MCD + 13.62, $r^2 = 0.92$, $n = 60$) (Fig. 13). A significant difference was found between sexes (ANCOVA: $F = 4.48$, $p = 0.037$, $n = 103$). Additionally, no significant difference was detected between mean age estimates of centrum from the anterior and posterior portions

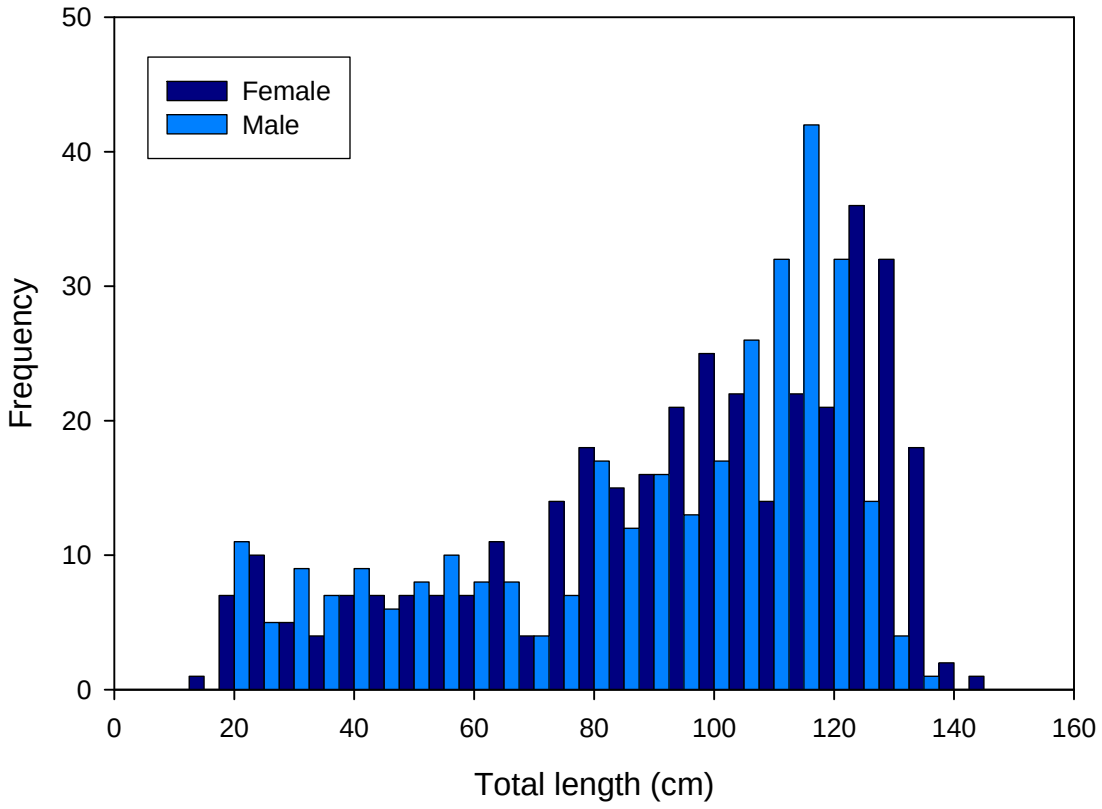

Fig. 8. Length frequencies of female (*n*=354) and male (*n*=318) *Raja rhina* examined from port sampling and fishery independent surveys, 2004-2006.

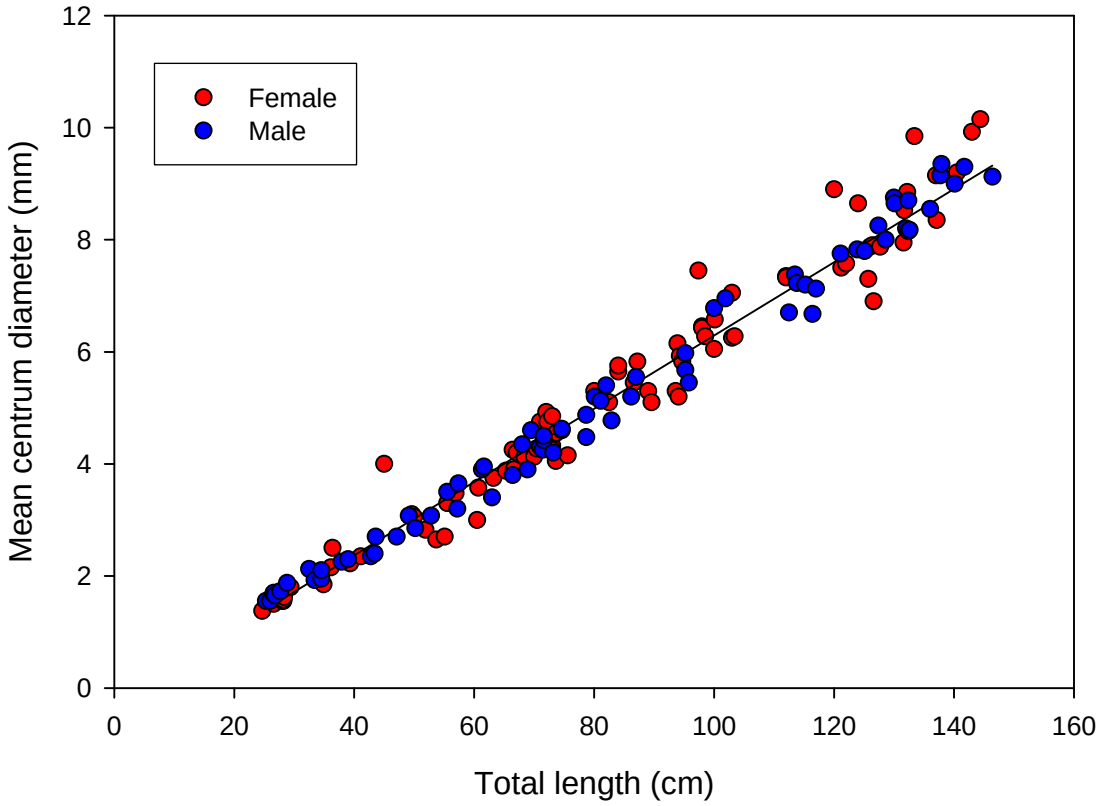

Fig. 9. Relationship between mean centrum diameter and total length for combined sexes of *Bathyraja aleutica* (*n*=157).

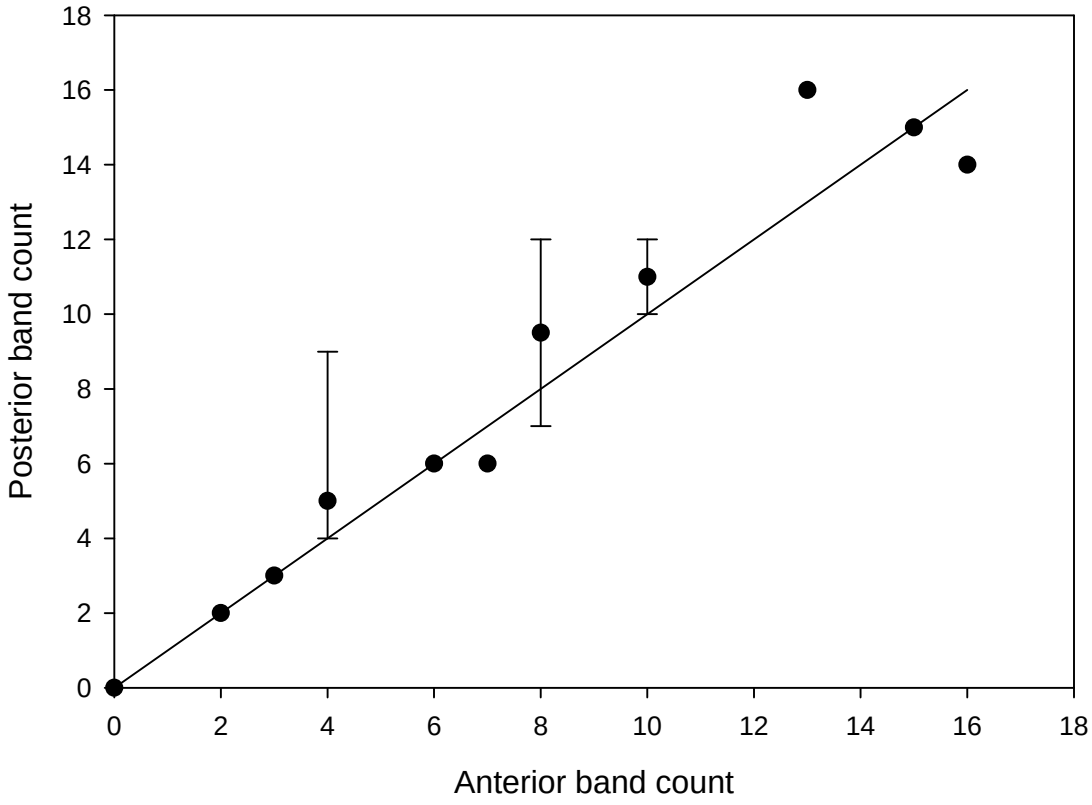

Fig. 10. Comparison of band counts from anterior and posterior vertebrae for *Bathyraja aleutica* (*n*=27). The 45º line represents 1:1 agreement between band counts. Bars demonstrate the range of values.

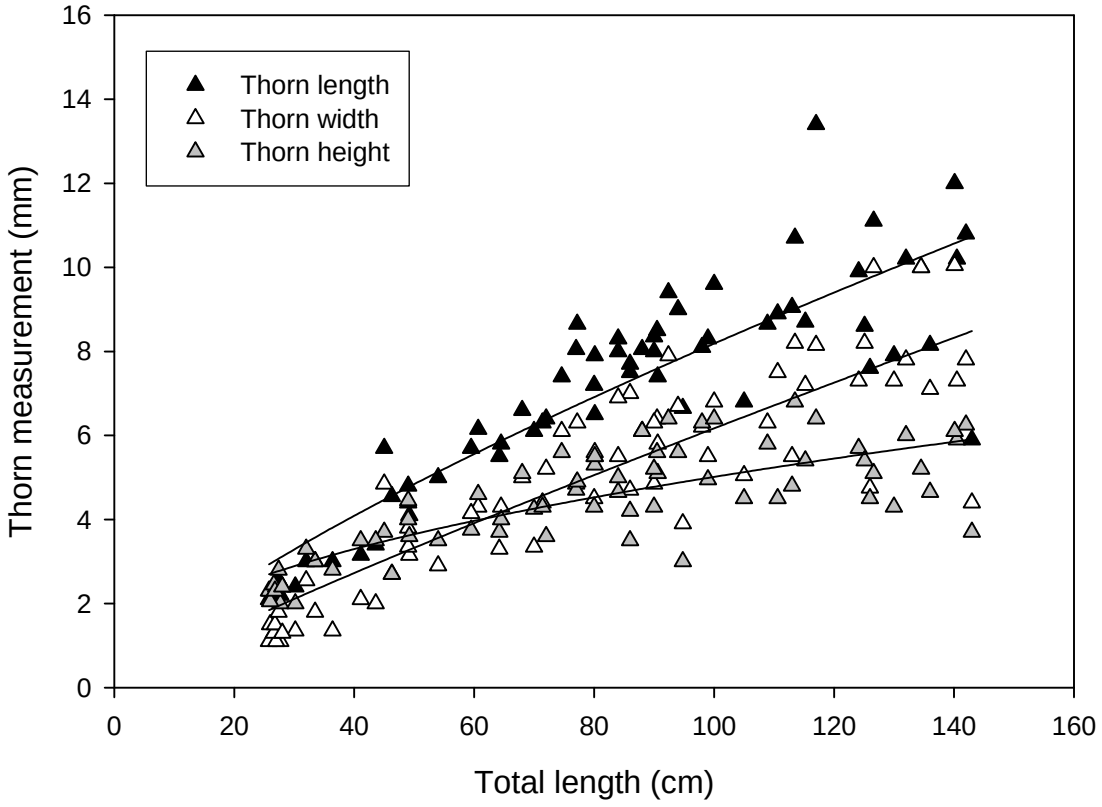

Fig. 11. Relationship between caudal thorn base length and total length of *Bathyraja aleutica* sexes combined (*n*=68).

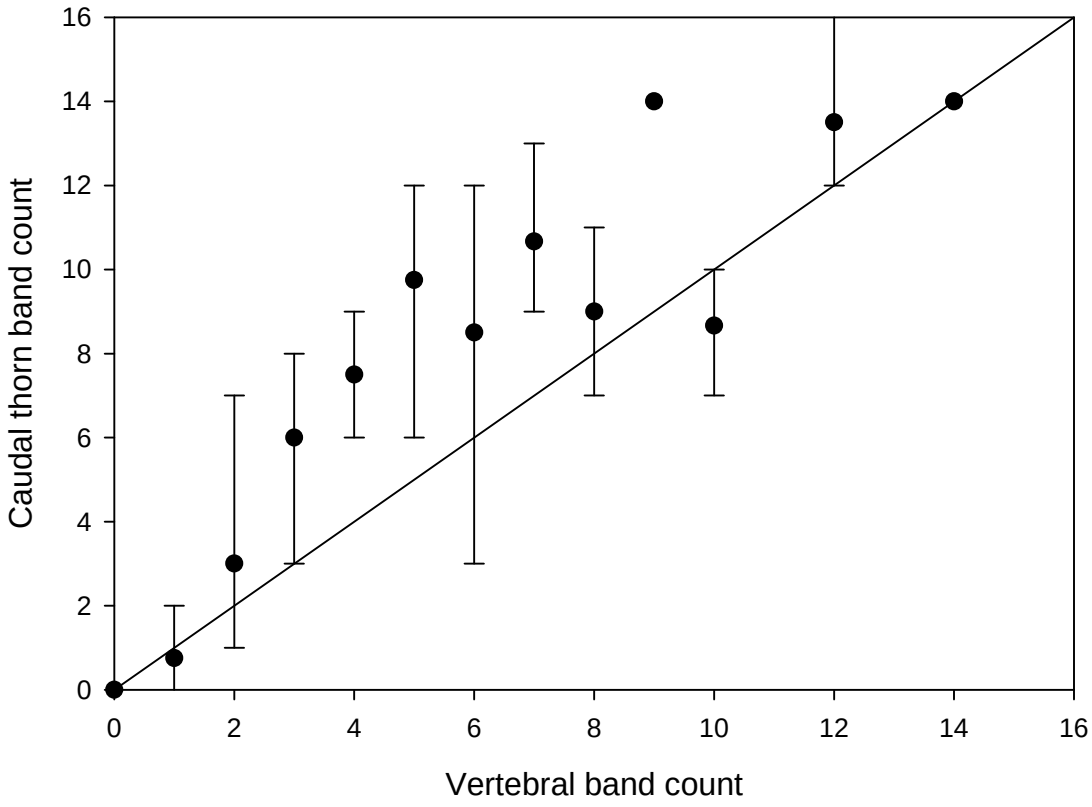

Fig. 12. Age bias plot of caudal thorn and vertebral band counts from *Bathyraja aleutica* (*n*=54). The 45º line represents 1:1 agreement between band counts. Bars indicate range of band counts.

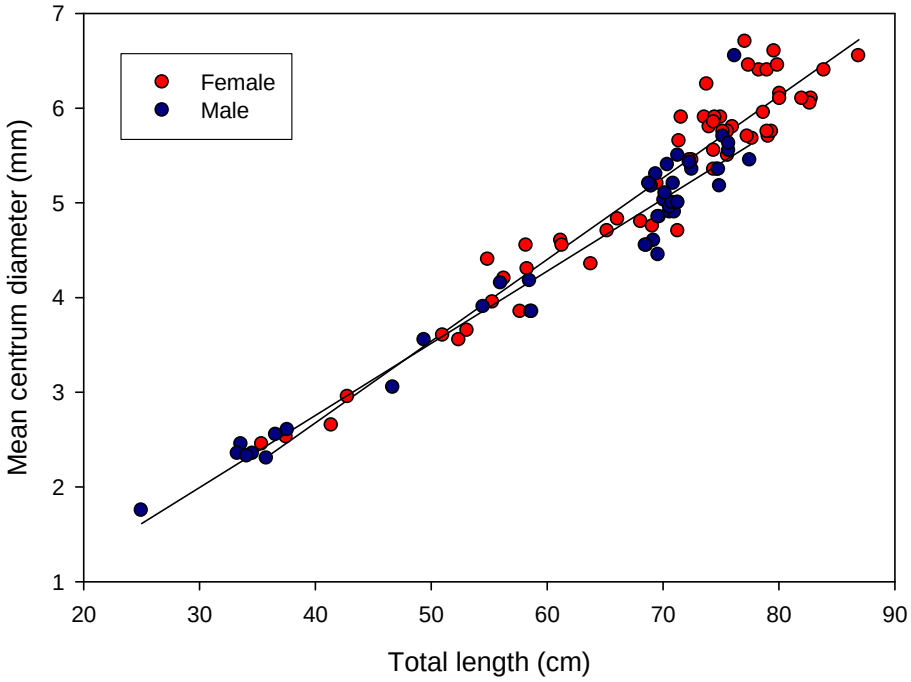

Fig. 13. The relationship between mean centrum diameter and total length for female (*n*=60) and male (*n*=43) *Bathyraja interrupta*.

of the vertebral column ($t = 0.53$, $p = 0.60$) (Fig. 14).

To assess thorn growth, 32 individuals were measured, and regressed against TL. Caudal thorn base width (TBW) showed the best fit compared with the base length ($r^2 = 0.57$), and the caudal thorn height ($r^2 = 0.34$) (Fig. 15a). As there was a significant difference in the width of the caudal thorn and TL between sexes, the models were run separately (ARSS: $F = 2.97$, $p = 0.04$). The relationship between TBW and TL was best described by a power model for both sexes (Females: $TBW = 0.0621 \times TL^{1.043}$, $r^2 = 0.65$, $n = 33$; Males: $TBW = 0.0612 \times TL^{1.023}$, $r^2 = 0.78$, $n = 59$) (Fig. 15b).

Of the 388 vertebrae examined, 64 were given readability scores of 2 or less, providing 324 vertebrae for statistical analysis. Of the 92 caudal thorns examined, 8 were given readability scores of 2 or less, providing 84 caudal thorns for analysis. Although age estimates from thorns were not normally distributed, parametric statistical tests were conducted as the Levene's test failed to show unequal variances between thorn and vertebrae (K-S Test: $z = 1.48$, $p = 0.025$, $n = 83$; Levene's test: $F = 0.971$, $df_1 = 1$, $df_2 = 164$, $p = 0.33$). Age estimates between caudal thorns and vertebral centra were significantly correlated, however, only 72% of the variability was explained by this relationship ($r = 0.72$, $p < 0.0001$) (Fig. 16). There was no significant difference in mean age estimates between structures ($t = -0.523$, $p = 0.602$, $n = 83$), though the age bias plot showed a tendency toward underestimation of ages among vertebrae from older individuals.

Precision and error analyses

Bathyraja aleutica. Age bias plots demonstrated no appreciable bias between age estimates from vertebral thin sections or caudal thorns (Figs. 17 and 18). Precision was calculated excluding those low quality samples that were not found to be in agreement, and excluding age 0 samples for vertebrae and caudal thorns. Overall precision among the three age estimates from vertebral thin sections was generally high (IAPE = 8.91%, CV = 11.45%, D = 8.10%). Precision of caudal thorn age estimates was lower than for vertebrae (IAPE = 10.84%, CV = 14.08%, D = 9.96%). Precision was poor between caudal thorn and vertebral thin section estimates from the same specimens (IAPE = 22.00%, CV = 31.11%, D = 22.00%).

Bathyraja interrupta. Visual assessment of the pair-wise age difference plots showed no obvious biases between reads for both vertebrae and caudal thorns. However, read 3 of the caudal thorns aged slightly higher (Figs. 19 and 20). Average percent error, CV and D were acceptable among both the three or four vertebral reads (IAPE = 9.13%, CV = 11.54%, D = 6.40%) and caudal thorn age estimates (IAPE = 7.73%, CV = 10.12%, D = 5.65%). Comparisons of estimated ages from vertebrae and thorns were less precise than for each structure alone (IAPE = 12.87%, CV = 18.21%, D = 12.87%).

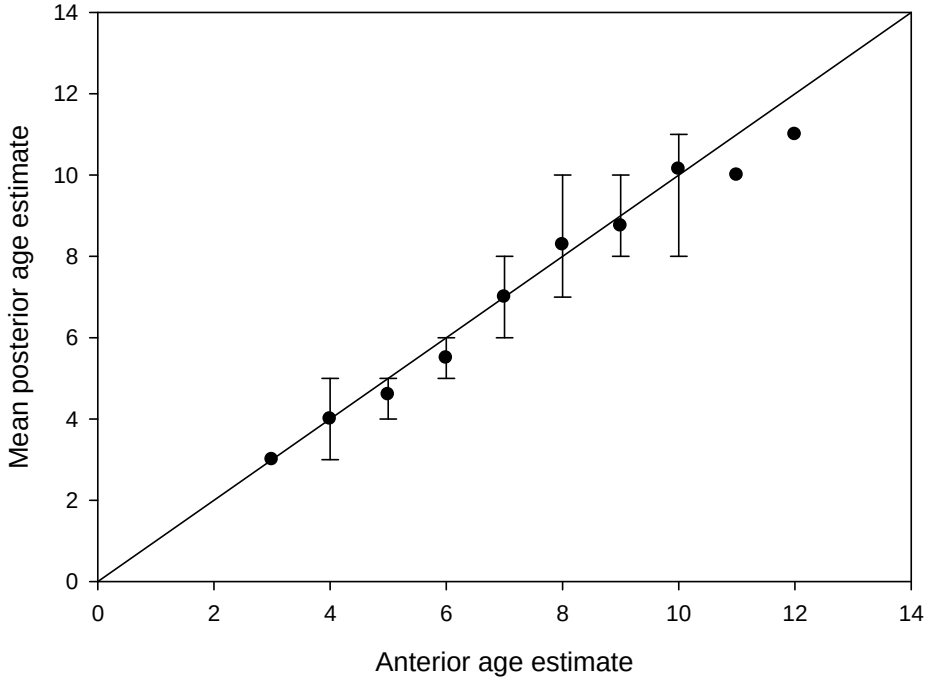

Fig. 14. The relationship between the mean posterior age estimates and anterior age estimates from vertebrae of *Bathyraja interrupta* (n=35). Bars demonstrate the range of values.

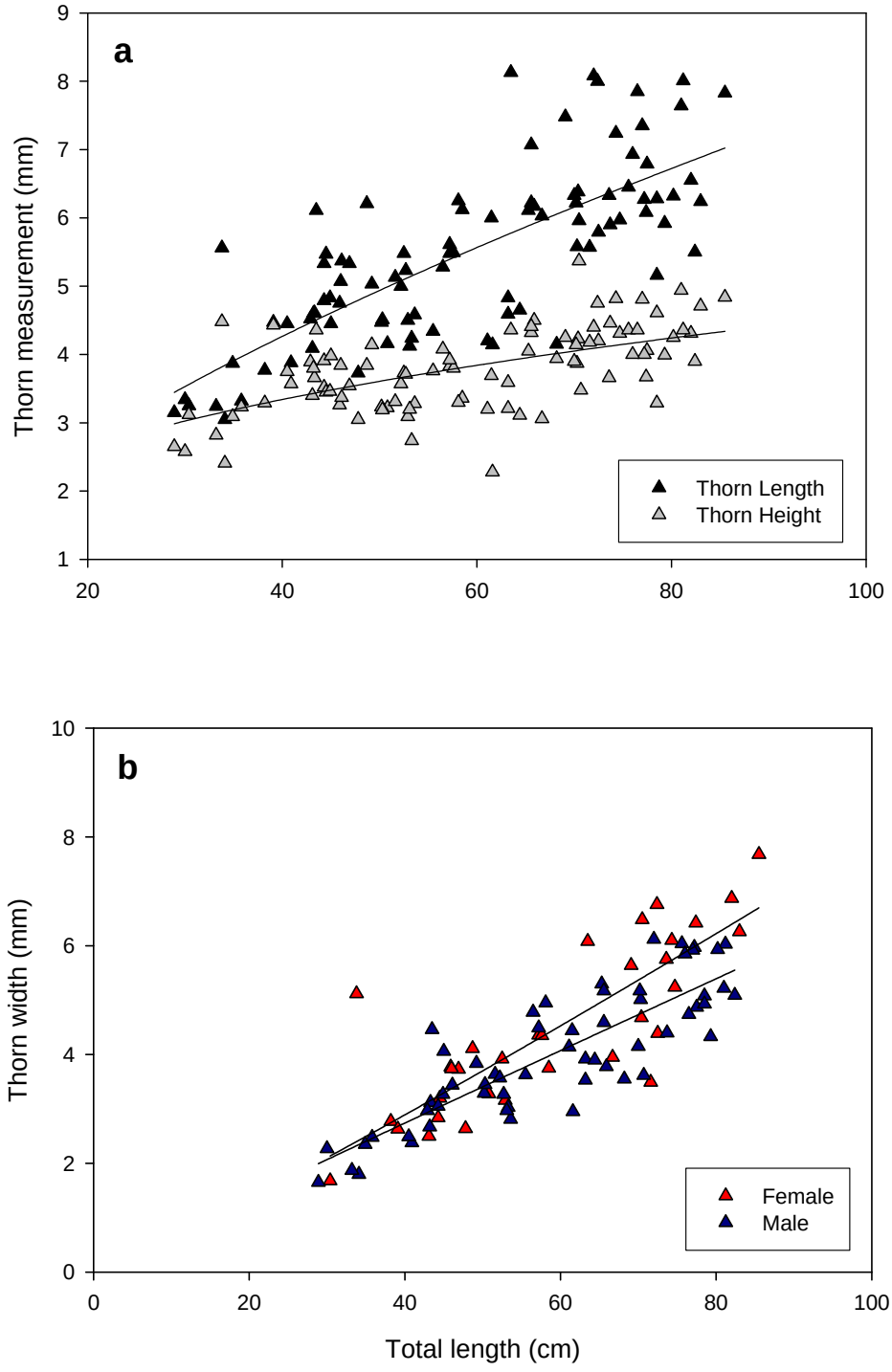

Fig. 15. The relationships between thorn height and length (**a**) and width (**b**) measurements and total length for *Bathyraja interrupta* (*n*=92).

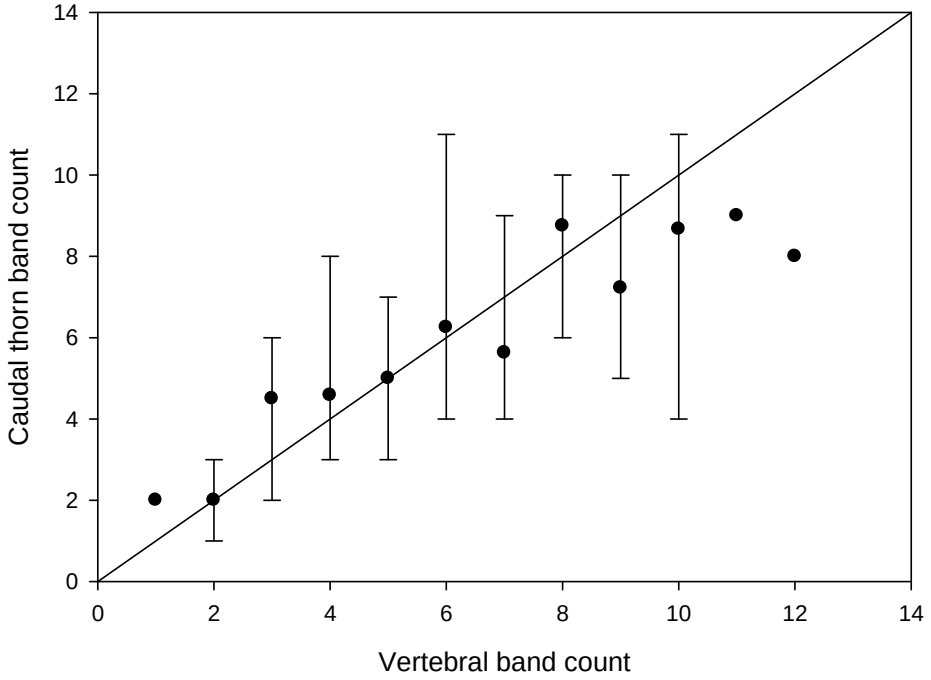

Fig. 16. The relationship between caudal thorn band counts and vertebral band counts from *Bathyraja interrupta* (*n*=81). The 45º line represents 1:1 agreement between band counts. Bars demonstrate the range of values.

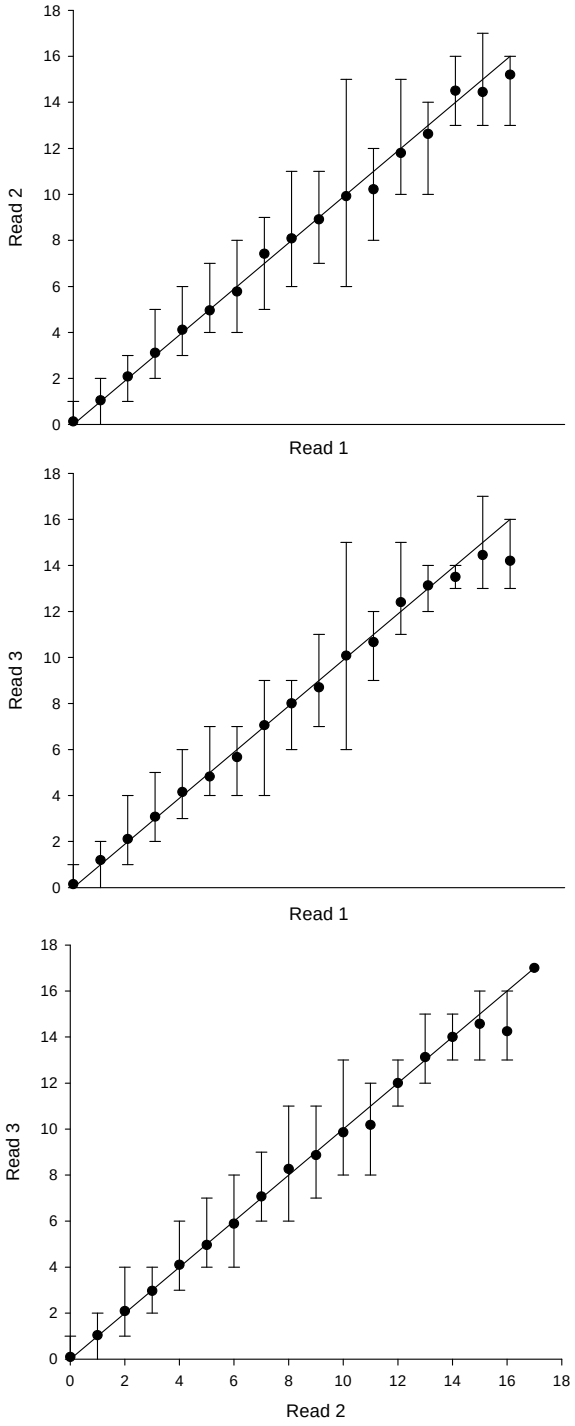

Fig. 17. Age bias plots of age estimates between independent reads of vertebral thin sections from *Bathyraja aleutica* (*n*=325). The 45º line represents 1:1 agreement between band counts. Bars demonstrate the range of values.

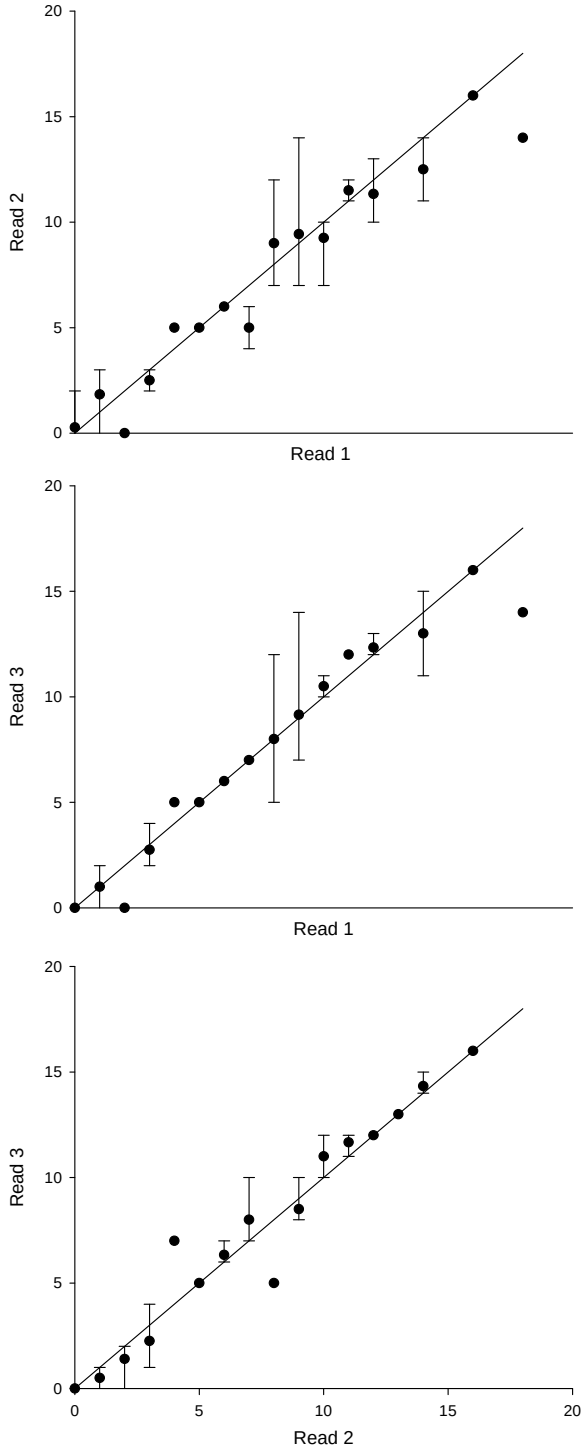

Fig. 18. Age bias plots of age estimates between independent reads of *Bathyraja aleutica* caudal thorns (*n*=54). The 45º line represents 1:1 agreement between band counts. Bars indicate the range of values.

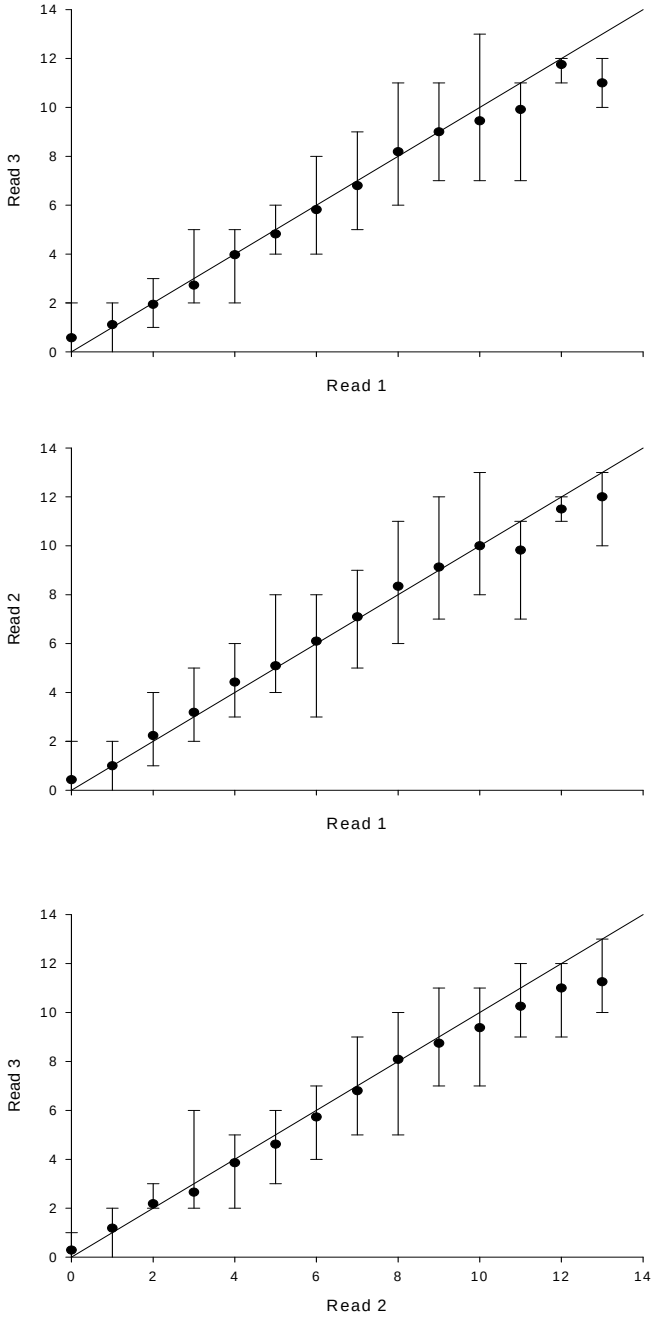

Fig. 19. Age bias plots of age estimates between independent reads of vertebral thin sections from *Bathyraja interrupta* (*n*=326). The 45º line represents 1:1 agreement between band counts. Bars indicate the range of values.

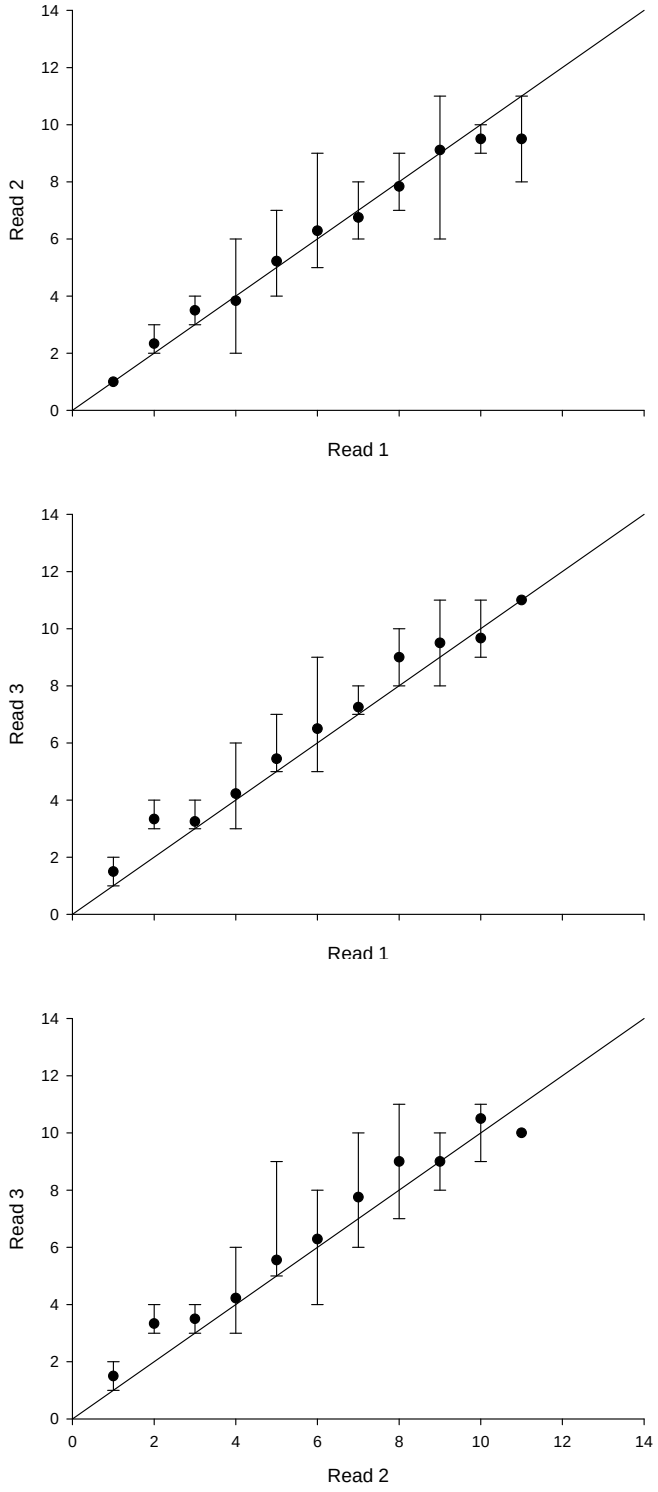

Fig. 20. Age bias plots of age estimates between independent reads of from three reads of *Bathyraja interrupta* caudal thorns (*n*=86). The 45º line represents 1:1 agreement between band counts. Bars indicate the range of values.

Age validation

Bathyraja aleutica. An annual pattern of band deposition could not be validated using marginal increment and edge analysis methods. Analyses were performed on 209 vertebral thin sections. Due to poor clarity of thin sections, about 48% of samples were removed from marginal increment analysis and 40% from edge analysis. The greatest mean MIR value (0.80) occurred in January, and the lowest (0.42) in March. There were no significant differences in mean MIRs among months (F =1.82, p = 0.08; Fig. 21). Comparison of edge types demonstrated that translucent bands were present most frequently at the edge during January and opaque bands during July.

Bathyraja interrupta. A total of 261 vertebral sections were examined for validation. There was no apparent pattern of edge classification among months, although it is important to note that this analysis was limited to six consecutive months, not a full year as recommended. A one-way ANOVA found no significant differences in mean MIRs among months (F = 0.903, df = 5, p = 0.481, n = 131) (Fig. 22).

Growth parameter estimates

Bathyraja aleutica. Vertebral thin section age estimates ranged from 0 to 16 years for males (n = 149) and 0 to 17 years for females (n = 176). The largest female was 153.4 cm TL and was aged to 15 years. The oldest female, aged to 17 years, was 144.4 cm TL. The largest male was 149.9 cm TL and aged to 13 years, whereas the oldest male, aged to 16 years, was 132.4 cm TL.

All growth models fit the length-at-age data well and were highly significant (p = <0.001; Table 4). The three parameter VBGF was biologically reasonable and had strong goodness-of-fit. Females reached a larger maximum size (L_∞ = 174.4 cm) and had a slightly lower growth coefficient (k = 0.10) than males (L_∞ = 170.5, k = 0.11), however differences in growth were not significant between sexes (ARSS, F = 0.27, p = 0.85). Therefore, data were combined for all models, and the resulting growth parameters for the three parameter VBGF were L_∞ = 172.6 cm, k = 0.11, t_o = -1.78 (Fig. 23).

Size at birth predicted by the VBGF (29.7 cm TL) and Gompertz models (31.8 cm TL) were greater than the smallest free-swimming individuals (20.6 cm TL female and 23.9 cm TL male) and previous estimates of size at birth (19.6-26.3 cm TL, modified from Teshima and Tomonaga 1986), indicating that these models may not adequately describe early growth. The two parameter VBGF with fixed length at birth (23.0 cm TL) had an estimated maximum length (L_∞ = 160.8), however, values of r^2 and MSE were lower and higher, respectively. The polynomial function provided the best statistical fit of all the models (Table 4).

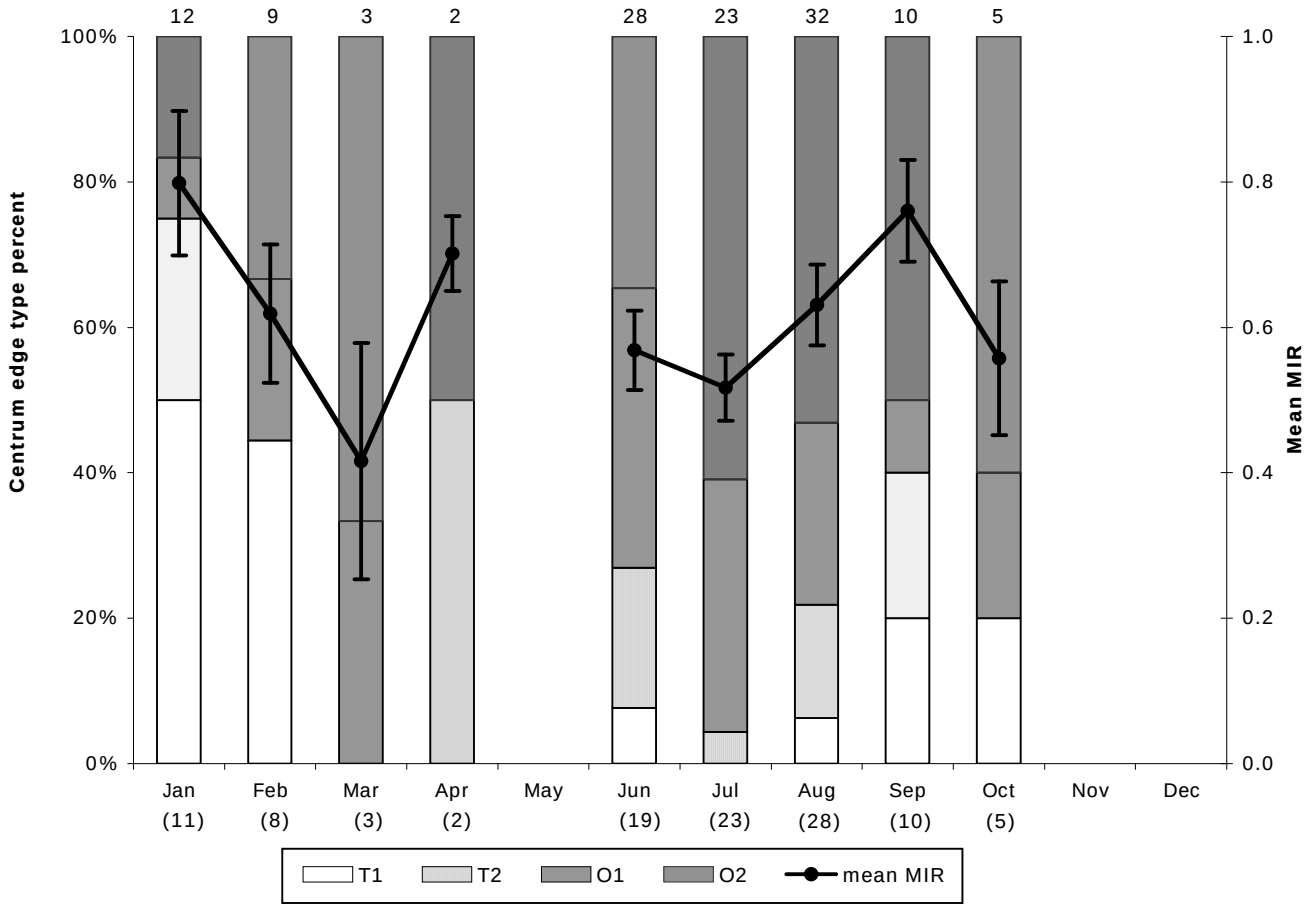

Fig. 21. Monthly variation in *Bathyraja aleutica* centrum edge type (n=124) and mean marginal increment ratio (MIR) ± 1 standard error (*n*=109) determined from pooled sexes. Values listed above the histogram represent the number of samples used in centrum edge analyses. Sample sizes included in MIR analyses are depicted below month in parentheses. T1, narrow translucent edge; T2, broad translucent edge; O1, narrow opaque edge; O2, broad opaque edge.

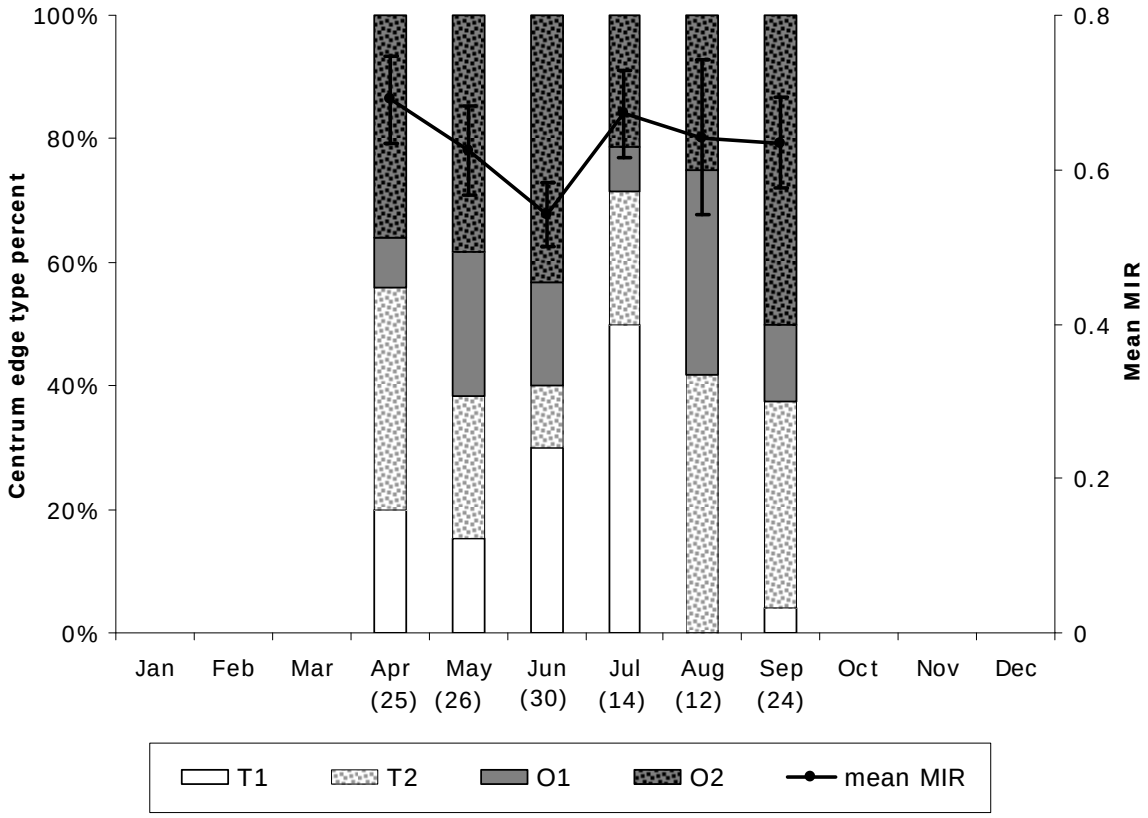

Fig. 22. Monthly variation in *Bathyraja interrupta* centrum edge type (n=131) and mean marginal increment ratio (MIR) ± 1 standard error (*n*=131) determined from pooled sexes. Values listed above the histogram represent the number of samples used in centrum edge analyses. Sample sizes included in MIR and edge type analyses are depicted below month in parentheses. T1, narrow translucent edge; T2, broad translucent edge; O1, narrow opaque edge; O2, broad opaque edge.

Table 4. Parameters for each growth model for males, females, and combined sexes of *Bathyraja aleutica*. VBGF, von Bertalanffy growth function; L_∞, asymptotic length; k, growth coefficient; t_0, theoretical age at 0 length; L_0, length at birth; g, instantaneous growth rate; P, shape parameter; y_o, a, and b, are constants.

Growth Model		L_∞	k	t_0	L_0	g	P	y_o	a	b	r^2	MSE	SEE	p
3 Parameter VBGF	Females	174.43	0.10	-1.86	30.3	-	-	-	-	-	0.9545	63.38	7.96	<0.0001
	Males	170.47	0.11	-1.69	29.0	-	-	-	-	-	0.9569	60.41	7.77	<0.0001
	Pooled	172.58	0.11	-1.78	29.7	-	-	-	-	-	0.9557	61.60	7.85	<0.0001
2 Parameter VBGF	Females	162.14	0.13	-	23.0	-	-	-	-	-	0.9455	75.59	8.69	<0.0001
	Males	158.93	0.14	-	23.0	-	-	-	-	-	0.9497	70.04	8.37	<0.0001
	Pooled	160.80	0.13	-	23.0	-	-	-	-	-	0.9476	72.71	8.53	<0.0001
Gompertz	Females	150.42	1.54	-	32.2	0.21	-	-	-	-	0.9535	64.85	8.05	<0.0001
	Males	147.63	1.55	-	31.3	0.22	-	-	-	-	0.9566	60.92	7.81	<0.0001
	Pooled	149.21	1.55	-	31.8	0.22	-	-	-	-	0.9550	62.59	7.91	<0.0001
Logistic	Females	142.28	-	3.56	-	0.32	-	-	-	-	0.9495	70.41	8.39	<0.0001
	Males	140.06	-	3.45	-	0.34	-	-	-	-	0.9531	65.84	8.11	<0.0001
	Pooled	141.30	-	3.51	-	0.33	-	-	-	-	0.9513	67.80	8.23	<0.0001
Richards	Females	176.99	0.10	-	0.83	-	-0.02	-	-	-	0.9546	63.75	7.98	<0.0001
	Males	172.28	0.11	-	0.83	-	-0.01	-	-	-	0.9569	60.83	7.80	<0.0001
	Pooled	175.40	0.11	-	0.83	-	-0.02	-	-	-	0.9558	61.79	7.86	<0.0001
Polynomial	Females	-	-	-	-	-	-	31.20	13.26	-0.39	0.9547	63.16	7.95	<0.0001
	Males	-	-	-	-	-	-	29.71	14.10	-0.45	0.9593	57.14	7.56	<0.0001
	Pooled	-	-	-	-	-	-	30.50	13.62	-0.42	0.9568	60.20	7.76	<0.0001

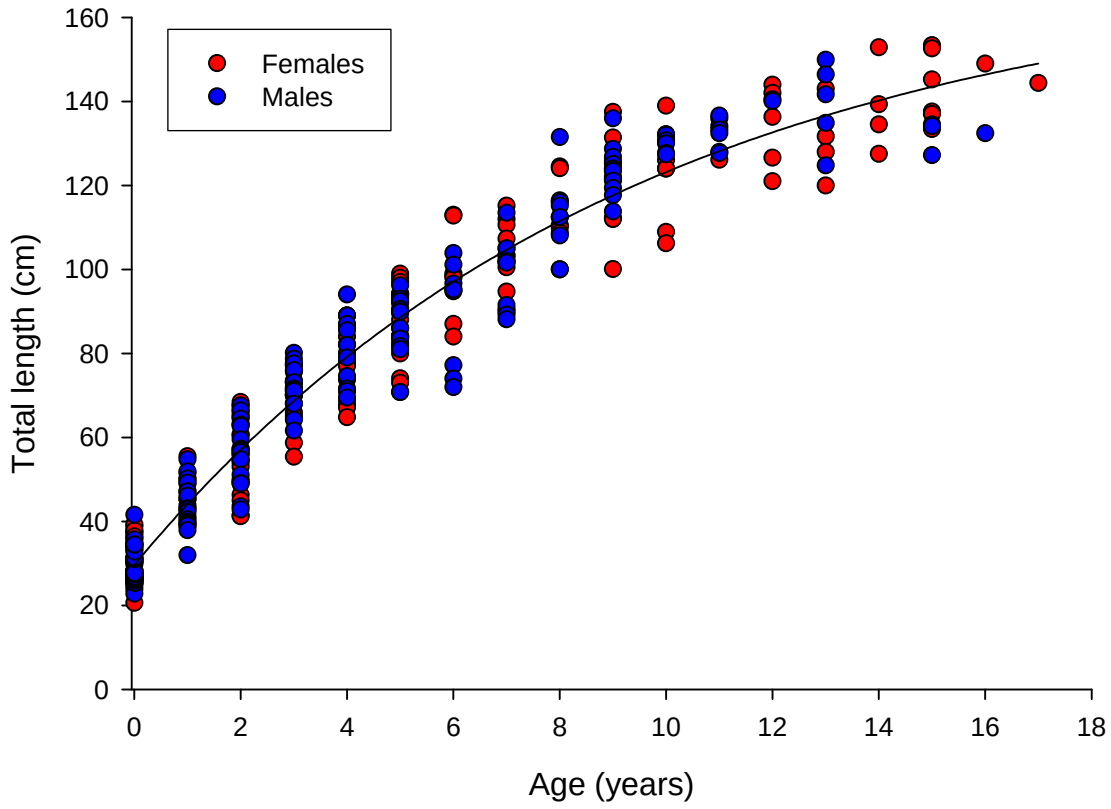

Fig. 23. von Bertalanffy growth function fitted to length-at-age data for combined sexes of *Bathyraja aleutica* (*n* = 325).

Bathyraja interrupta. Ages estimated from vertebral centra indicate a minimum longevity of 12 years for males and 13 for females. Both the largest female aged (87.1 cm TL) and the largest male (82.4 cm TL) were estimated to be 9 years old. The oldest female measured 86.9 cm TL and was estimated to be 13 years old. The oldest male was estimated to be 12 years old and was 78.5 cm TL.

All growth models fit the length-at-age data and were highly significant (p = <0.001), however the CV was lower than expected from results of other elasmobranch age and growth studies. Growth models were initially run separately, however, there was not enough evidence to support differences in growth parameters between sexes; therefore sexes were pooled (ARSS: VBGF three parameter: F = 0.8259, p = 0.48; VBGF two parameter: F = 1.8217, p = 0.14; Gompertz: F = 1.1499, p = 0.33; Logistic: F = 1.4805, p = 0.2198; Richards: F = 0.6155, p = 0.61). Using the coefficient of variation (r^2), residual mean squared error (MSE), and significance levels to examine goodness-of-fit of the model, the logistic model provided best fit the age at length data, closely followed by the Gompertz model (Table 5, Fig. 24).

The Logistic, Gompertz and Richards's models had the most biologically realistic L_∞ estimates, while the L_∞ estimates from both VBGFs were much higher than the reported maximum sizes for *B. interrupta* (Table 5). Estimates of k from the 3 and two parameter VBGFs were reasonable. Estimates of L_0 based on the three parameter VBGF (21.4 cm) and Gompertz model (22.1 cm) were much greater than estimated size after hatching (13.0 to 14.0 cm for *B. interrupta* from the eastern Bering Sea; Jerry Hoff, NMFS-AFSC, pers. comm.). However, the smallest individuals reported in this study was a 20.3 cm female and an 18.9 cm male, and the initial two parameter VBGF model was based on these estimates of L_0. An additional two parameter model was generated using 13.5 cm as an estimate of L_0, which gave lower estimates of L_∞ and higher k values.

Maturity and reproduction

Bathyraja aleutica. Reproductive observations were recorded from 267 female and 279 male *B. aleutica*. Females and males were similar in maturity, with females maturing over slightly longer lengths but shorter age ranges (Figs. 25 and 26). Maturity was attained from 111.6 to 137.6 cm TL for females, and corresponded to ages of 9 to 12 years. Males matured between 117.7 and 133.3 cm TL, which corresponded to ages of 7 to 11 years. Based on maturity ogives, TL_{50} was estimated as 124.1 cm for females and 122.8 cm for males. Corresponding median ages at maturity were estimated as 10.4 and 10.2 years for females and males, respectively. All females greater than 137.6 cm were classified as mature. A female of 137.5 cm TL was the largest immature specimen, and the smallest mature female was 111.6 cm TL. All males greater than 133.3 cm TL were determined to be mature. A male measuring 132.6 cm TL was the largest immature specimen, and the smallest mature male was 117.7 cm TL.

Table 5. Parameters for each growth model for males, females and pooled sexes of *Bathyraja interrupta*. Parameter abbreviations indicate VBGF, von Bertalanffy growth function; L_∞, asymptotic length; k, growth coefficient; t_0, theoretical age at 0 length; L_0, length at birth; g, instantaneous growth rate; P, shape parameter; y_o, a, and b, are constants.

Growth Model		L_∞	k	t_0	L_0	g	P	y_0	a	b	r^2	MSE	SEE	p
3 Parameter VBGF	Females	138.95	0.07	-2.65	23.5	_	_	_	_	_	0.864	36.98	6.08	<0.0001
	Males	116.73	0.09	-1.99	19.1	_	_	_	_	_	0.880	28.83	5.37	<0.0001
	Pooled	126.40	0.08	-2.32	21.4	_	_	_	_	_	0.872	33.00	5.75	<0.0001
2 Parameter VBGF	Females	129.35	0.07	_	20.3 (set)	_	_	_	_	_	0.864	36.90	6.07	<0.0001
	Males	114.34	0.10	_	18.9 (set)	_	_	_	_	_	0.880	28.66	5.35	<0.0001
	Pooled	117.85	0.09	_	18.9 (set)	_	_	_	_	_	0.871	33.10	5.75	<0.0001
2 Parameter VBGF	Females	107.09	0.12	_	13.5 (set)	_	_	_	_	_	0.851	40.54	6.37	<0.0001
	Males	100.45	0.13	_	13.5 (set)	_	_	_	_	_	0.873	30.36	5.51	<0.0001
	Pooled	103.09	0.13	_	13.5 (set)	_	_	_	_	_	0.861	35.64	5.97	<0.0001
Gompertz	Females	102.08	1.49	_	23.0	0.17	_	_	_	_	0.869	35.65	5.97	<0.0001
	Males	92.31	1.49	_	20.8	0.21	_	_	_	_	0.887	27.19	5.21	<0.0001
	Pooled	97.27	1.48	_	22.1	0.19	_	_	_	_	0.877	31.62	5.62	<0.0001
Logistic	Females	91.80	_	3.76	_	0.28	_	_	_	_	0.873	34.71	5.89	<0.0001
	Males	85.00	_	3.13	_	0.33	_	_	_	_	0.891	26.22	5.12	<0.0001
	Pooled	88.73	_	3.45	_	0.30	_	_	_	_	0.880	30.77	5.55	<0.0001
Richards	Females	96.66	0.06	_	0.84	_	0.36	_	_	_	0.864	37.21	6.10	<0.0001
	Males	86.38	0.09	_	0.83	_	0.30	_	_	_	0.880	29.02	5.39	<0.0001
	Pooled	90.11	0.08	_	0.84	_	0.34	_	_	_	0.872	33.11	5.75	<0.0001
Polynomial	Females	_	_	_	_	_	_	21.52	7.51	-0.19	0.866	36.47	6.04	<0.0001
	Males	_	_	_	_	_	_	19.14	8.74	-0.29	0.884	27.97	5.29	<0.0001
	Pooled	_	_	_	_	_	_	20.56	8.02	-0.23	0.874	32.37	5.69	<0.0001

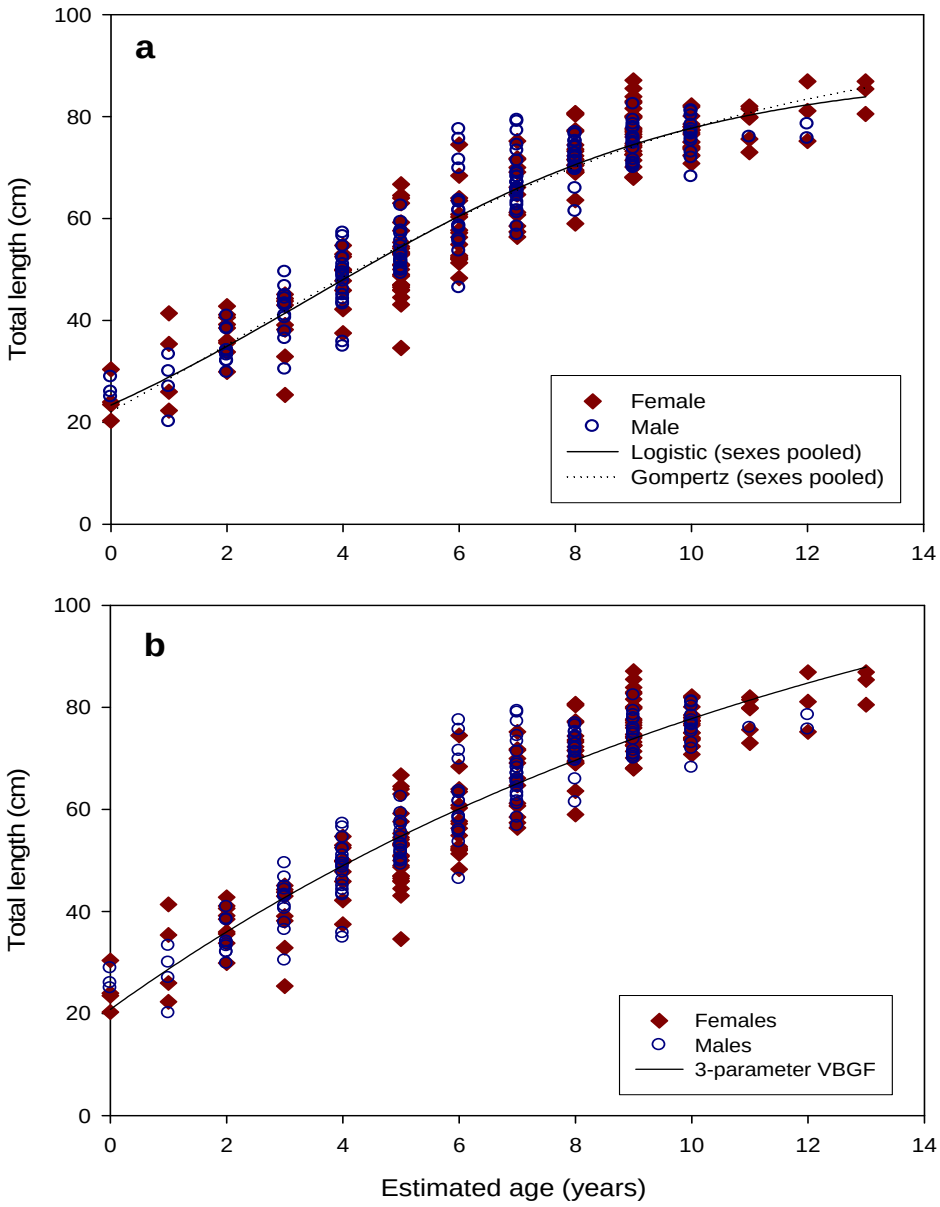

Fig. 24. Logistic and Gompertz models of growth with sexes pooled (**a**) and the three parameter VBGF with sexes pooled (**b**) fitted to total length at age data for *Bathyraja interrupta*.

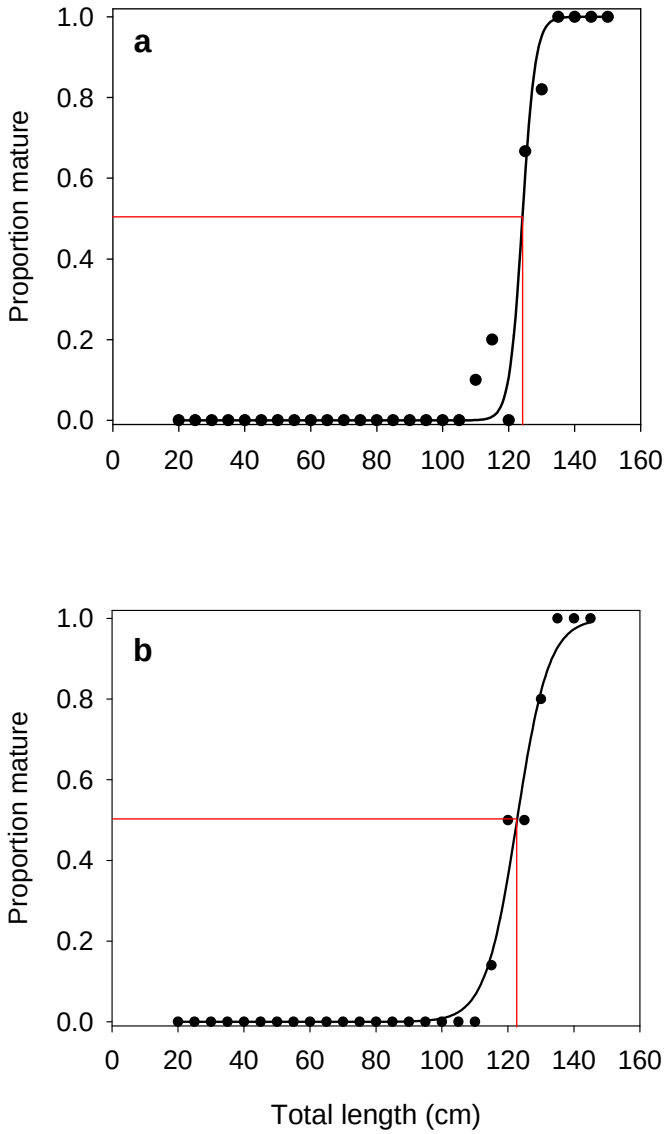

Fig. 25. Estimated median size at maturity for female (**a**) and male (**b**) *Bathyraja aleutica*. Size at 50% maturity corresponds to 124.4 and 122.8 cm total length for females and males, respectively.

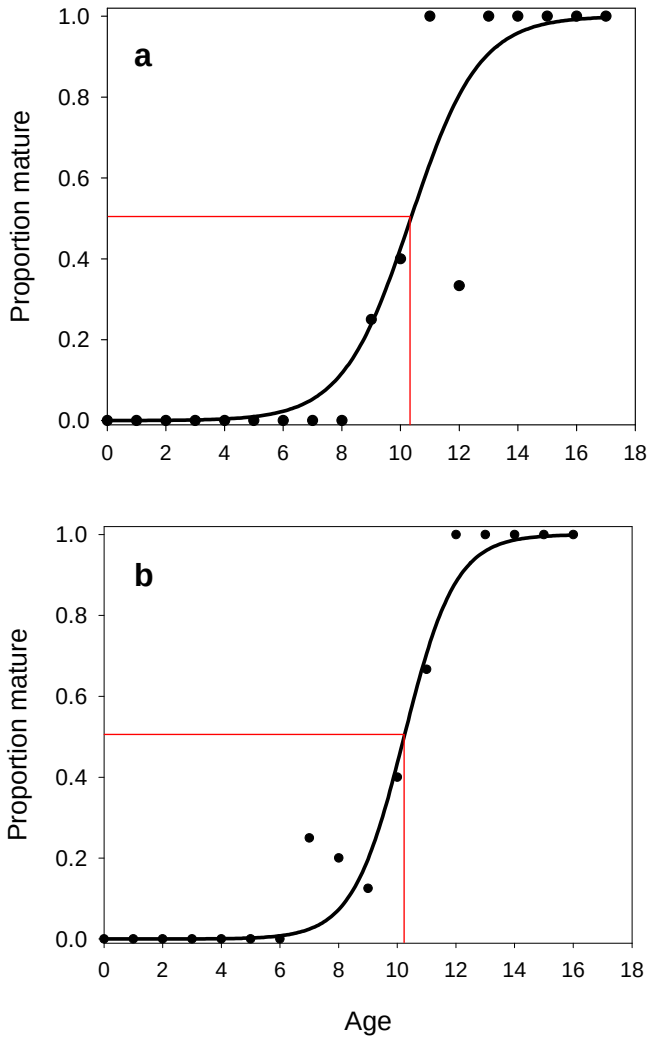

Fig. 26. Estimated median age at maturity for female (**a**) and male (**b**) *Bathyraja aleutica*. Median age at maturity corresponds to 10.4 and 10.2 years for females and males, respectively.

Onset of maturity was indicated by measures of external morphology as well. In females, oviducal gland widths ranged from 1 to 88 mm, and uterus widths from 1 to 39 mm. Abrupt changes in the relationships between widths of both female reproductive organs and TL began at ~110 cm TL (Fig 27). Inner clasper length ranged from 9 to 266 mm, and exceeded 200 mm in all mature males. A sharp increase in the inner clasper length – TL relationship was apparent at ~115 cm TL (Fig. 28).

Analysis of histological samples also reflected onset of maturity in males. Mature spermatocysts occurred in each month sampled, with a slight increase in the proportion of mature spermatocysts from June to August (Fig 29). Mature spermatocysts were visible among males by 116.4 cm TL, and the proportion of mature spermatocysts was greater than 5% in all males over 129.2 cm TL (Fig. 30).

The number of mature ova in left and right ovaries was highly correlated but not significantly different ($t = 1.129$, $p = 0.285$, $n = 11$) (Fig 31). Differences were not significant among months in maximum ova diameter (KW $\chi^2 = 3.508$, $p = 0.173$, $n = 15$) or total number of mature ova (KW $\chi^2 = 0.700$, $p = 0.705$, $n = 11$), although the latter increased by month (Fig. 32). The proportion of gravid females also was similar among months sampled ($\chi^2 = 0.84$, $n = 28$) (Fig. 33)

Maximum ova diameter appeared to increase with female size at ~130 cm TL, but relationships between maximum ova diameter or number of mature ova with TL (ova diameter: $r^2 = 0.35$; number of ova: $r^2 = 0.14$; Fig. 34a) or age (ova diameter: $r^2 = 0.05$; number of ova: $r^2 = 0.004$; Fig 34b) were not significant.

Bathyraja interrupta. The largest immature female was 79.1 cm TL and the smallest mature female was 66.6 cm. Similarly, the largest immature male was 73.7 cm TL, while the smallest mature male was 63.2 cm TL. TL_{50} was estimated as 68 cm TL for males and 70 cm TL for females, respectively (Males: $r^2 = 0.88$, $p < 0.0001$, $n = 40$; Females: $r^2 = 0.99$, $p < 0.0001$, $n = 43$) (Fig. 35). Corresponding median ages at maturity were estimated as 7 and 7.5 years for males and females respectively (males: $r^2 = 0.99$, $p < 0.0001$, $n = 12$; females: $r^2 = 0.997$, $p < 0.0001$, $n = 14$) (Fig. 36).

Inner clasper length ranged from 9 to 216 mm, with a sharp increase at approximately 55cm TL (Fig. 37). Oviducal widths ranged from 1 to 61 mm and uterus widths ranged from 1 to 34 mm (excluding gravid females). An increase in the width of the oviducal gland in females occurred near 60 cm TL (Fig. 38a). Uterus widths show a sharp increase between 60 and 70 cm TL (Fig. 38b).

Of the 70 testes prepared for histology, 67 were useable for analysis. Males with mature spermatocysts occurred in each month studied (Fig. 39). While the proportions varied amongst months, so did the sample size. Spermatocysts began to mature in males of 62.0 cm TL or greater and were present in all males over 66 cm TL (Fig. 40).

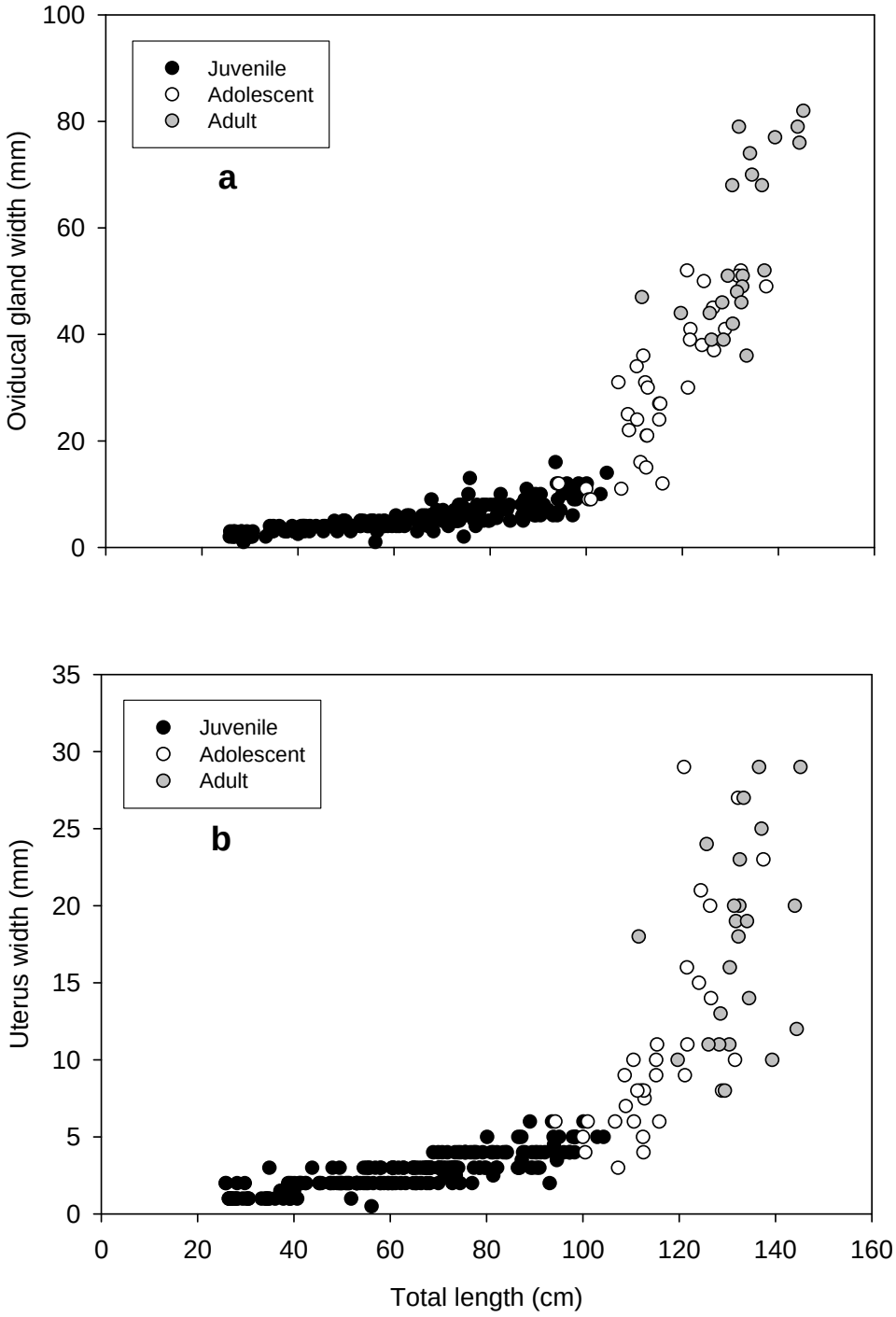

Fig. 27. Relationships between oviducal gland width (**a**; n=260) and uterus width (**b**; *n*=259) with total length based on reproductive classifications of female *Bathyraja aleutica*.

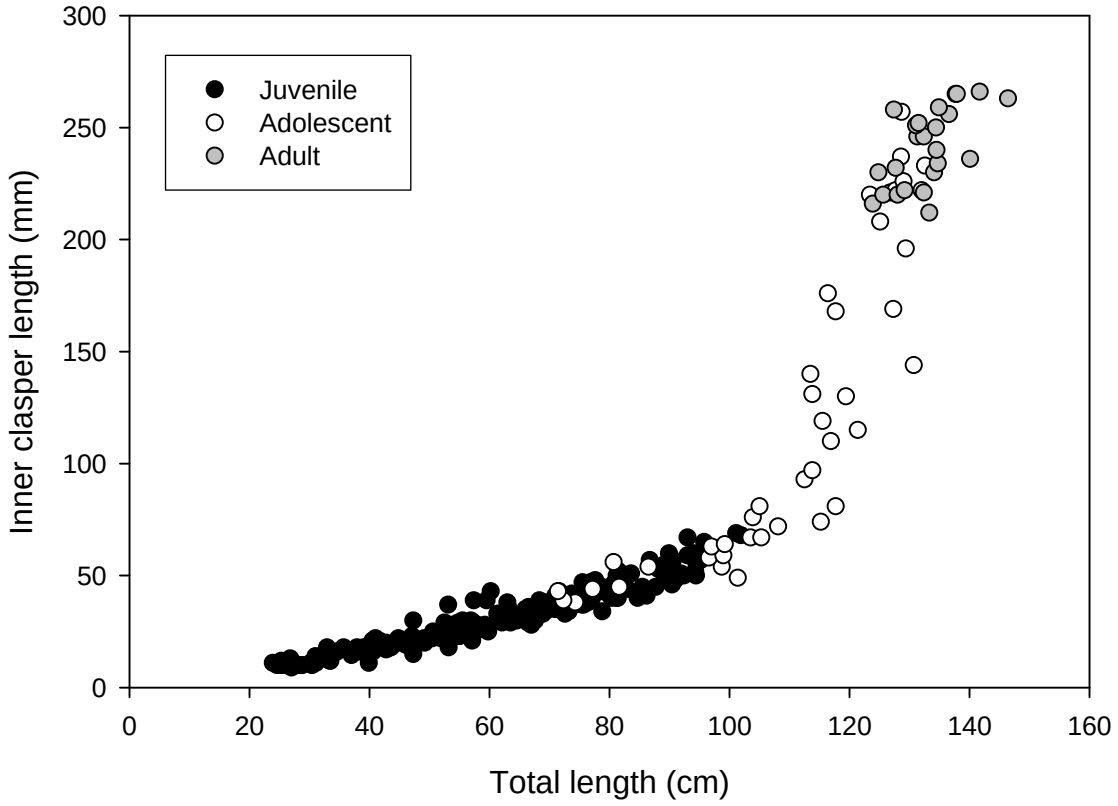

Fig. 28. Relationship between inner clasper length and total length based on reproductive classification of 278 male *Bathyraja aleutica*.

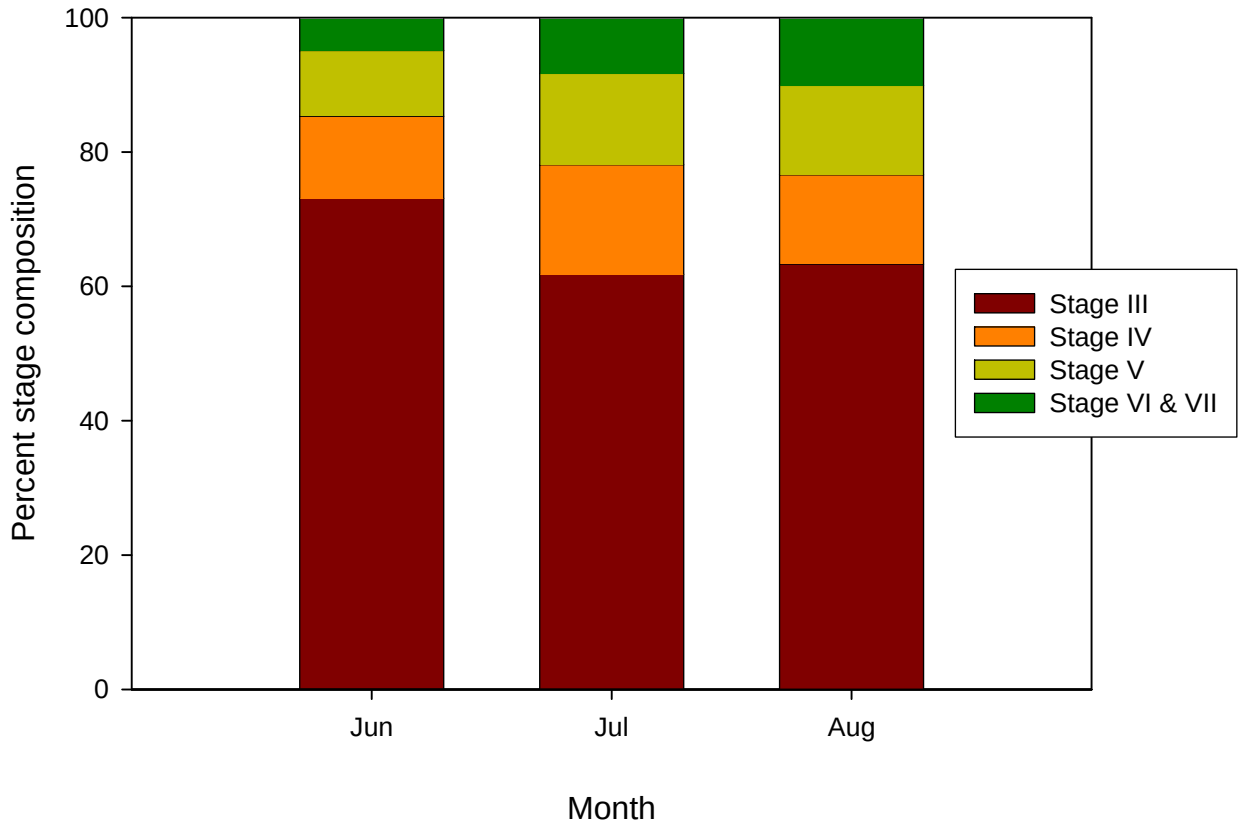

Fig. 29. Monthly changes in spermatogenesis in male *Bathyraja aleutica* (*n*=11). The percent stage composition is the mean proportion of each stage occupied along a transect line across one representative full lobe cross section of a testis.

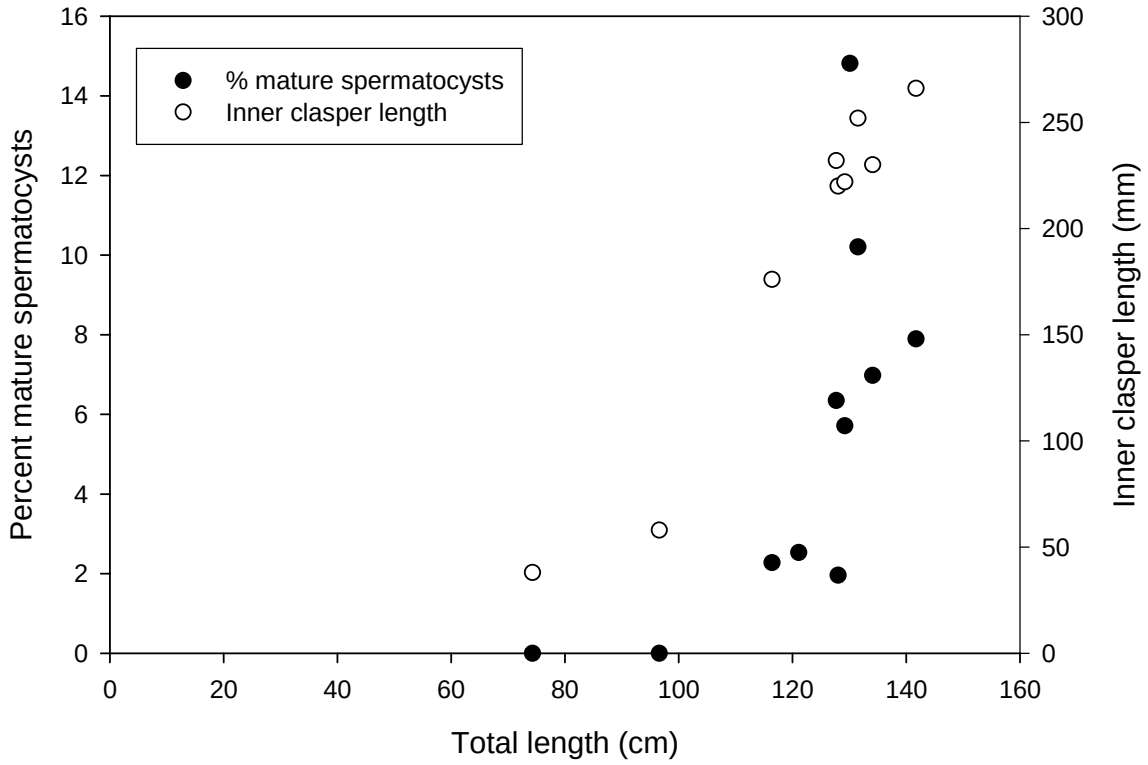

Fig. 30. Relationship between proportion of mature spermatocysts, inner clasper length, and total length based on histological examination of 11 mature male *Bathyraja aleutica*.

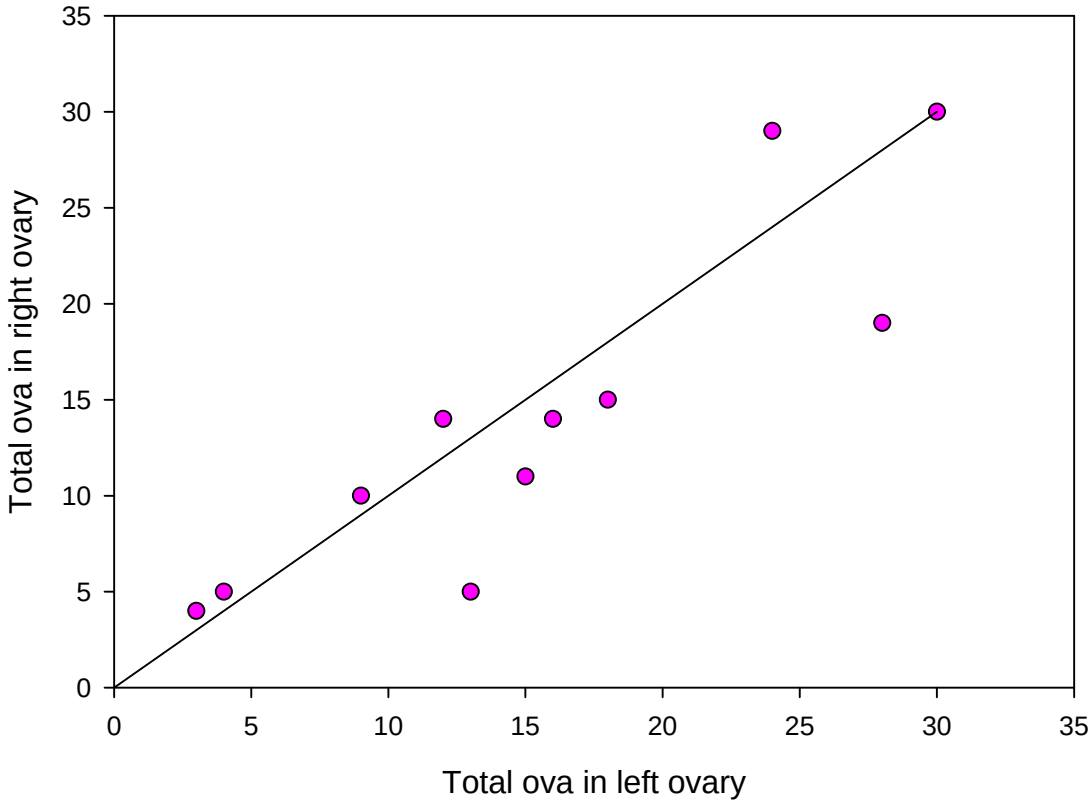

Fig. 31. Comparison between total number of ova in left and right ovaries based on the examination of 11 mature female *Bathyraja aleutica*. The 45º line represents 1:1 agreement between number of ova.

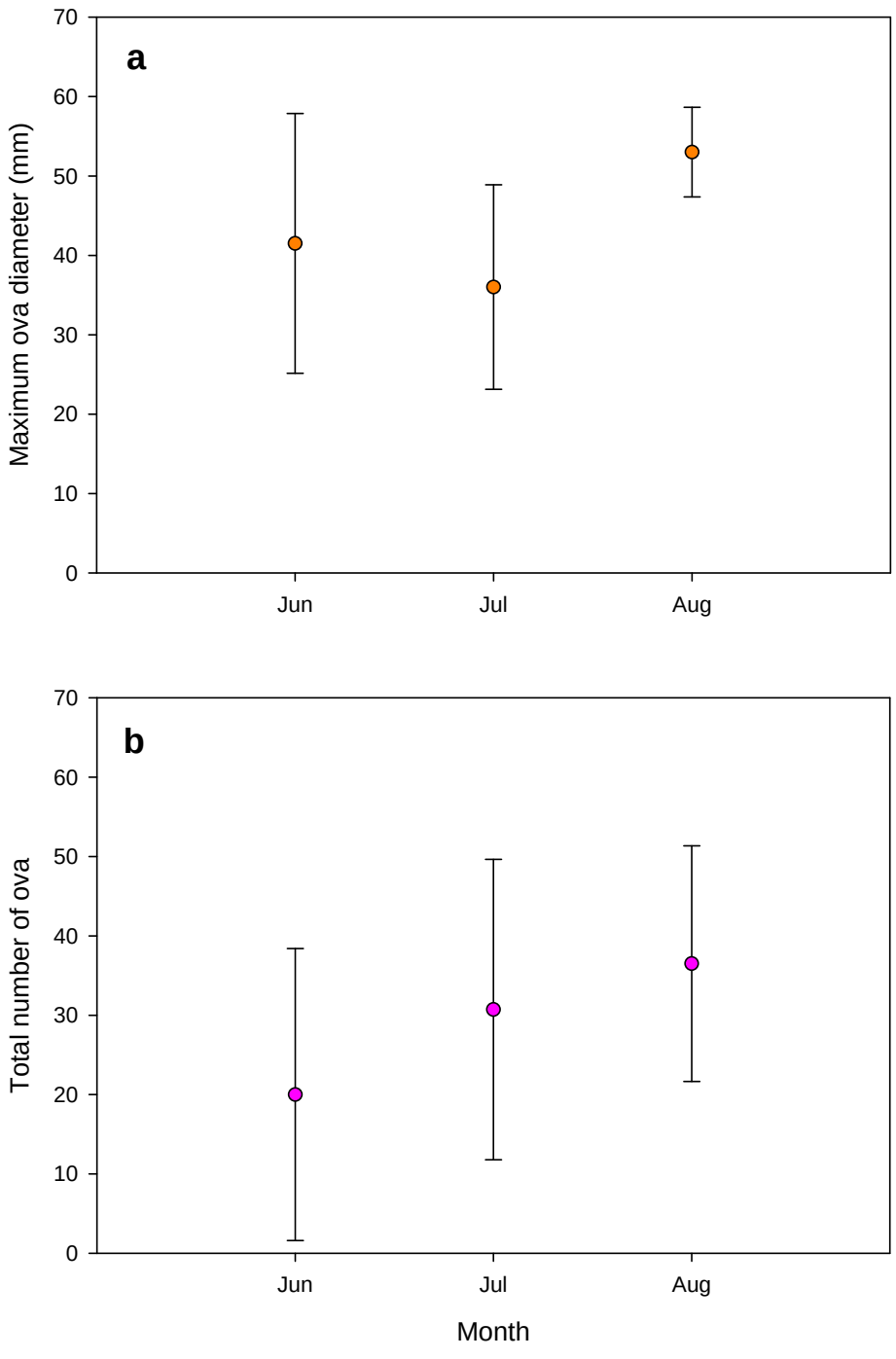

Fig. 32. Relationships between mean maximum ova diameter (**a**; *n*=11) and total number of ova (**b**; *n*=11) by month based on the examinations of mature female *Bathyraja aleutica*. Error bars represent ± one standard deviation.

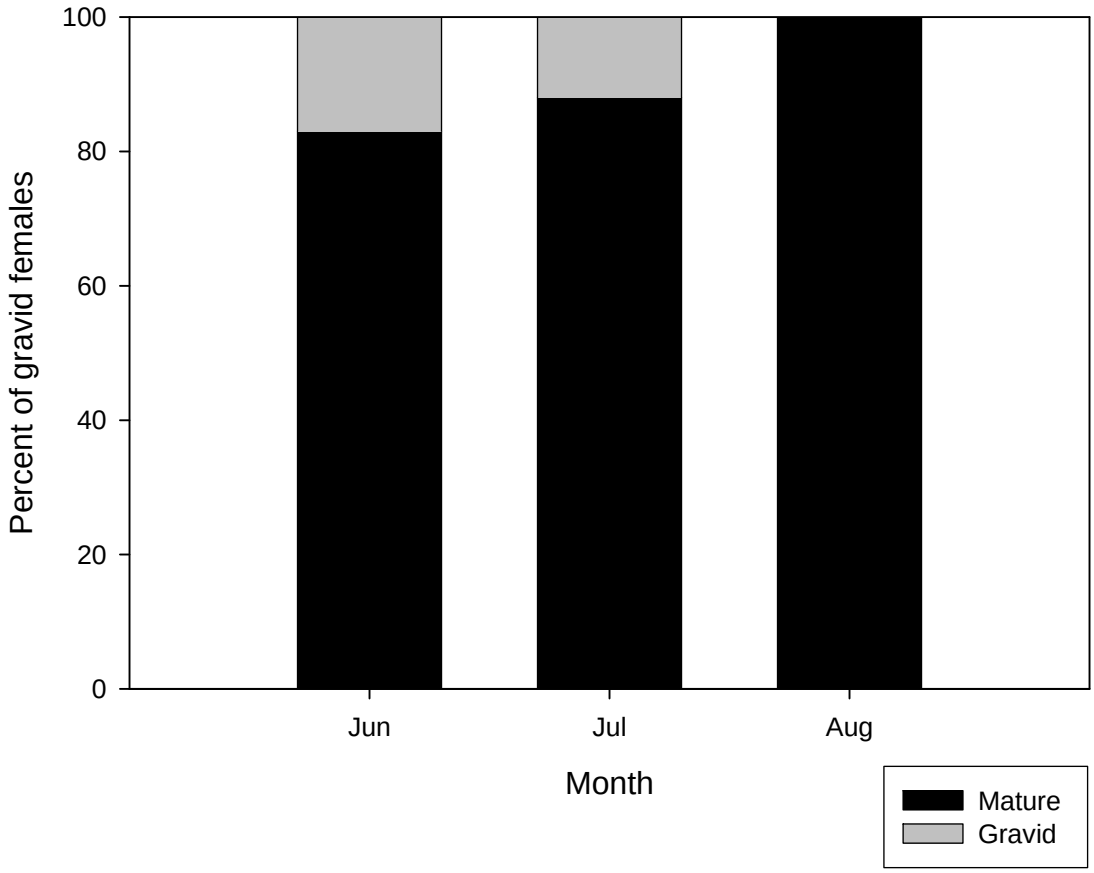

Fig. 33. The percentage of gravid *Bathyraja aleutica* among sampled months.

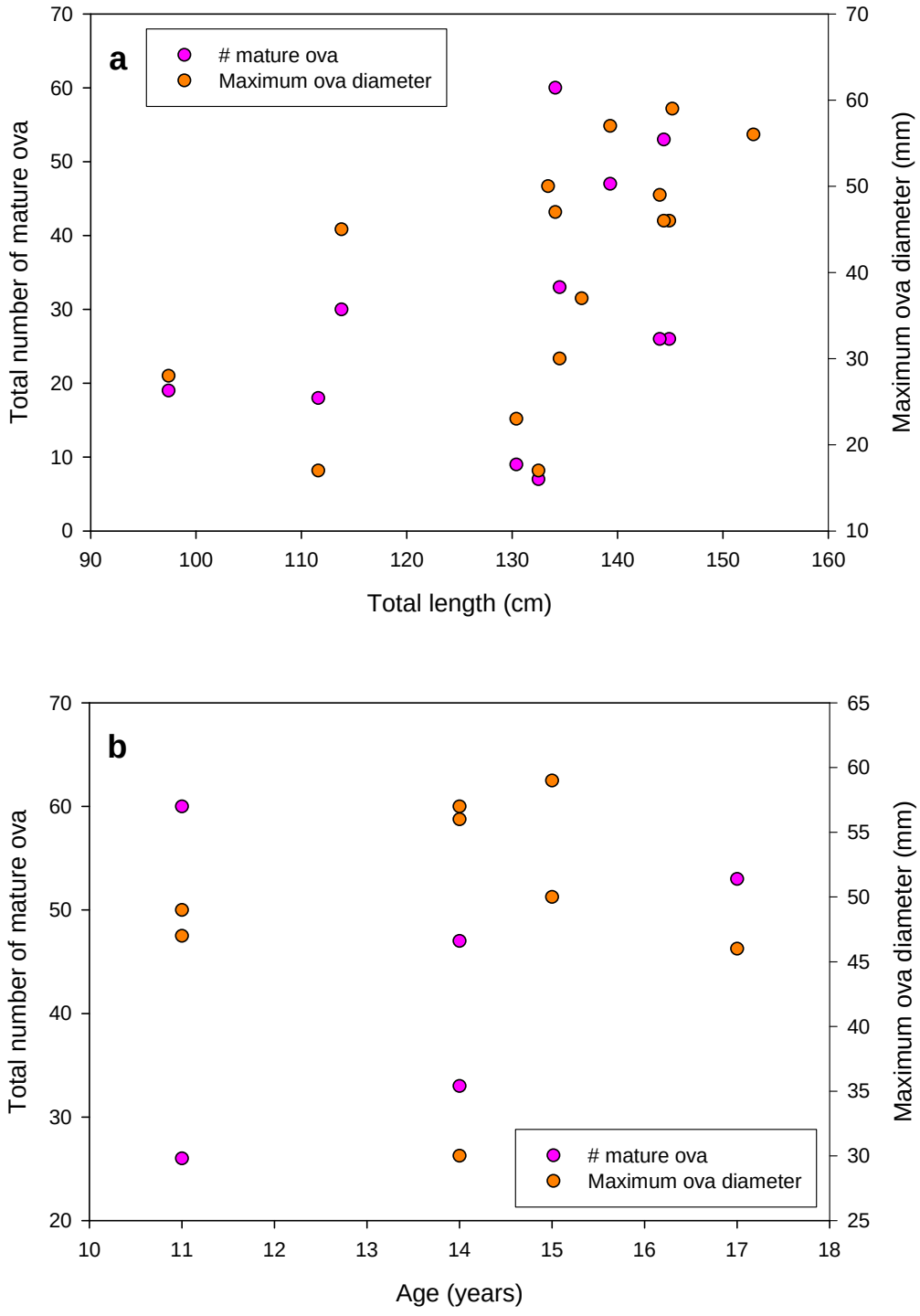

Fig. 34. The relationships between number of mature ova (n=11) or maximum ova diameter (n=15) and total length **(a)**, and between number of mature ova (n=5) or maximum ova diameter (n=8) and age **(b)** for *Bathyraja aleutica.*

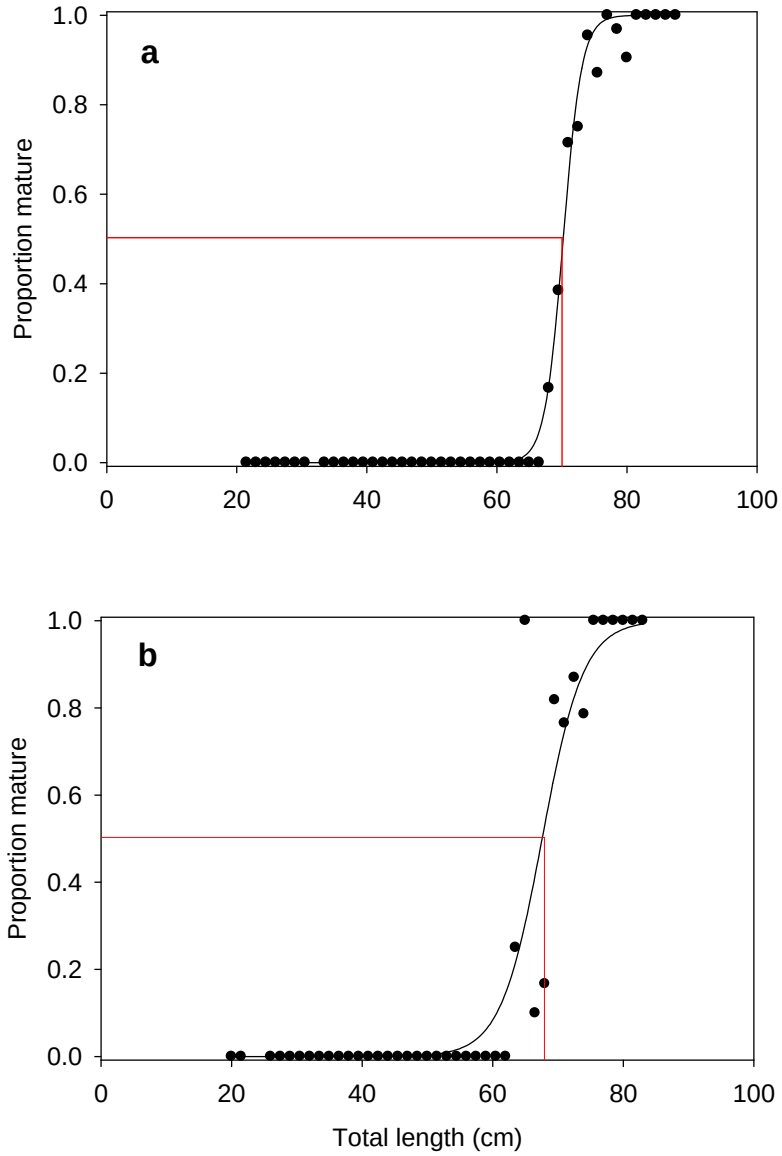

Fig. 35. Estimated median size at maturity for female **(a)** and male **(b)** *Bathyraja interrupta* from the Gulf of Alaska. Median size at maturity corresponds to 70.2 and 67.6cm TL for females and males, respectively.

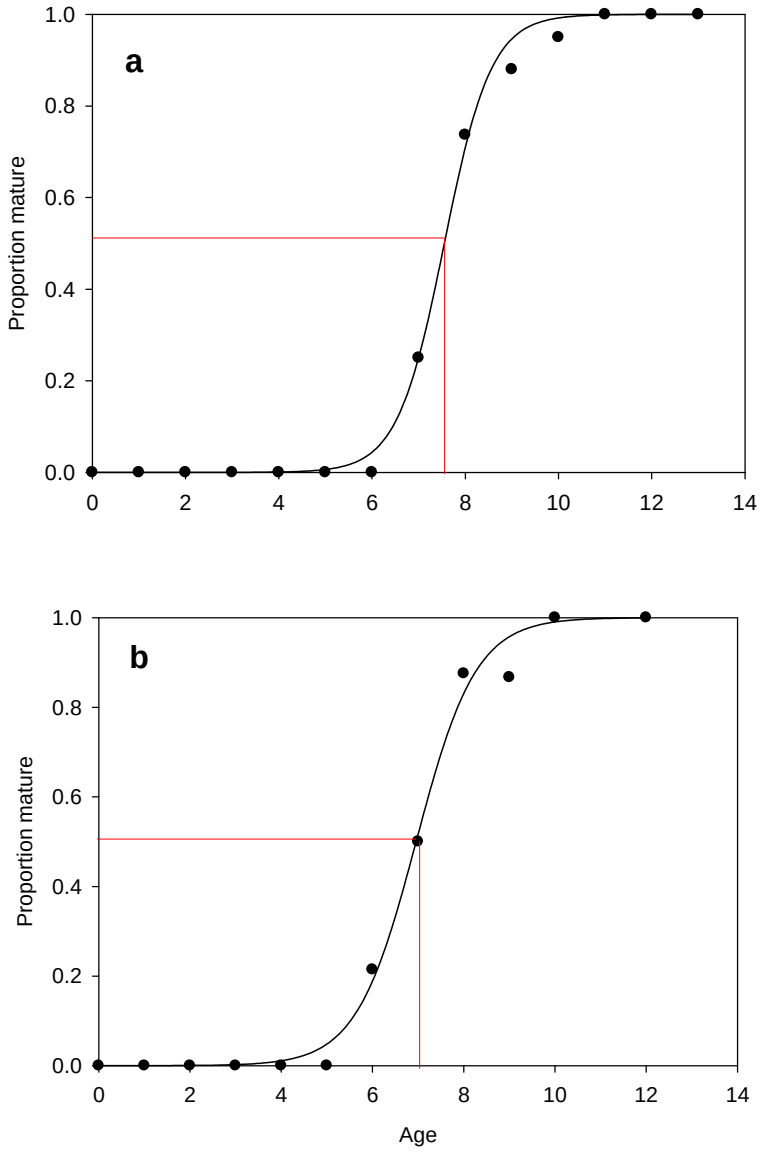

Fig. 36. Estimated median age at maturity for female **(a)** and male **(b)** *Bathyraja interrupta* from the Gulf of Alaska. Median size at maturity corresponds to 7.5 and 7 years for females and males, respectively.

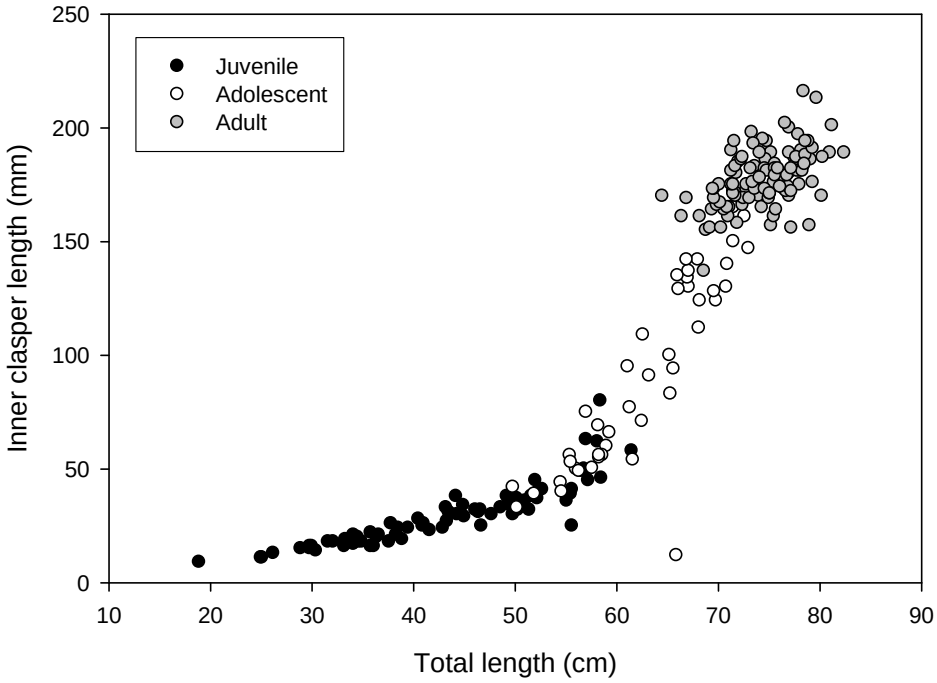

Fig. 37. Relationship between clasper length and total length based on the reproductive classifications of *Bathyraja interrupta* (*n*=261).

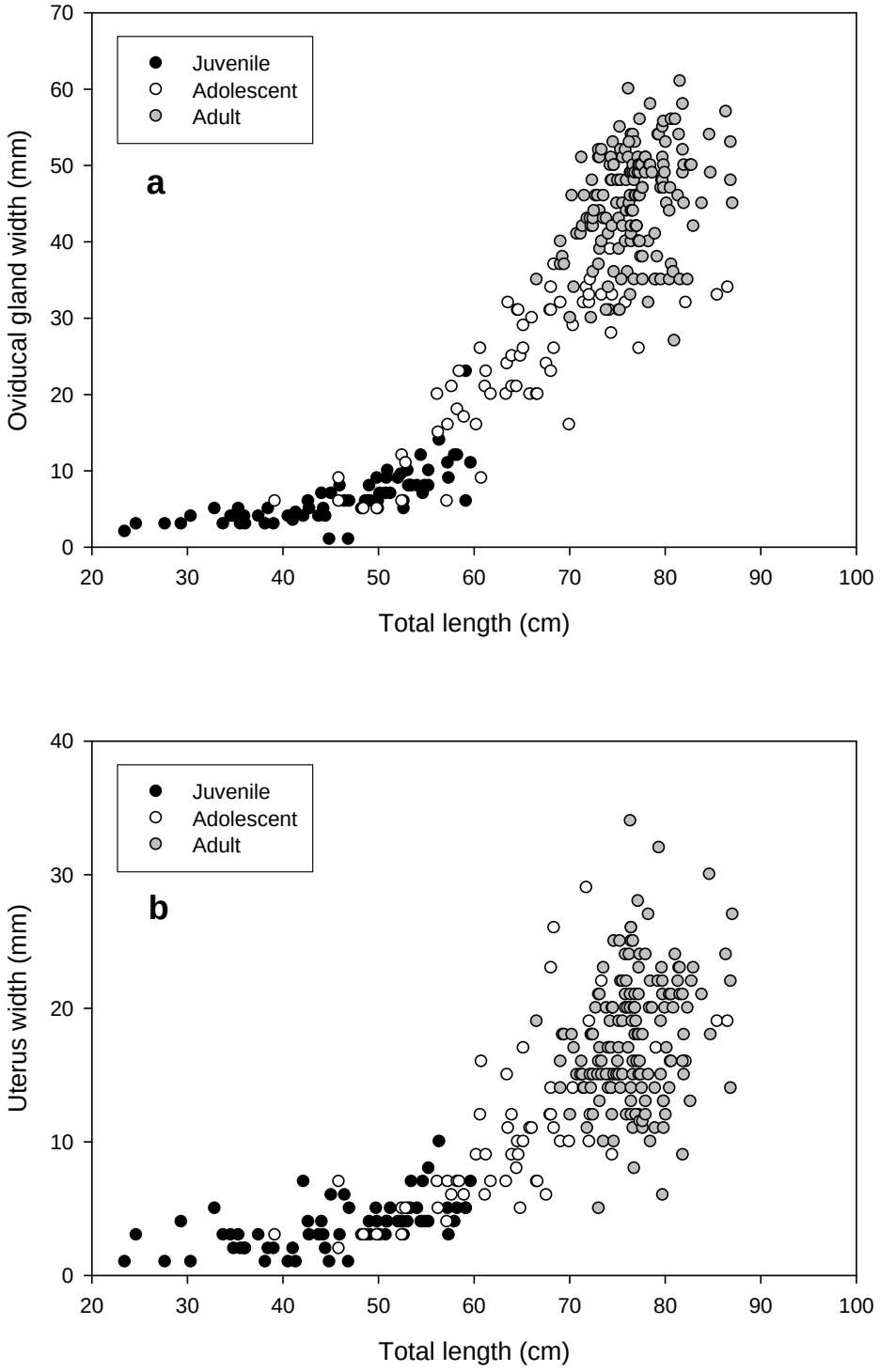

Fig. 38. Relationship between oviducal gland width (**a**; *n*=297) and uterus width (**b**; *n*=287) with total length based on the reproductive classifications of *Bathyraja interrupta*.

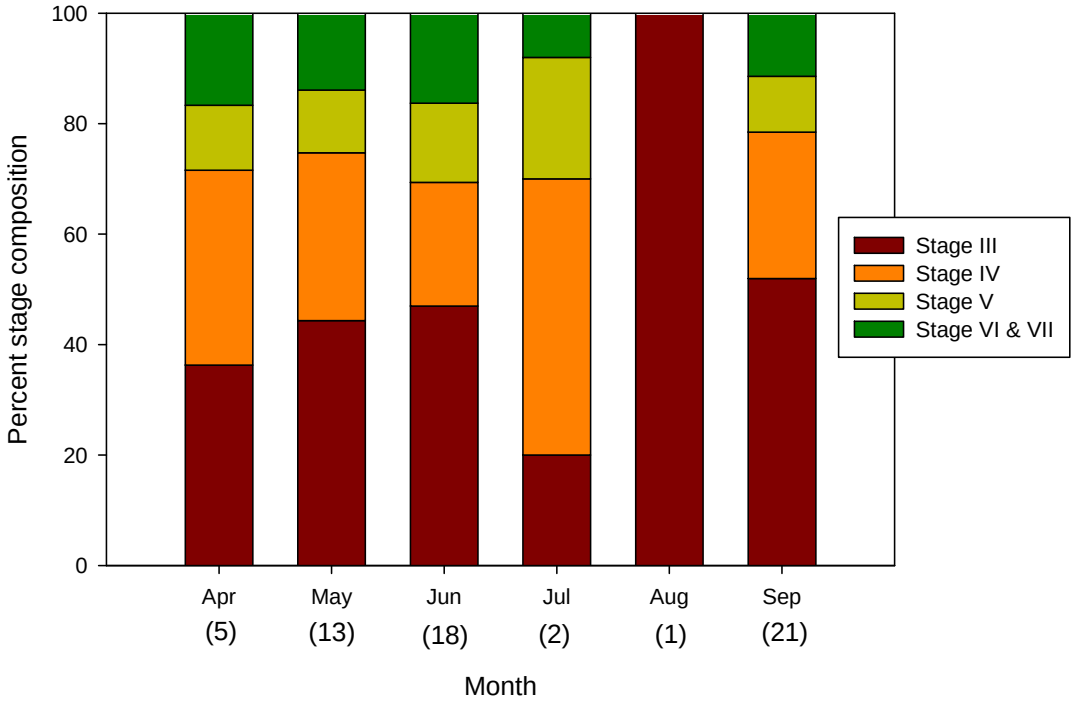

Fig. 39. Percent stage compositions of spermatocysts by month for *Bathyraja interrupta*. Sample sizes are presented in parentheses.

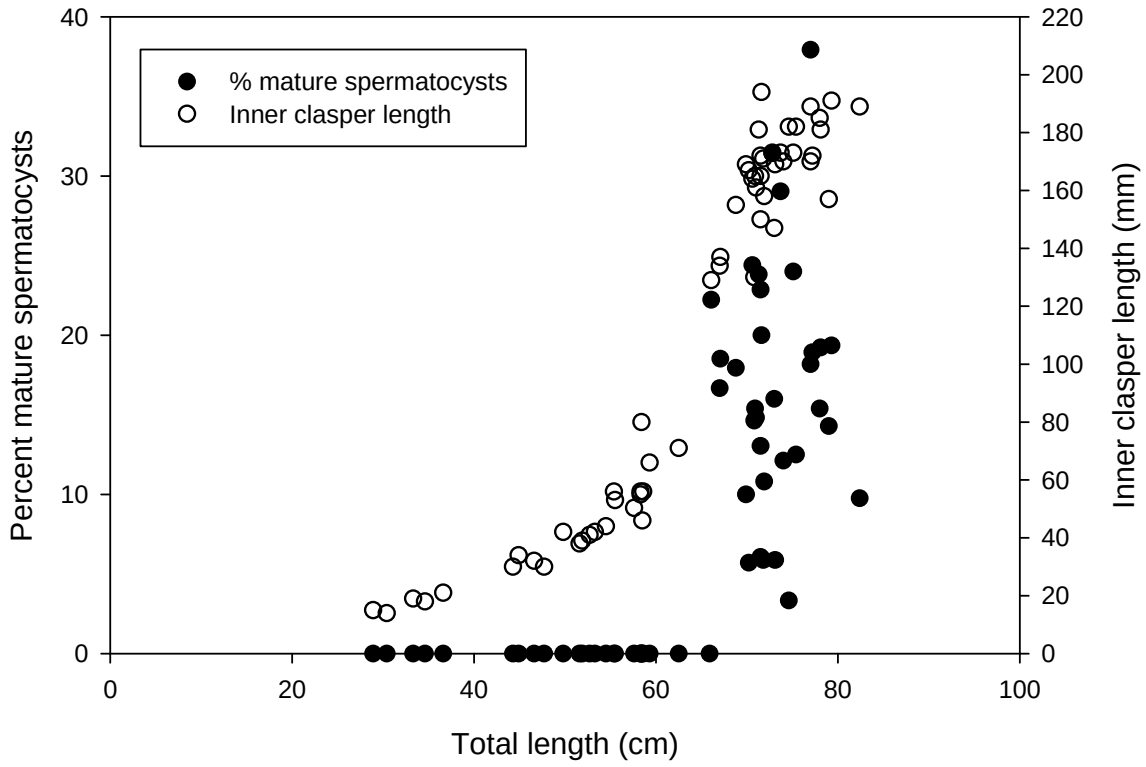

Fig. 40. Relationships between the percent of mature spermatocysts and total length as well as inner clasper length and total length for *Bathyraja interrupta* (*n*=60).

No difference was found in the mean number of mature ova in the left and right ovaries (paired t-test: $t = -0.226$, $p = 0.82$, $n = 122$). A one-way ANOVA, followed by Tukey's post-hoc test found significant differences in the mean number of mature ova among months ($F = 14.28$, $p < 0.0001$, $n = 122$) (Fig. 41a). All months were found to be significantly different from each other except April and August ($p = 1.00$), May and June ($p = 0.30$), May and July ($p = 0.30$), and June and July ($p = 1.00$). There was a significant difference found among months (KW $X^2 = 14.46$, df = 5, $p = 0.01$). The mean diameter was significantly smaller in September than all five preceding months ($Q = 3.01$, $Q_{0.05, 6} = 2.94$, $p < 0.05$). All comparisons between months April through August found no significant differences (Fig. 41b). A Chi-square (χ^2) test comparing the proportion of mature females with developing egg cases *in utero* failed to reject the null hypothesis of equal proportions among months ($X^2 = 9.0$, $p > 0.10$, $n = 182$) (Fig. 42).

No relationship was found between TL or age of the mature female and the number of mature ova (Fig. 43a) (TL: $r^2 = 0.15$, $p < 0.0001$, $n = 122$; Age: $r^2 = 0.02$, $p = 0.25$, $n = 57$) or the greatest ova diameter respectively (TL: $r^2 = 0.008$, $p = 0.24$, $n = 166$; Age: $r^2 = 0.003$, $p = 0.70$, $n = 58$) (Fig. 43b).

Raja binoculata. Female *R. binoculata* attained maturity at greater sizes than males. TL_{50} was estimated as 148.6 and 119.2 cm TL for females and males, respectively (Fig. 44). No gravid females were observed. Among females, the smallest mature specimen was 125.8 cm TL and the largest immature individual was 139.1 cm TL. The smallest mature male was 124.0 cm TL and the largest immature male was 126.1 cm TL. All males examined that were greater than 127.0 cm TL were determined to be mature.

Gradual increases in the relationship between the width of female reproductive organs and specimen TL generally coincided with the onset of maturity among female *R. binoculata*. A notable increase in the relationship between oviducal gland width and TL was observed at approximately 100 cm TL (Fig. 45a). Oviducal gland widths of mature (adult) individuals ranged from approximately 50 to 125 mm TL. Uterus widths increased markedly among specimens in excess of 140 cm TL, but were also associated with high variability among specimens (Fig. 45b). Considerable overlap was observed among groups based on their maturity classifications and both oviducal gland width and uterus width in relation to TL.

A gradual increase in the proportion of clasper length to TL was evident between approximately 99 and 119 cm TL indicating the onset of male sexual maturity in male *R. binoculata* (Fig. 46). Clasper lengths of specimens classified as juveniles did not exceed 100 mm. Mature males were found to have clasper lengths that exceeded 200 mm in length.

Testes samples for histological analysis of *Raja binoculata* were collected from three months: April, August, and September. Examination of histological stages III through VI of spermatogenesis did

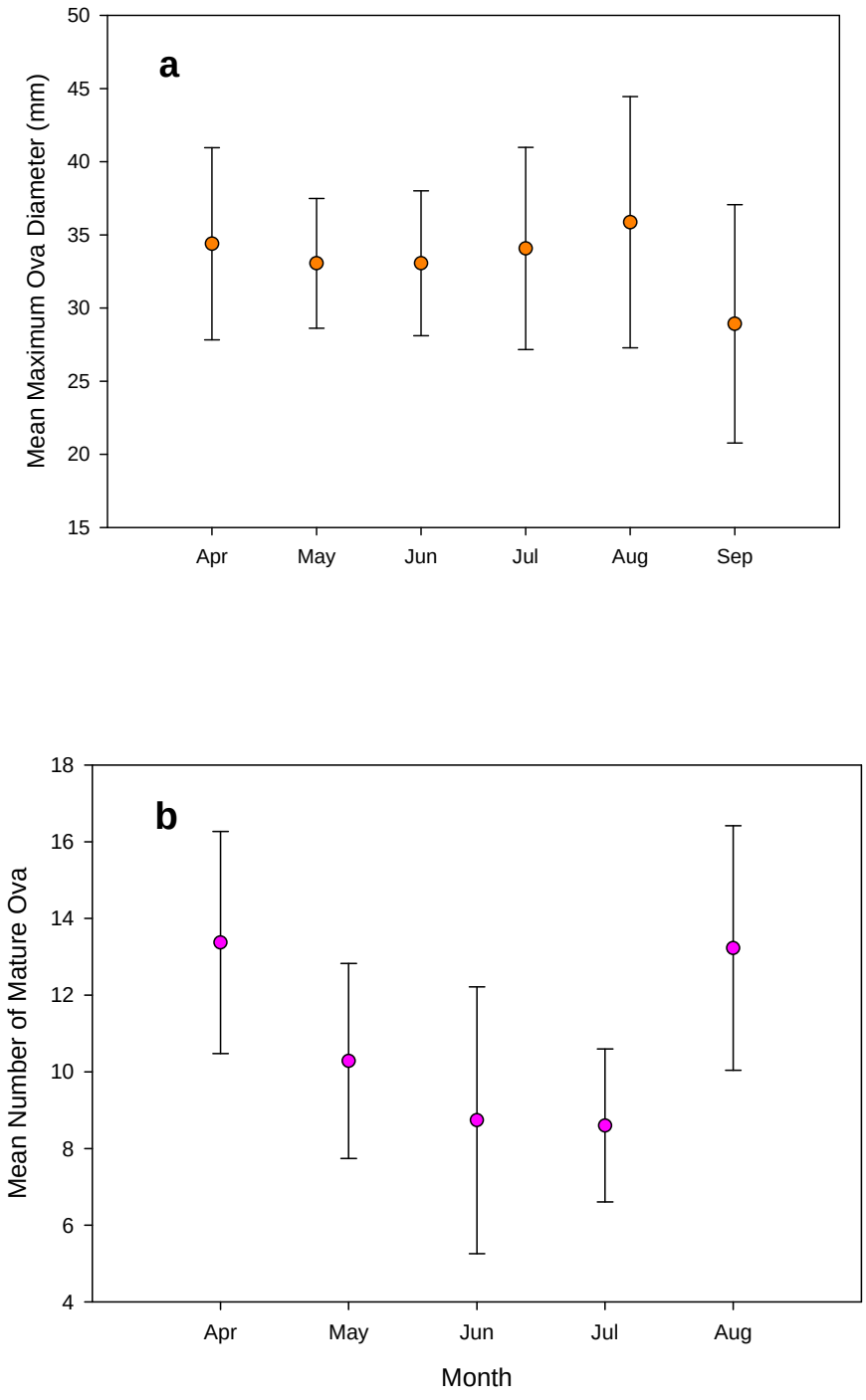

Fig. 41. Relationships between the mean maximum ova diameter (**a**) and mean number of mature ova (**b**) among months based on the examination of mature female *Bathyraja interrupta* (*n*=122). Error bars represent ± one standard deviation.

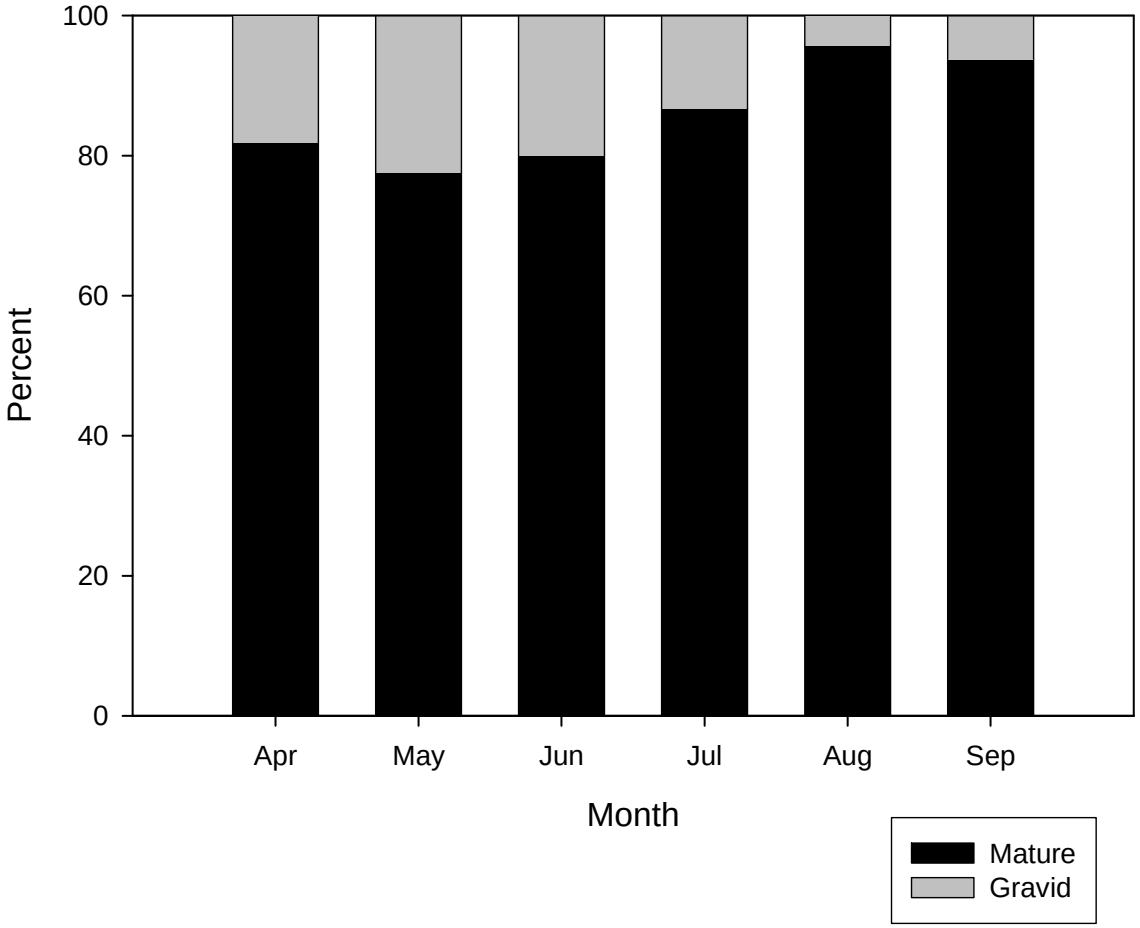

Fig. 42. The percentage of gravid *Bathyraja interrupta* among sampled months.

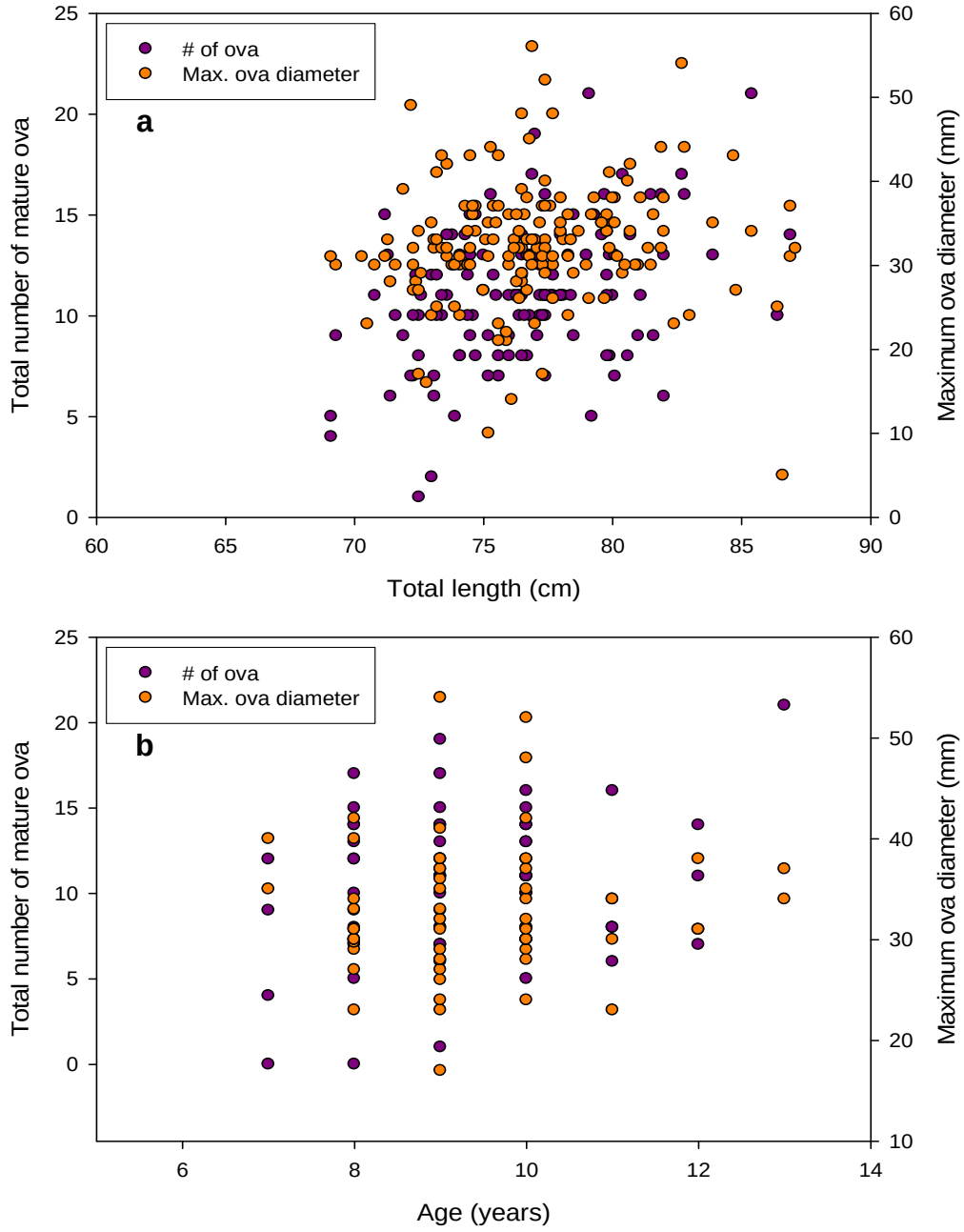

Fig. 43. Relationships between maximum ova diameter (**a**; *n*=167) and total number of mature ova (**b**; *n*=122) with total length for mature female *Bathyraja interrupta*.

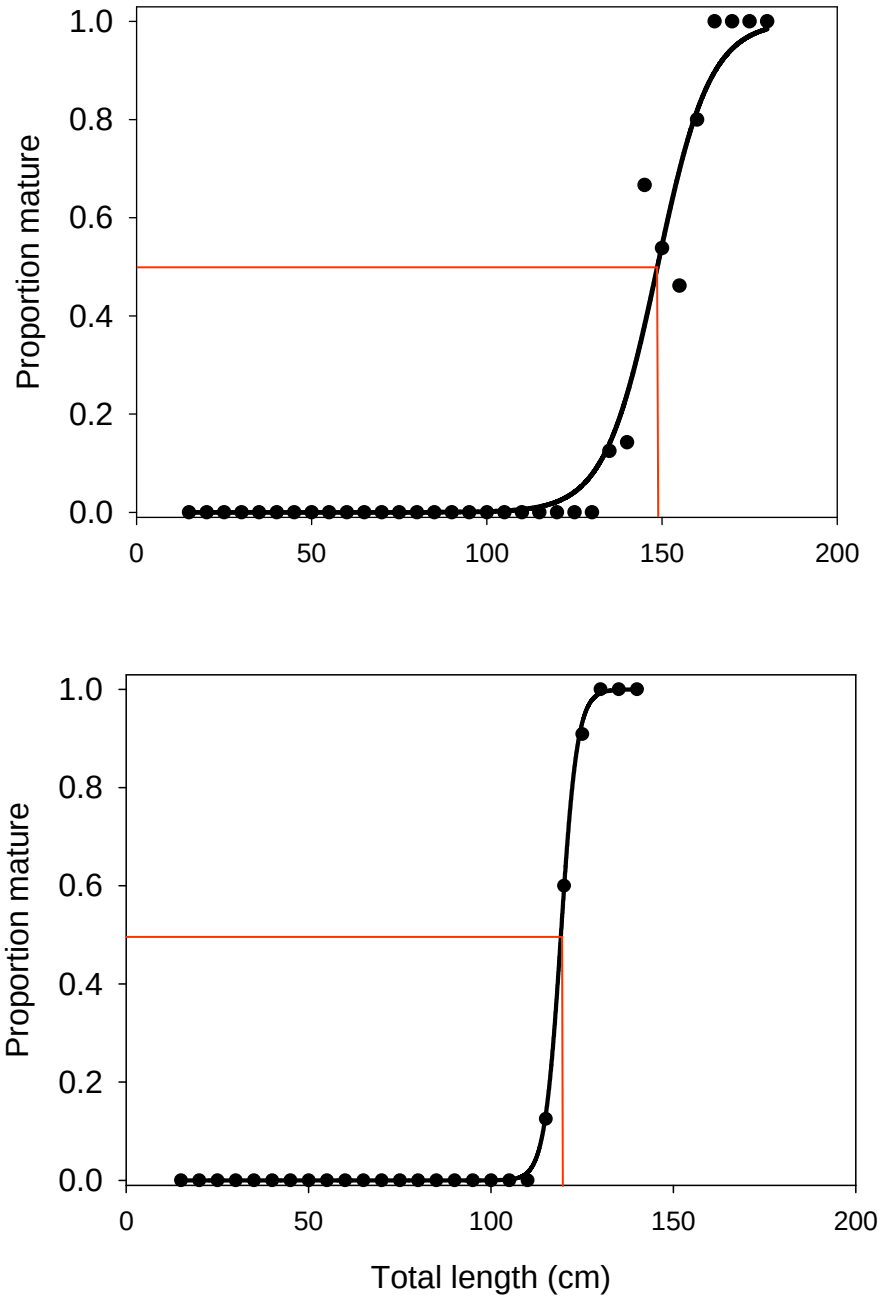

Fig. 44. Estimated median size at maturity for female (*n*=297; **a**) and male (*n*=138; **b**) *Raja binoculata*. Size at 50% maturity corresponds to 148.6 and 119.2 cm TL for females and males, respectively.

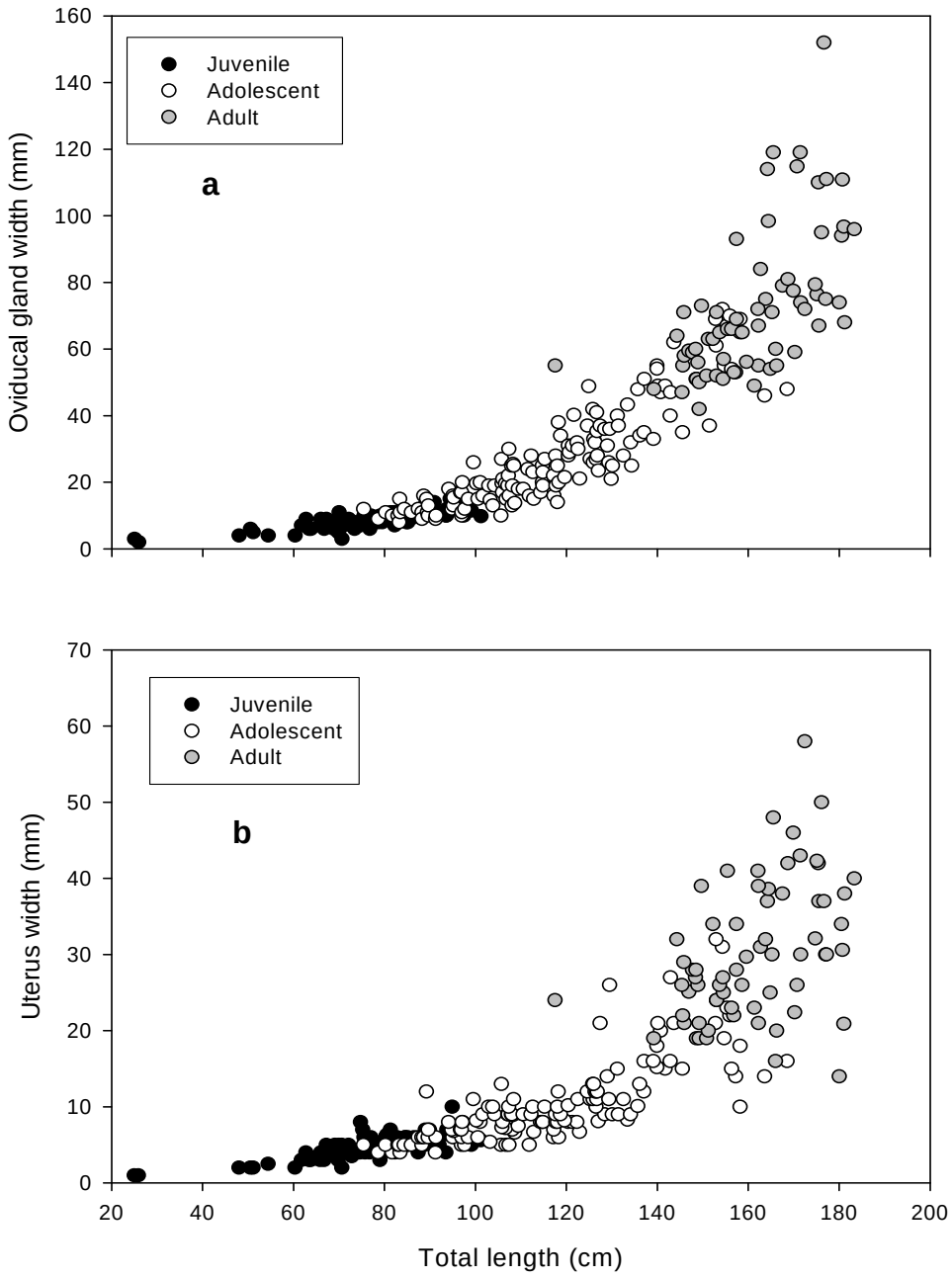

Fig. 45. Relationships between oviducal gland width (**a**; *n*=292) and uterus width (**b**; *n*=277) with total length based on the reproductive classifications of *Raja binoculata*.

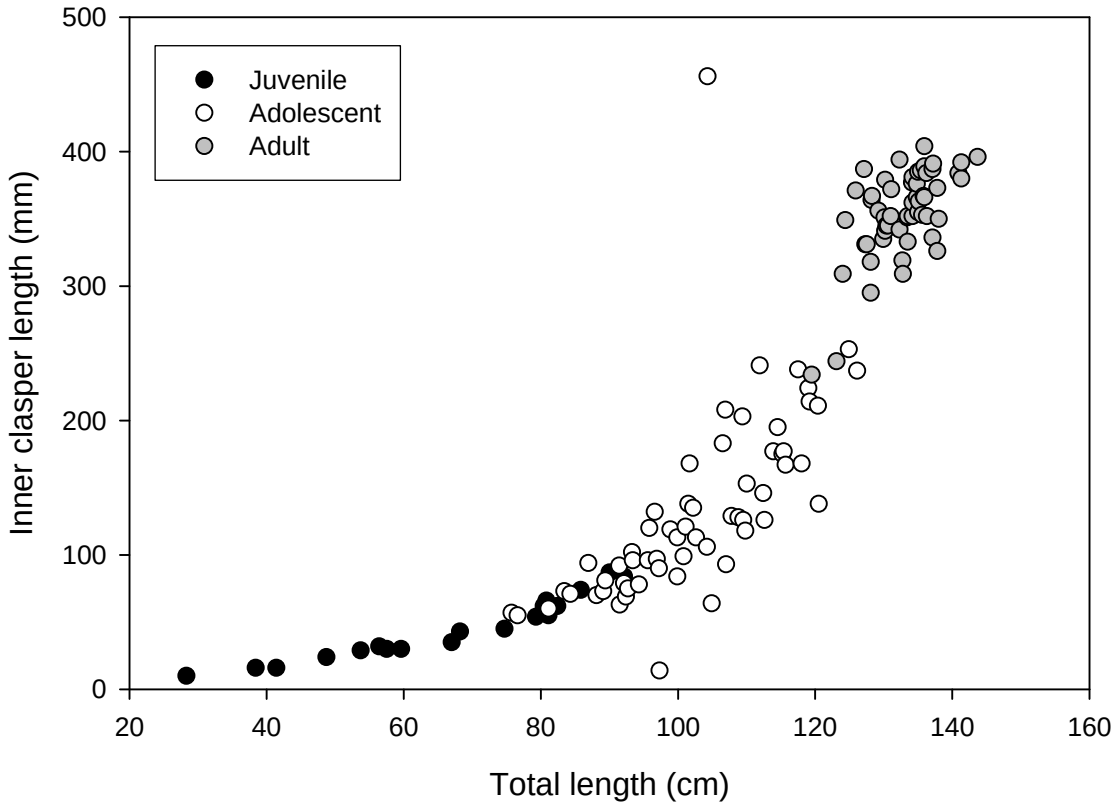

Fig. 46. Relationship between clasper length and total length based on the reproductive classification of 135 *Raja binoculata*.

not reveal any significant differences in the relative proportion of these four stages among the three months sampled (Fig. 47). The production and maintenance of mature spermatocysts within the testes appears to persist during these three months. There did not appear to be any notable reduction of mature spermatocysts between the spring (April) and late summer (August and September) months. The percentage increase in mature spermatocysts corresponded closely with clasper development (Figure 48).

Raja rhina. Female *R. rhina* were found to mature at slightly greater sizes than males. TL_{50} was estimated as 113.1 cm TL for females and 102.9 cm TL in males (Fig. 49). The smallest mature female measured 102.2 cm TL and the largest immature female was 123.0 cm TL. The smallest male classified as mature (adult) was 101.0 cm TL and the largest adolescent male (immature) examined measured 111.2 cm TL.

Oviducal gland width and uterus width to TL relationships revealed sharp increases in size of these reproductive organs at or near 110 cm TL among female *R. rhina* (Fig. 50a). Oviducal gland widths of approximately 40 mm or greater were measured among those females that were assigned maturity status of adults. Greater variability among uterus width to TL and maturity status was more evident than that observed within oviducal gland width to TL relationships. A range of uterine widths of 8 mm to greater than 50 mm was recorded among adult females. Differences among uterus widths between juveniles and adolescents were minimal (Fig. 50b).

No significant trend was detected between maximum ovarian diameter and month among female *R. rhina* (Fig. 51). Average maximum ova diameter values were largest among June specimens. However, variance among specimens and months was high. Among the 74 mature females examined, maximum ova diameters ranged from 10 mm to 57 mm in diameter. Mature ova were observed in females during all months sampled.

No trend was observed between maximum ovarian fecundity and female TL for *R. rhina* (Fig. 52). Ovarian ova were frequently damaged during collection or as a result of extended waits following specimen capture and processing, limiting the number of specimens from which accurate counts could be obtained to 49 individuals. Maximum average ovarian fecundity was highly variable among months. Counts ranged from 2 to 61 ova.

Plots of clasper length to TL showed a notable upward shift in this relationship near 105 cm TL, indicating the onset of maturity among male *R. rhina* (Fig. 53). Specimens classified as adult typically had clasper lengths measuring in excess of 250 mm. Overlap in the clasper size of adolescents and juveniles were evident between 70 and 110 cm TL.

Testes samples for histological analysis of *R. rhina* were collected from five months, between April and September. Examination of histological stages III through VI of spermatogenesis did not reveal

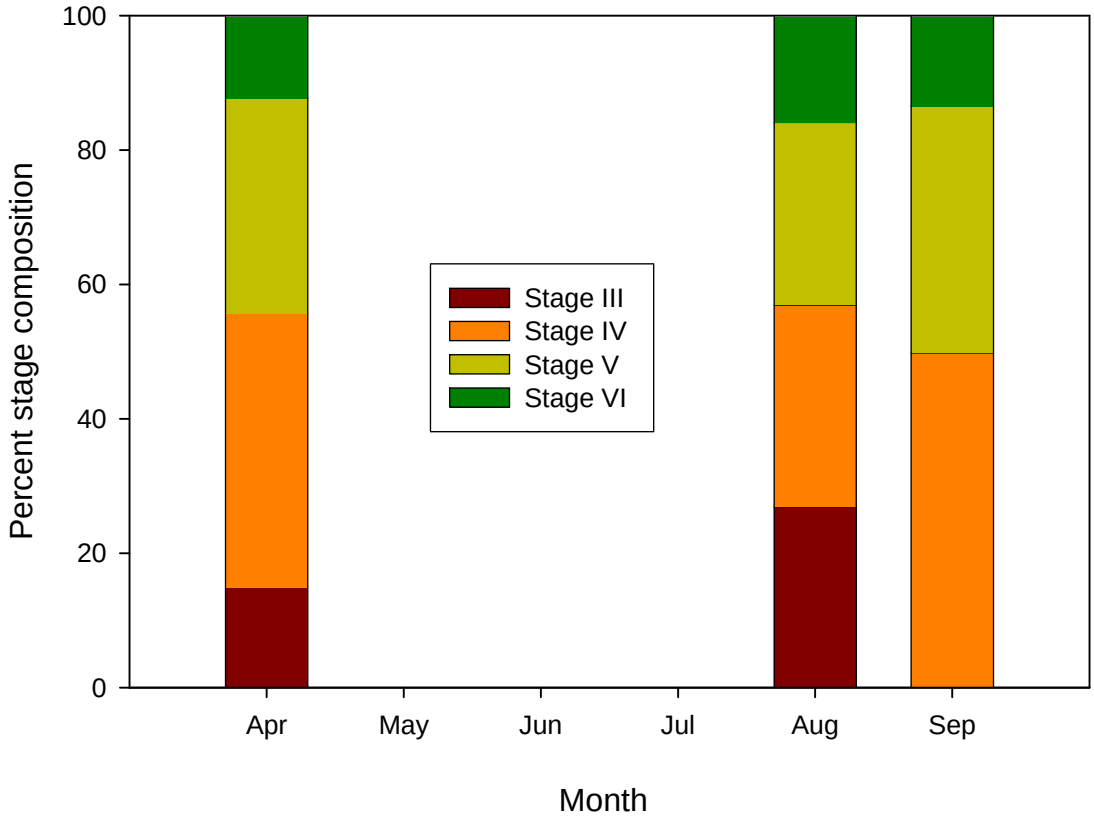

Fig. 47. Monthly changes in spermatogenesis in male *Raja binoculata*. The percent stage composition is the mean proportion of each stage occupied along a transect line across one representative full lobe cross section of a testes, and expressed as the mean. Sample sizes are presented in parentheses.

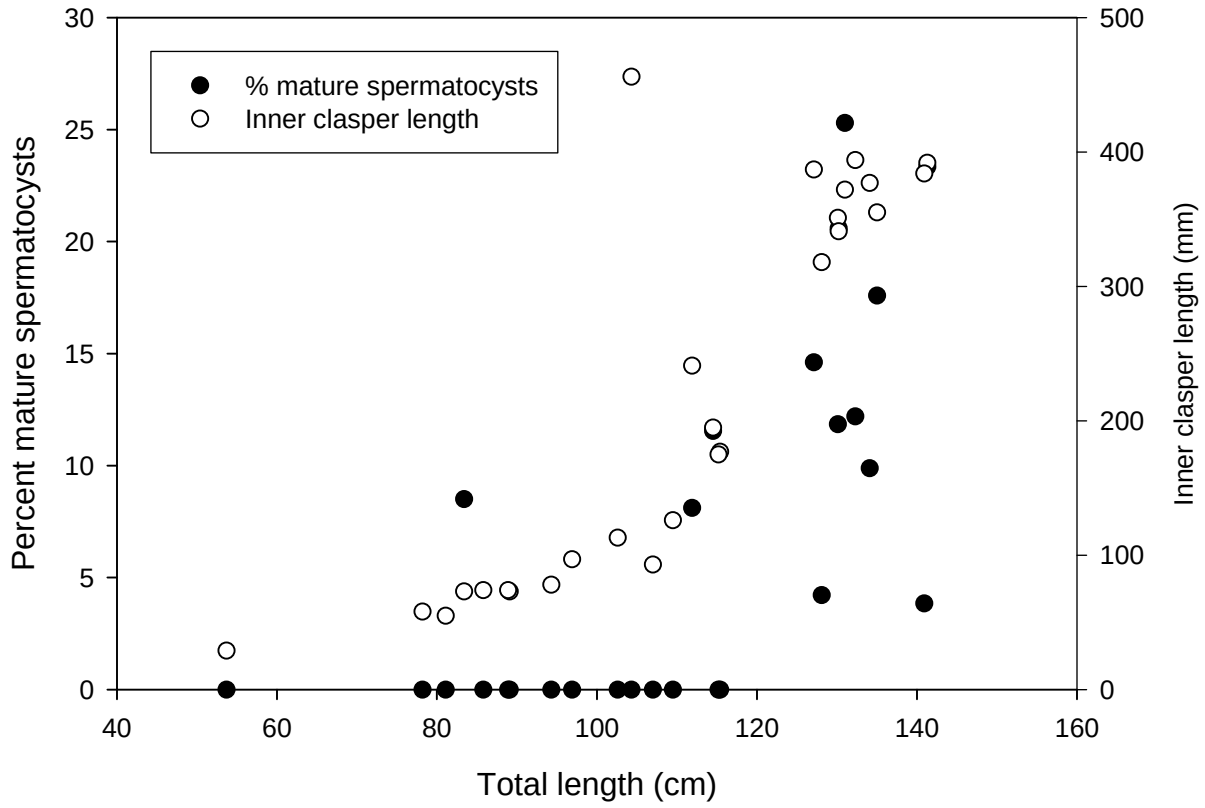

Fig. 48. Relationship between the proportion of mature spermatocysts, inner clasper length, and total length for *Raja binoculata* (*n*=26).

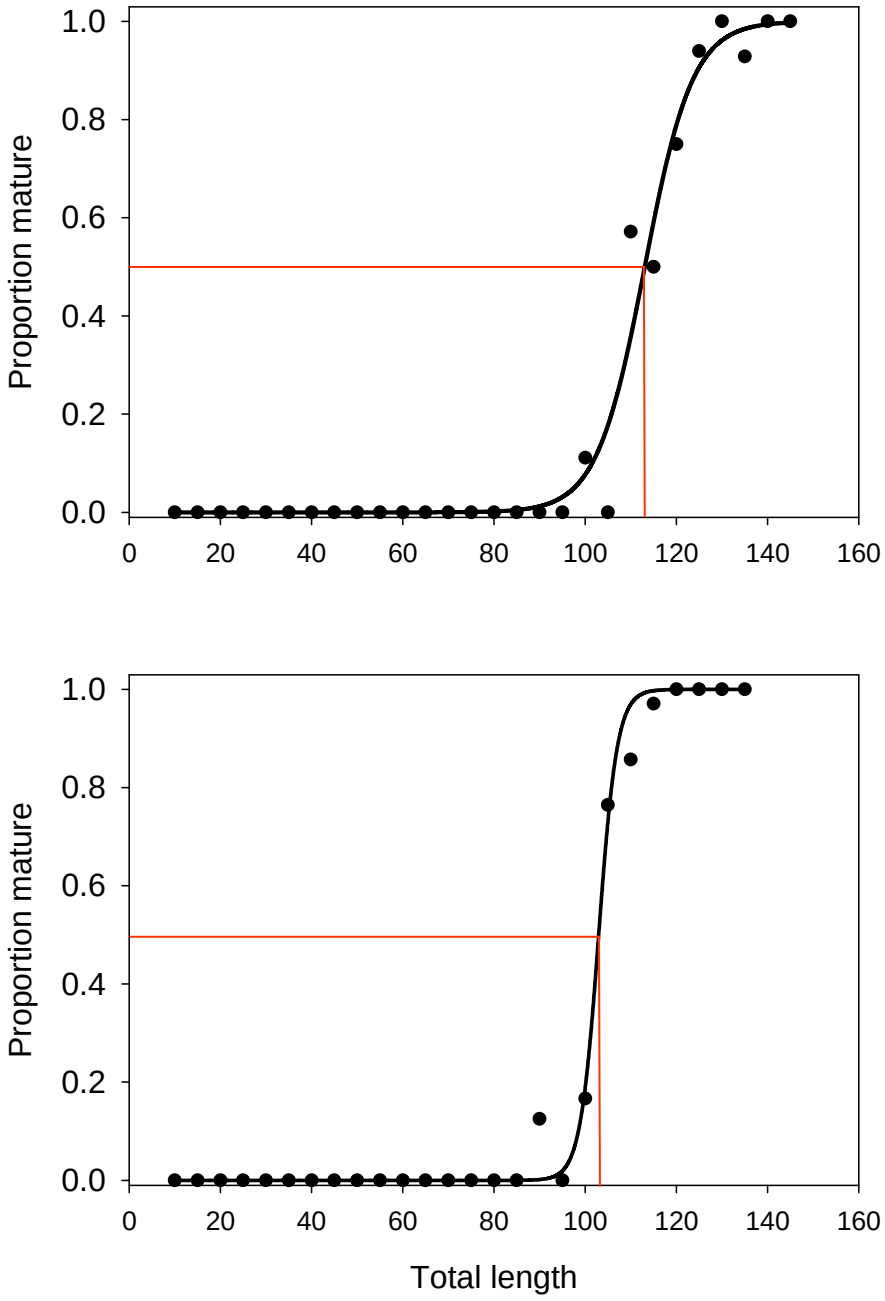

Fig. 49. Estimated median size at maturity for female (*n*=223; **a**) and male (*n*=216; **b**) *Raja rhina*. Size at 50% maturity corresponds to 113.1 and 102.9 cm TL for females and males, respectively.

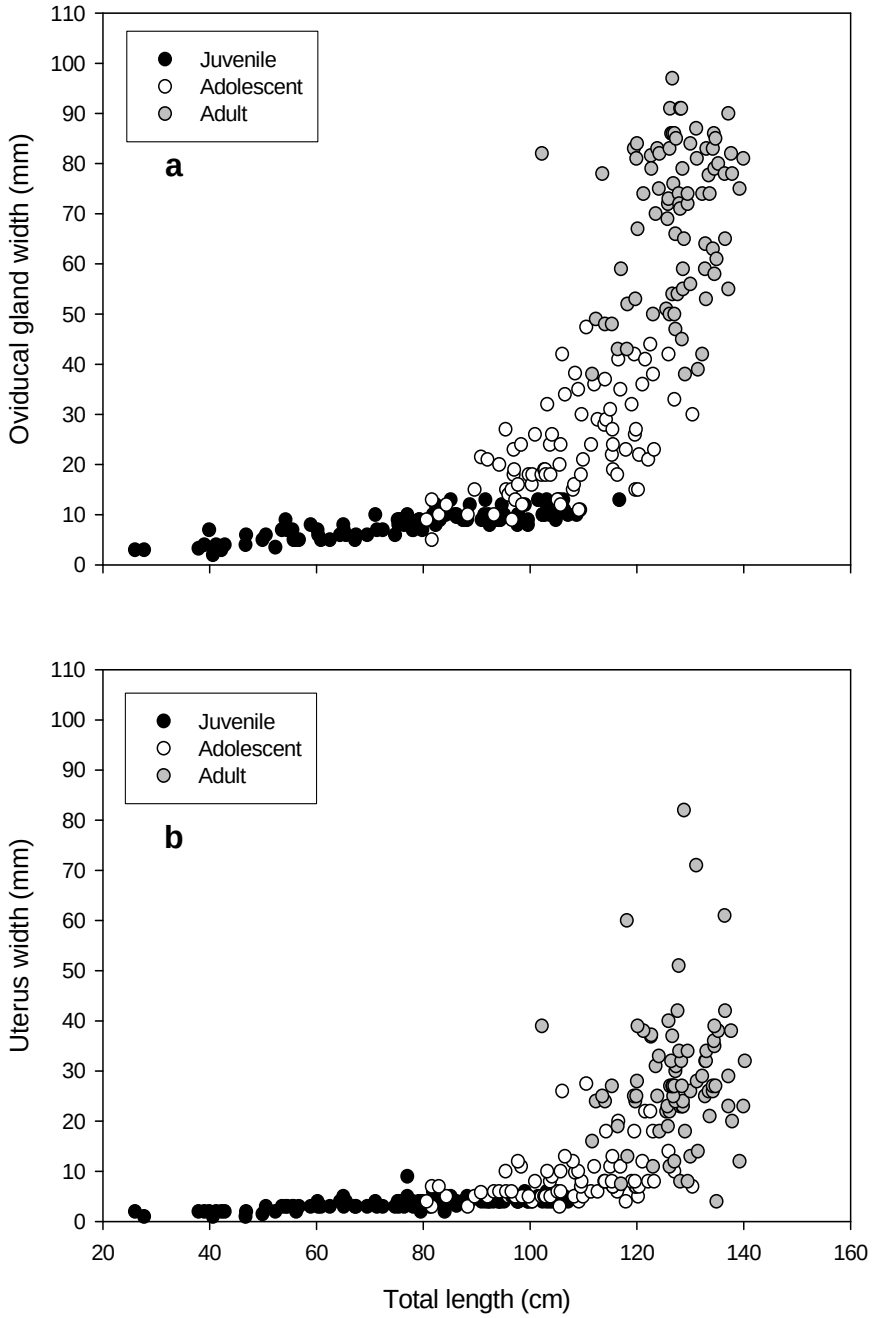

Fig. 50. Relationships between oviducal gland width (**a**; *n*=272) and uterus width (**b**; *n*=269) and total length based on reproductive classifications of *Raja rhina*.

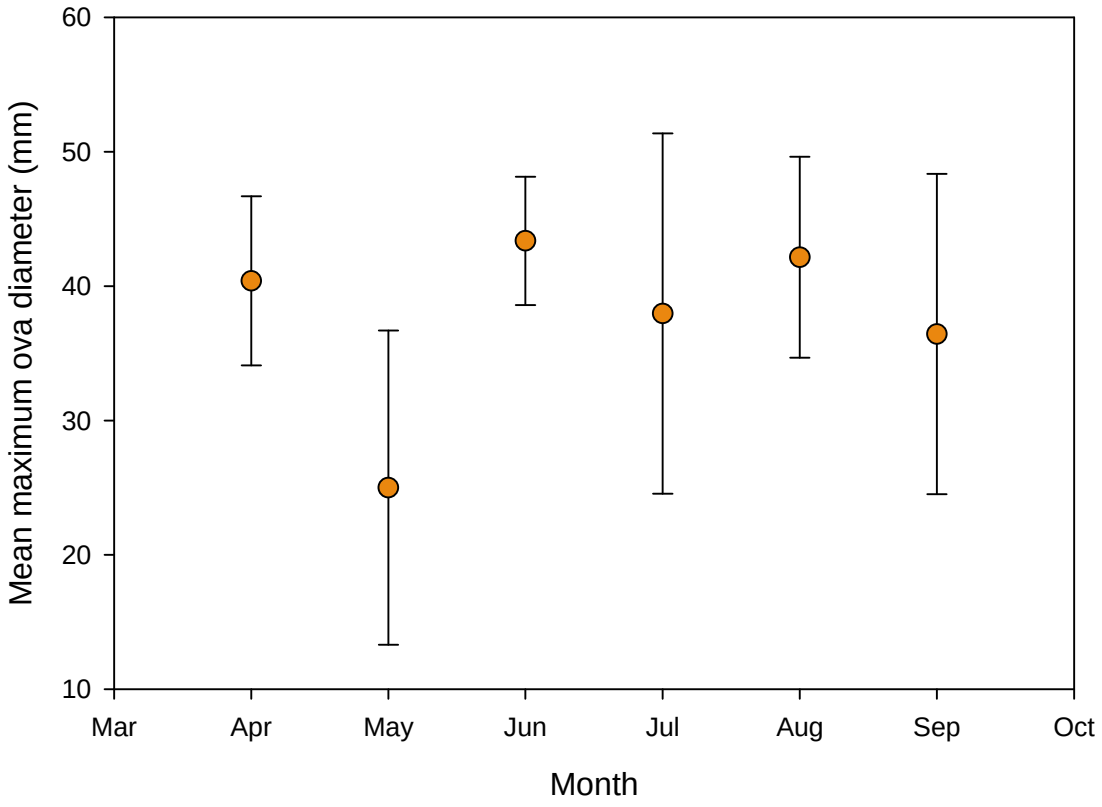

Fig. 51. Relationship between mean maximum ova diameter and month based on the examination of 74 mature *Raja rhina*. Error bars represent ± one standard deviation.

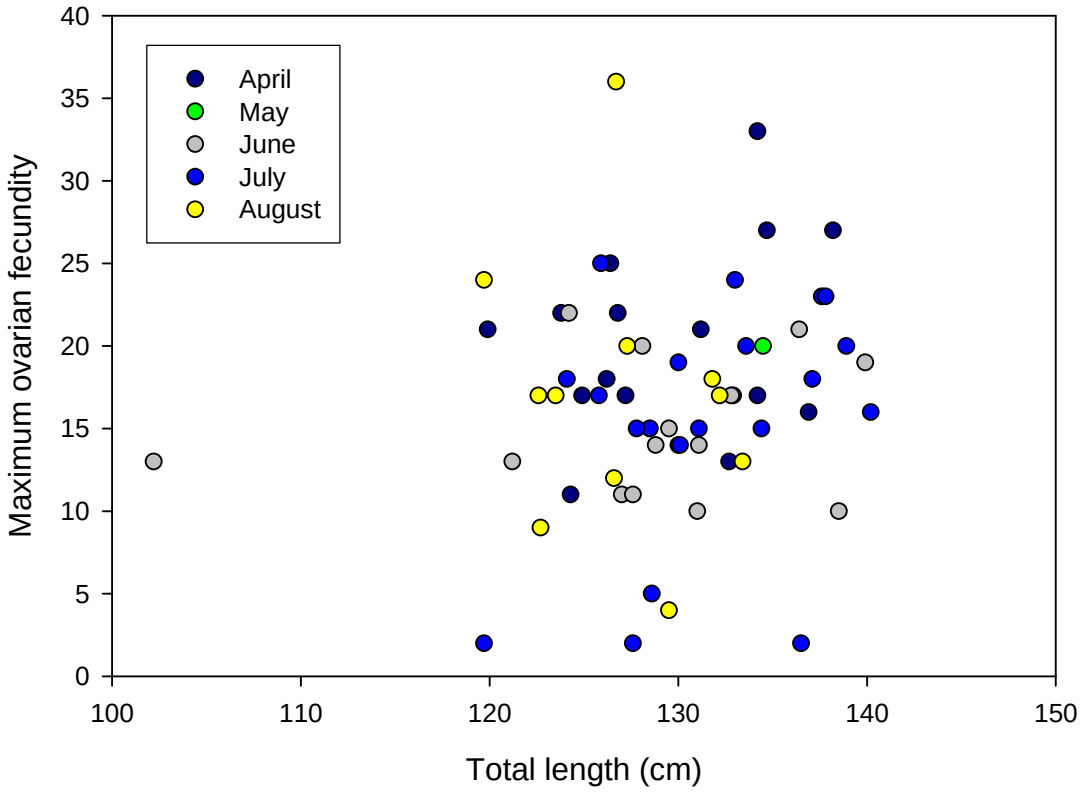

Fig. 52. Relationship between the maximum number of mature ova recorded and total length by month. Counts of mature ova are summed from both ovaries from 49 *Raja rhina*.

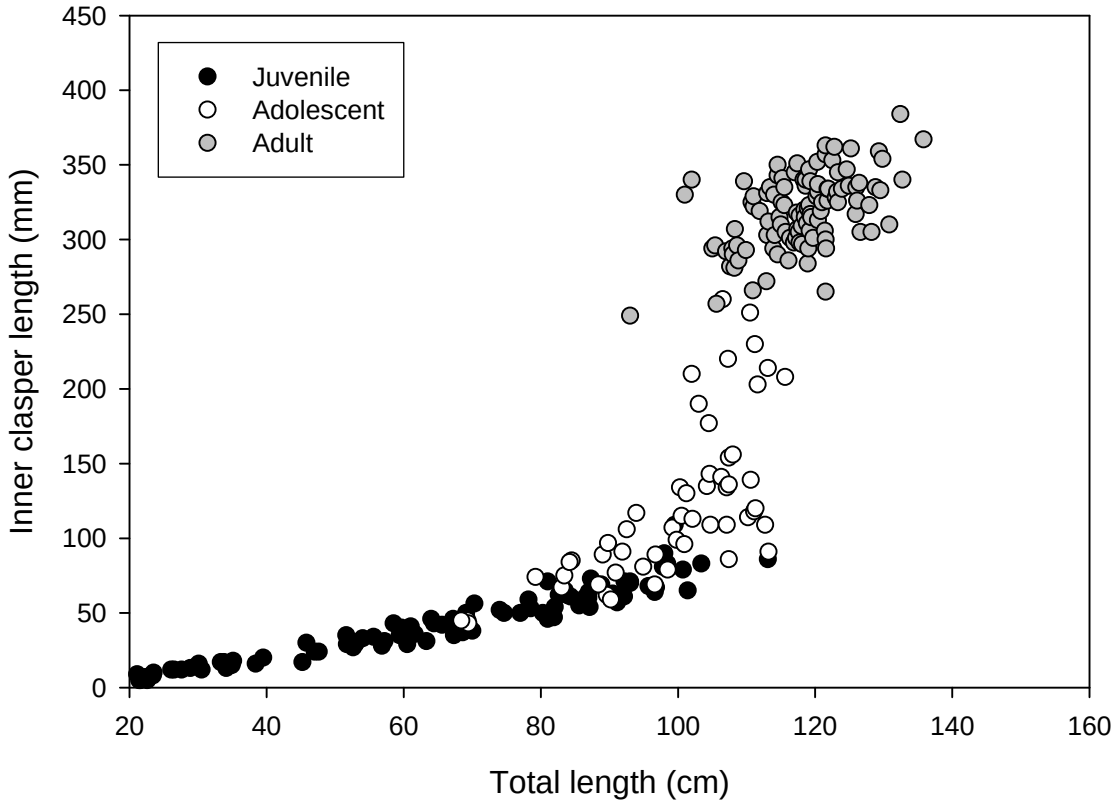

Fig. 53. Relationship between clasper length and total length based on the reproductive classification of 255 *Raja rhina*.

any notable change in the relative proportion of these four stages among the five months sampled (Fig. 54). The production and maintenance of mature spermatocysts within the testes appears to persist throughout the spring and summer, with no notable changes among those examined. The increase in the proportion of mature spermatocysts occurred primarily in those individuals over 100 cm TL and appeared to mirror development of the claspers (Fig. 55).

Demographic analysis

Natural mortality and survivorship estimates calculated from six indirect methods produced a broad range of rates, within and among skate species (Table 6). Variation among these estimates was greatest for *B. interrupta* and least in *R. binoculata*. Overall annual survivorship was determined to be lowest for *B. interrupta* and highest for *R. rhina*. The longevity-based method of Campana et al. (2001) consistently generated the lowest survivorship values.

Probabilistic models developed to incorporate uncertainty and variability in vital rates projected positive values of λ for each skate species examined (Table 7). Confidence limits were narrowly distributed around the mean values of all demographic parameters. Average annual population growth rates ranged from 20% to 36% for *R. rhina* and *B. interrupta*, respectively, in the absence of fishing pressure. Minimum λ estimated from population projections were 1.16 yr^{-1} for *B. aleutica*, 1.20 yr^{-1} for *B. interrupta*, 1.23 yr^{-1} *R. binoculata*, and 1.14 yr^{-1} for *R. rhina* were calculated during the 1,500 simulations. Mean λ projections suggest that average fishing mortalities of 0.22 yr^{-1} for *B. aleutica*, 0.31 yr^{-1} for *B. interrupta*, 0.29 yr^{-1} *R. binoculata*, and 0.25 yr^{-1} for *R. rhina* would result in no net population growth (λ = 1.0). Mean R_o values were greatest for *R. binoculata*. Despite a projected range of approximately eight years in Ā among species, t_{x2} and *rT* estimates were relatively similar, ranging between 2.35-3.82 (t_{x2}) and 3.33-4.31 (*rT*).

Age-specific reproductive values (V_x) rise rapidly near the onset of first reproduction and then gradually fall with increasing ages. The average 13 year old female *B. aleutica* may be expected to produce 178 offspring (Fig. 56). *Bathyraja interrupta* may have a peak output of 131 female offspring at age 10, whereas this value falls to less than 100 by age 17 (Fig. 57). Maximum V_x of 206 offspring were predicted to occur within age 13 *R. binoculata*, declining to values similar to those of immature age classes by age 25 (Fig. 58). An estimated 237 offspring may be produced by the average 18 year old *R. rhina*, with projected V_x declining below 100 female individuals produced annually by age 27 (Fig. 59).

Elasticity patterns indicate that population growth rates of each skate assessed are more strongly influenced by survival of the juvenile age classes than survival of neonates or changes in fecundity (Table 8). Fertility elasticities ranged from 0.05 for *R. rhina* to 0.09 in *B. interrupta*. Juvenile elasticities ranked as the highest values in all population projections, ranging from a minimum 0.73 for *R. binoculata* to a

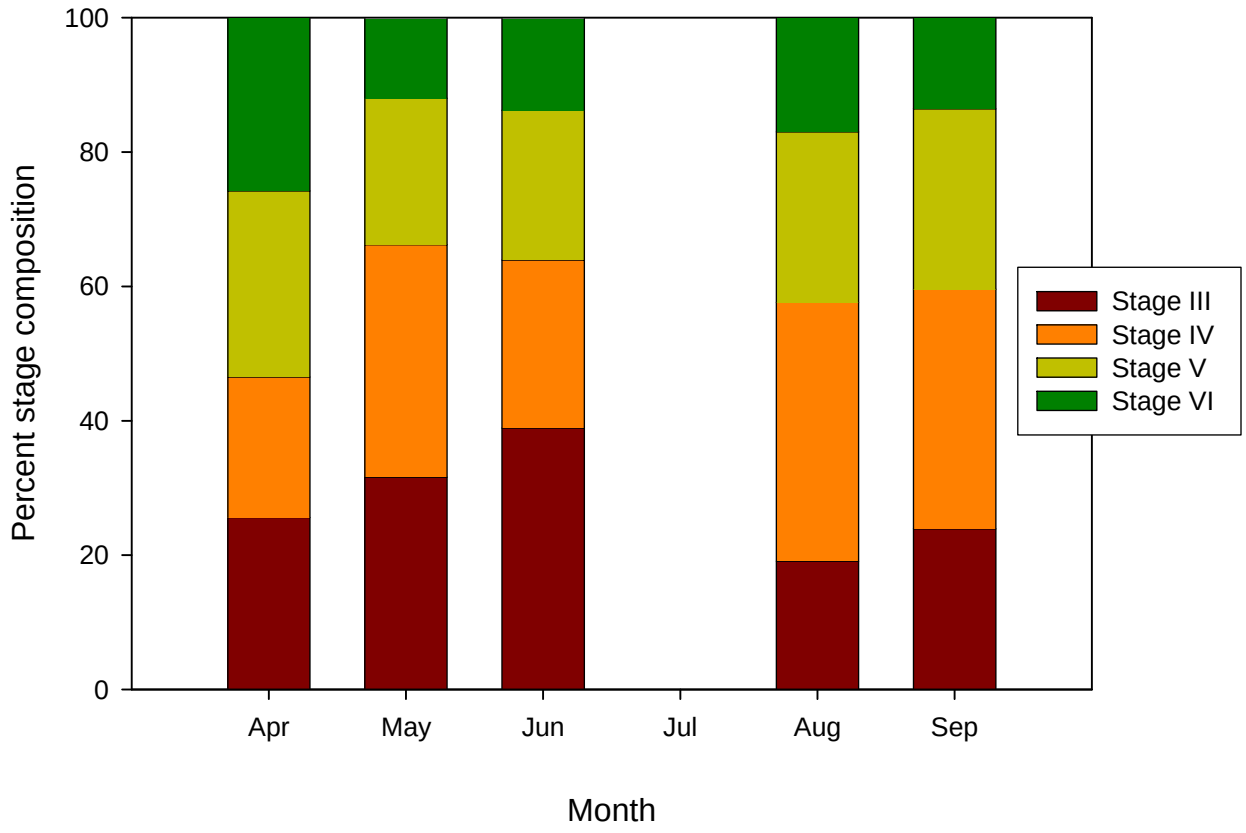

Fig. 54. Monthly changes in spermatogenesis in male *Raja rhina*. The percent stage composition is the mean proportion of each stage occupied along a transect line across one representative full lobe cross section of a testes, and expressed as the mean. Sample sizes are presented in parentheses.

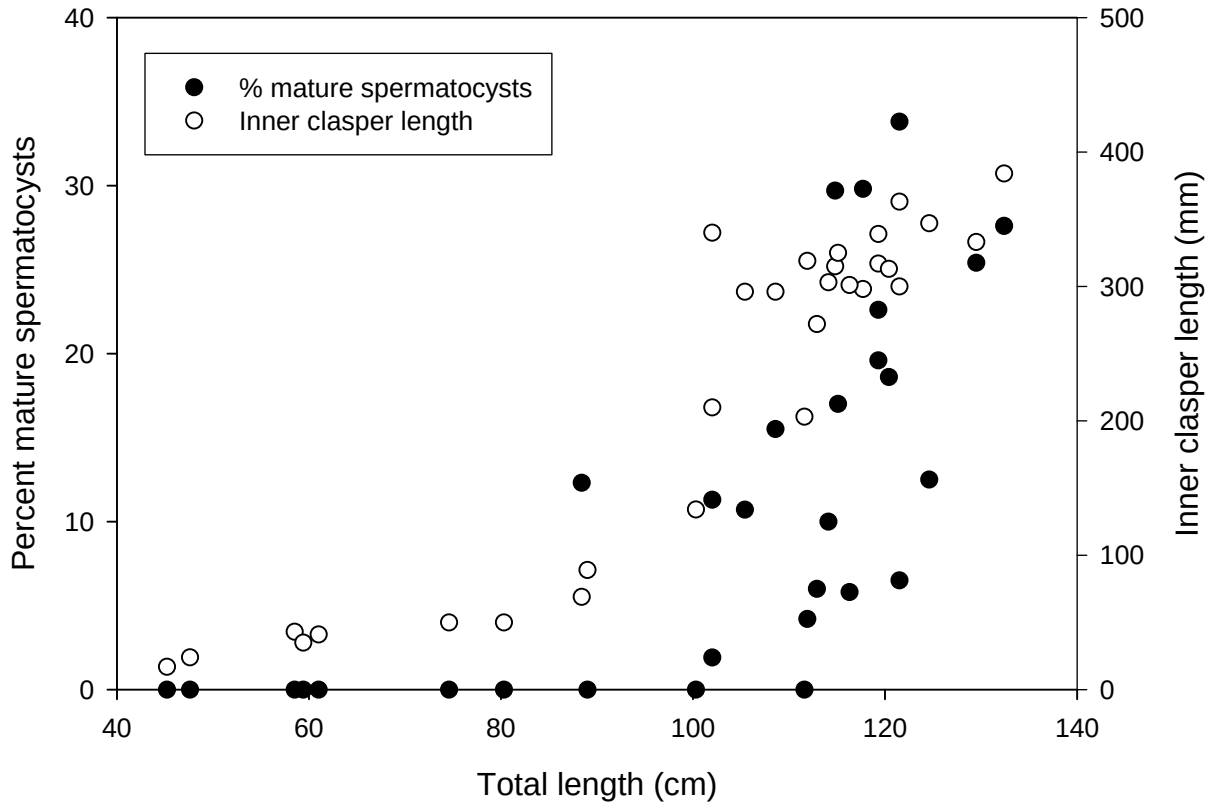

Fig. 55. Relationship between proportion of mature spermatocysts, inner clasper length, and total length for (*n*=30) male *Raja rhina*.

Table 6. Formulas and resulting indirect estimates for natural mortality (M) and survivorship (S_x) applied in demographic models of Aleutian (*Bathyraja aleutica*), Bering (*B. interrupta*), big (*Raja binoculata*), and longnose (*R. rhina*) skates.

Method	*Bathyraja aleutica*		*Bathyraja interrupta*		*Raja binoculata*		*Raja rhina*	
	M (yr^{-1})	S_x(yr^{-1})	M (yr^{-1})	S_x(yr^{-1})	M (yr^{-1})	S_x(yr^{-1})	M (yr^{-1})	S_x(yr^{-1})
Hoenig (1983)								
1. $\ln M = 1.46 - 1.01 * (\ln \omega)$	0.23	0.79	0.30	0.74	0.16	0.85	0.19	0.83
2. $\ln M = 1.44 - 0.982 * (\ln \omega)$	0.25	0.78	0.32	0.73	0.17	0.84	0.20	0.82
Jensen (1996)								
3. $M = 1.65/\alpha$	0.16	0.85	0.22	0.80	0.17	0.85	0.11	0.90
4. $M = 1.50 * k$	0.16	0.85	0.10	0.91	0.12	0.89	0.06	0.95
5. $M = 1.6 * k$	0.17	0.84	0.10	0.90	0.13	0.88	0.06	0.94
Campana et al. (2001)								
6. $M = -\ln 0.01/\omega$	0.26	0.77	0.33	0.72	0.18	0.84	0.21	0.81

Table 7. Estimates of finite population growth rates (λ), net reproductive rates (R_o), the average age of the parents of the offspring (Ā), population doubling times (t_{x2}), and rates of increase per generation (rT) projected from deterministic and probabilistic life table models for Aleutian (*Bathyraja aleutica*), Bering (*B. interrupta*), big (*Raja binoculata*), and longnose (*R. rhina*) skates. LCL and UCL represent the lower 2.5 % and upper 97.5% confidence limits. Results reflect uncertainty in median age of first reproduction, age-specific survivorship, age-specific fecundity, and longevity based on 1,500 Monte Carlo simulations.

Species	λ	LCL	UCL	R_0	LCL	UCL	Ā	LCL	UCL	t_{x2}	LCL	UCL	rT	LCL	UCL
Bathyraja aleutica	1.252	1.251	1.253	23.26	23.06	23.45	13.24	13.21	13.27	3.14	3.13	3.16	3.33	3.32	3.34
Bathyraja interrupta	1.360	1.357	1.362	30.29	29.92	30.65	10.32	10.28	10.35	2.35	2.34	2.37	3.69	3.67	3.71
Raja binoculata	1.334	1.333	1.336	48.69	48.26	49.12	12.44	12.41	12.47	2.45	2.44	2.46	4.31	4.30	4.33
Raja rhina	1.202	1.201	1.203	36.47	36.12	36.83	18.66	18.63	18.68	3.82	3.81	3.83	3.72	3.70	3.73

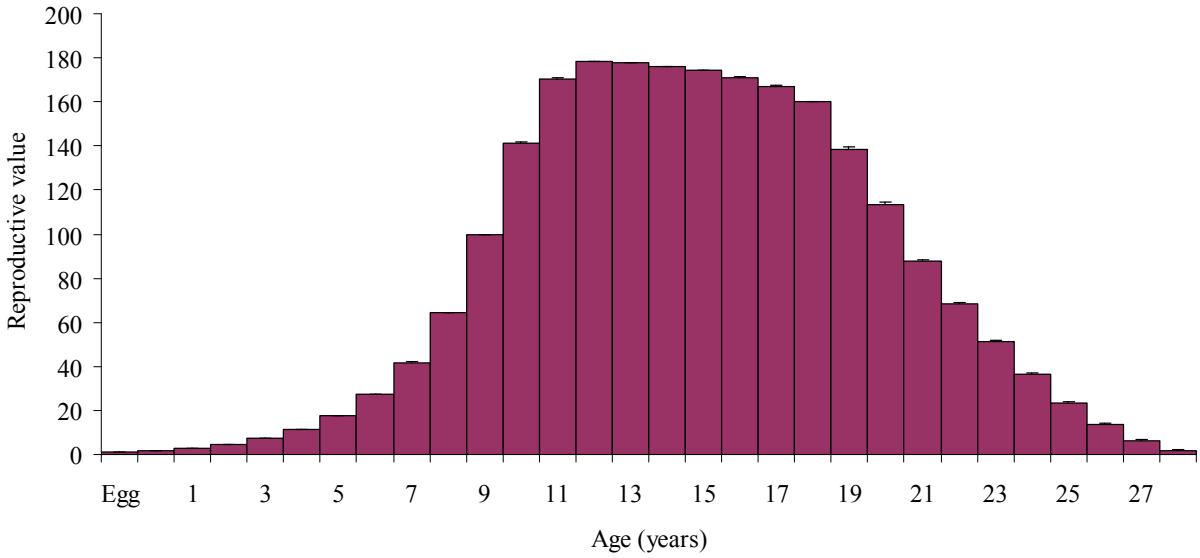

Fig. 56. Age-specific reproductive values (V_x) projected from 1,500 Monte Carlo simulations for *Bathyraja aleutica*. Error bars represent upper 97.5% confidence limits.

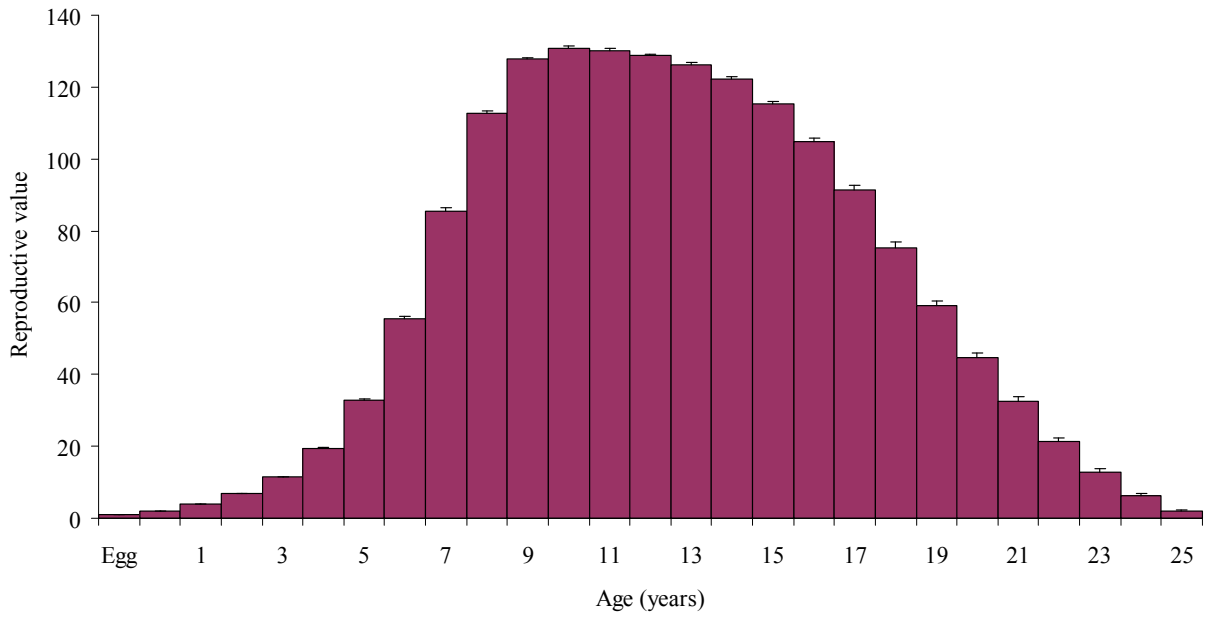

Fig. 57. Age-specific reproductive values (V_x) projected from 1,500 Monte Carlo simulations for *Bathyraja interrupta* from the Gulf of Alaska. Error bars represent upper 97.5% confidence limits.

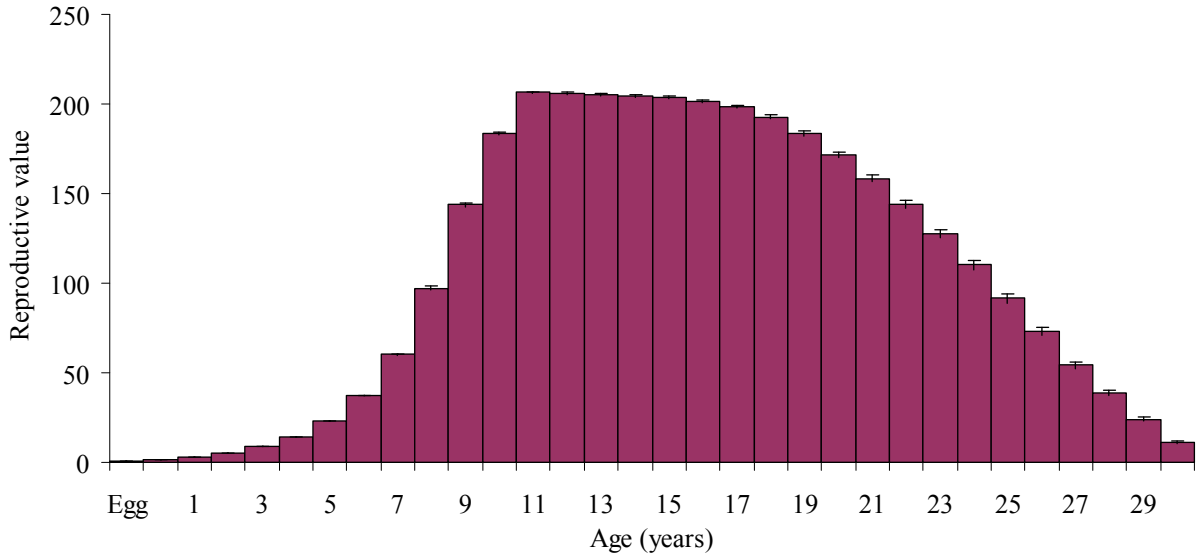

Fig. 58. Age-specific reproductive values (V_x) generated from 1,500 Monte Carlo simulations for *Raja binoculata* from the Gulf of Alaska. Error bars represent upper 97.5% confidence limits.

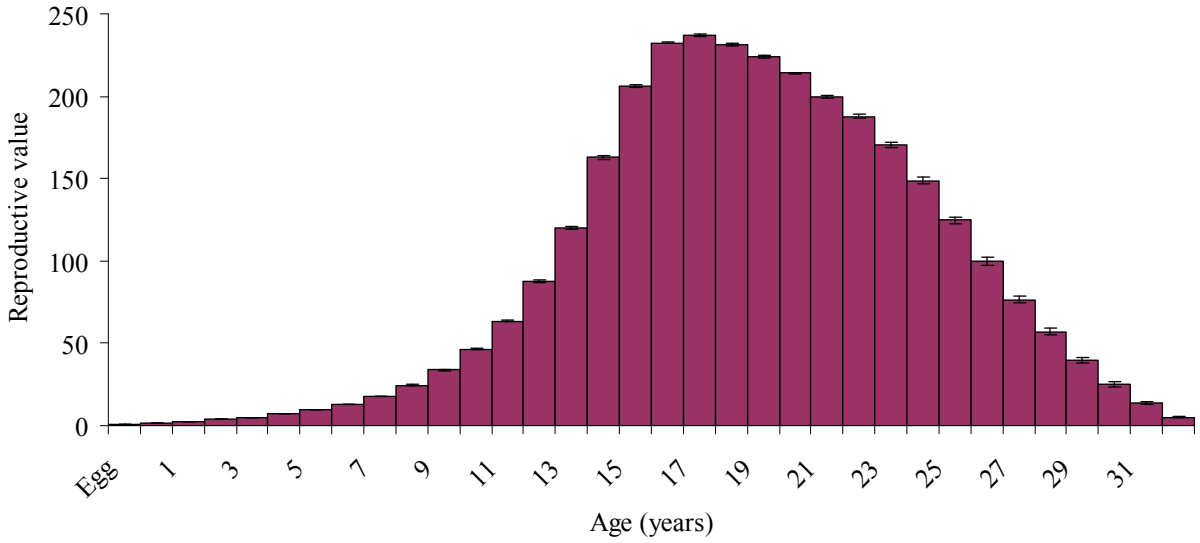

Fig. 59. Age-specific reproductive values (V_x) generated from 1,500 Monte Carlo simulations for *Raja rhina* from the Gulf of Alaska. Error bars represent upper 97.5% and lower 2.5% confidence limits.

Table 8. Mean fertility, juvenile survivorship, and adult survivorship elasticities and corresponding elasticity ratios summed across relevant age classes for Aleutian (*Bathyraja aleutica*), Bering (*B. interrupta*), big (*Raja binoculata*), and longnose (*R. rhina*) skates. Estimates are based on 1,500 Monte Carlo simulations.

	Mean Elasticity			Elasticity Ratios		
Species	Fertility	Juvenile	Adult	Adult : Age 0	Juvenile : Age 0	Adult : Juvenile
Bathyraja aleutica	0.07	0.81	0.12	1.72	11.52	0.15
Bathyraja interrupta	0.09	0.79	0.12	1.36	8.96	0.15
Raja binoculata	0.07	0.73	0.19	2.57	9.87	0.26
Raja rhina	0.05	0.78	0.17	3.28	15.37	0.21

maximum of 0.81 for *B. aleutica*. Mean adult elasticity values were equal to or exceeded 0.12 in each species, and ranked highest for *R. binoculata*. Mean juvenile survival to fertility elasticity ratios were highest for *R. rhina*, indicating that a 10% decrease in juvenile survival would require an increase in excess of 150% in fertility or egg stage survival to return the population to its original growth rate.

Discussion

Age determination

The utility of caudal thorns as ageing structures has been inconsistent among bathyrajid skates (Gallagher and Nolan 1999, Perez 2005, Davis et al. 2007). A recent study on another Alaskan species, *B. parmifera*, found caudal thorns provided age estimates similar to those obtained from vertebral centra (Matta and Gunderson 2007). In *B. aleutica*, both vertebral centra and caudal thorns grew proportionally to TL, indicating that each structure was suitable for age estimation. However, comparison between the structures suggested that caudal thorns might not be appropriate for ageing. Caudal thorn size was more variable with skate TL, as indicated by the curved regression and weaker coefficient of determination. CV values exceed 10% in most shark ageing studies (Campana 2001), therefore, although CV was more favorable for vertebral centra, precision of age estimates within both structures were both considered acceptable for *B. aleutica*. Precision between the structures was poor, however, with caudal thorns biased towards older ages, indicating either greater variability in thorn ages, or an underestimation of ages from vertebral centra. This bias may have resulted from the reader ageing the vertebral centra prior to the caudal thorns, as experienced readers tend to discern more bands in ageing structures (Officer et al. 1996, Gallagher et al. 2006).

The vertebral band pairs of *B. interrupta* were especially difficult to discern as it was uncommon to have clear banding in the intermedialia; consequently the corpus calcareum was relied upon. Many of the larger vertebrae showed cloudiness toward the focus, which may have concealed bands deposited early in life, possibly leading to under-ageing (Fig. 60). This may have contributed to the slightly lower goodness of fit values for the growth models in comparison with other skate age and growth studies. Several other elasmobranch studies have found similar problems with higher variability in banding with increased size (Abdel-Aziz 1992, Casey et al. 1985, Ferreira and Vooren 1991, Gallagher and Nolan 1999, Licandeo et al. 2006, McFarlane and King 2006). Further research will be required to determine the nature of this 'cloudiness', which may be caused by ontogenetic changes in diet and or temperature, or reabsorption of certain materials deposited in the vertebral matrix (Licandeo et al. 2006). McFarlane and King (2006) used mean distances from the focus to the first and second bands from vertebrae in which they were visible to estimate the number of 'missing' bands in cloudy vertebrae from *R. binoculata*. A

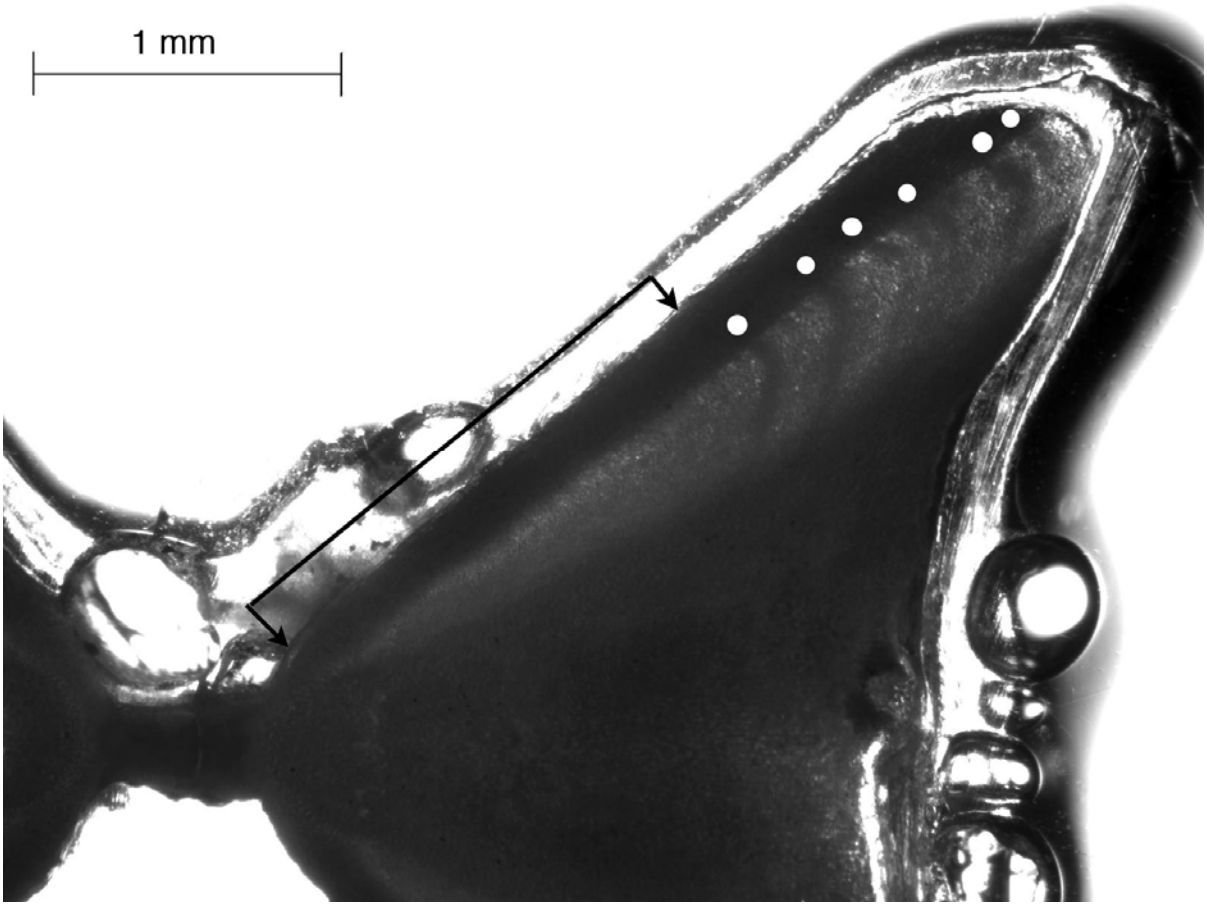

Fig. 60. Vertebral thin section from a male, 75.1 cm TL *Bathyraja interrupta* displaying the "cloudiness" typically associated with early bands. The arrows delineate the region of cloudiness, while the white dots show clearly visible bands.

similar technique is in progress for *B. interrupta*.

A significant, although weak relationship between age estimates was derived from caudal thorns and vertebrae of *B. interrupta*. This may be because of the difficulties encountered with ageing the vertebrae, which were not encountered when ageing the thorns. This difference is reflected in the age bias plot of vertebral age estimate against caudal thorn age estimate. The overall precision was higher for thorns when compared to vertebrae, similar to the findings of Gallagher and Nolan (1999), which suggests that thorns of *B. interrupta* may be easier to interpret. The results of this study do not rule out the possibility that the caudal thorn may be a useful ageing tool for *B. interrupta*. In the future, if the challenges of distinguishing the bands on the vertebrae are overcome, then the relationship between age estimates from these two structures may be stronger.

Among batoids, maximum observed ages range from 3 to 28 years (Cailliet and Goldman 2004). Maximum ages estimated for *B. aleutica* and *B. interrupta* were 17 and 13 years for females and 16 and 12 years for males, respectively. Previous studies reported maximum ages of 18 years in *B. kincaidii* (Perez 2005), 17 years in *B. parmifera* (Matta and Gunderson 2007), and 20 years in *B. trachura* (Davis et al. 2007). *Bathyraja aleutica* and *B. interrupta* generally fall within the mid-range of longevity estimates for skates (Sulikowski et al. 2005a). Because there is a possibility that under-ageing occurred, particularly for *B. interrupta*, it is important to consider the longevity provided as a minimum. Additional analyses of the age and growth of *B. interrupta* is currently underway as part of a master's thesis by one of the authors (S.M. Ainsley).

Age validation

Validation of annual band deposition was not demonstrated in either *B. aleutica* or *B. interrupta*. For *B. aleutica*, centrum edge analysis may suggest a trend, as the majority of translucent bands were present in January and opaque bands in July (excluding March, as $n = 3$), but differences could not easily be statistically tested. The MIR was not significantly different among months, but the 0.08 p-value was close to the set statistical significance level of 0.05, possibly indicating a biological change occurring in the vertebrae over time. Natanson et al. (2007) noted similar results for female *Malacoraja senta*, although mean monthly MIRs were significantly different for males, and timing of MIR peaks was incongruent between sexes. MIRs were combined for male and female *B. aleutica*, and may have attributed to their variability. Resolution of an annual banding pattern may also have been precluded by lack of data for all months, low sample size for some available months, and inclusion of samples from multiple years. Poor edge clarity due to reduced calcification, overpolishing, or lack of photographic resolution resulted in fewer samples available for edge analysis. However, MIR analyses have supported the depositional pattern of one opaque and one translucent band being laid down each year for a number

of other skate species, including *B. parmifera* (Matta and Gunderson 2007), *Amblyraja radiata* (Sulikowski et al. 2005b), and *R. texana* (Sulikowski et al. 2007a). We therefore assumed a pattern of annual band deposition for *B. aleutica*. However, because of the possibility of over or underestimation of ages in this study, estimates for fisheries management must be used cautiously (Campana 2001).

There was no pattern in either the MIRs or edge analyses to support an annual pattern of band deposition in the vertebrae of *B. interrupta*. It is important to note, however, that samples for this study were limited to six consecutive months. The six months studied were also the same months in which one would expect the least difference in MIR amongst month. Matta and Gunderson (2007) found support for annual band deposition in *Bathyraja parmifera* from the EBS. The mean MIRs for the summer months found by Matta and Gunderson (2007) were comparable to those found in this study for *B. interrupta*. However, the lowest MIRs found by Matta and Gunderson (2007) occurred in January and February, while the highest MIRs were found in November and December, all months not included in this study. This suggests that if samples of *B. interrupta* from the fall and winter months were available a pattern might be apparent. Despite lack of validation, it is assumed for this study that a single band pair is deposited per year, as there is substantial evidence that this is true for other skate species (Holden and Vince 1973, Ryland and Ajayi 1984, Waring 1984, Abdel-Aziz 1992, Natanson 1993, Sulikowski et al. 2005b, Natanson et al. 2007). In addition, Natanson et al. (2007) found a difference in MIR values between sexes. This is an area of research that may be examined in the future for *B. interrupta*. Further attempts at validation in both *B. interrupta* and *B. aleutica* are necessary.

Growth parameter estimates

Chondrichthyan age and growth studies primarily apply the three parameter VBGF. However, because of limitations identified with this growth function, the application and comparison of alternative models is suggested (Cailliet et al. 2006). Based on the criteria of statistical fit, biological relevance, and convenience (Roff 1979, Moreau 1987, Cailliet et al. 2006), the three parameter VBGF best fit the length-at-age data of *B. aleutica* (Table 4). Goodness-of-fit estimates (r^2, MSE, SEE) were nearly identical between three parameter VBGF and Richards models. Samples included most of the reported size range, however, L_∞ may be slightly overestimated due to the low number of samples in the oldest age classes. Although estimates of L_∞ from the two parameter VBGF approximated the maximum length of ~161 cm TL observed by Zenger (2004), making it also a biologically reasonable model, statistical fit was reduced. Gompertz and logistic functions fit the data well, but estimates of L_∞ in both models were less than the maximum observed length of 153.4 cm TL. Model generated estimates of L_o were greater than reported sizes at birth, and may indicate the limited ability of the three parameter VBGF to describe early growth (Gamito 1998). This may also reflect the use of whole ages, as prescribing ages with half-year increments

may have provided more precise model fits, especially during initial growth (Frisk and Miller 2006, Smith et al. 2007). Statistical fit of *B. aleutica* growth was best for the polynomial function, however, the resulting parameters cannot be directly compared biologically with other studies.

The von Bertalanffy growth coefficient (k) is commonly used to compare life history strategies and address the potential vulnerability of a population. Although most elasmobranchs are generally considered to exhibit slow growth, reported estimates of k among skates are broad (Musick 1999, Cailliet and Goldman 2004). Published growth coefficients range from 0.05 yr^{-1} for *Dipturus pullopunctata* (Walmsley-Hart et al. 1999) to 0.50 yr^{-1} for *Raja miraletus* (Abdel-Aziz 1992). *Bathyraja aleutica* is a moderately slow growing, large bodied species, with $k = 0.11$ yr^{-1}. Compared to other smaller Alaskan skates, the growth coefficient was similar to *B. parmifera* ($k = 0.10$ yr^{-1}; Matta and Gunderson 2007) and *B. interrupta* ($k = 0.08$ yr^{-1}; this study). Likewise, growth rates were much greater than comparably sized *R. rhina* ($k = 0.037$-0.056 yr^{-1}), but within the range of estimates for the larger species, *R. binoculata* ($k =$ 0.080-0.152 yr^{-1}) (Gburski et al. 2007).

Each of the six models of *B. interrupta* growth demonstrated good fit, explaining about 86-89% of the variation. The logistic and Gompertz models best fit *B. interrupta* age at length data, and also provided estimates of L_∞ that were closer to the maximum reported size. McFarlane and King (2006) and Carlson and Baremore (2005) similarly found the logistic model provided the best fit and more biologically realistic parameters, for growth of *R. rhina* and the spinner shark, *Carcharhinus brevipinna*, respectively. Neer and Cailliet (2001), Neer and Thompson (2005), and Matta and Gunderson (2007) have also reported that the Gompertz model provided the best fit and most reasonable parameters in elasmobranch ageing studies.

As with many skate age and growth studies the three parameter VBGF gave unrealistically high L_∞ values for *B. interrupta* (Sulikowski et al. 2005a, McFarlane and King 2006, Davis 2007). This effect has been attributed to rareness of larger specimens included within these studies (Sulikowski et al. 2005a). The standard three parameter VBGF has been criticized heavily over the years (Knight 1968, Roff 1980), however it is still the most commonly used growth model in fisheries science. The use of polynomial equations has been advocated several times by critics of the VBFG, however the benefits are usually discussed in situations in which there is no apparent asymptotic behavior of the data (Roff 1980). TL at age appears to asymptote in *B. interrupta*, therefore the results are very similar between three parameter VBGF and polynomial models (Table 5). The benefit of using the VBGF is that the parameters given are not arbitrary constants, but have at least some biological meaning. Even so, in the case of *B. interrupta* neither model was practical.

A recent study has found the two-parameter VBGF to be a useful model to describe skate growth (Davis 2007). The two-parameter model uses a set length at time 0, which is obtained from the smallest

free-swimming individuals as well as the largest embryos. The TLs at age zero for the samples examined in this study were much higher than expected, more than double the estimated size at birth of 13.0 to 14.0 cm TL for *B. interrupta* (Jerry Hoff, NMFS-AFSC, pers. comm.). The two parameter VBGF based on the estimated size at birth (13.5 cm) gave more realistic results than the model based on the smallest observed individuals from this study. The larger individuals in this study estimated to be age 0 might in fact be older. Due to the cloudiness within vertebral thin-sections, these age estimates may not be reflective of true age. As the MIRs and edge analyses were not able to clarify a pattern of band deposition, further studies are needed to clarify this issue.

Maturity and reproduction

The maximum size of *B. interrupta* and *R. rhina* found in this study exceeded that presently reported in the literature (Mecklenburg et al. 2002, Ebert 2005). Maximum sizes from this study were 87.1 and 145.0 for *B. interrupta* and *R. rhina* respectively, exceeding previous estimates by up to ~7 cm for *R. rhina*. These new size records were both from female specimens, although there was modest difference in maximum observed length between males and females.

Female elasmobranchs typically attain greater sizes than males (Cortés 2004), and this pattern was evident in all species in this study. Striking differences in maximum total lengths between the sexes were only observed for *R. binoculata*, with females attaining sizes that were greater than those of males by more than 40 cm TL. Females were found to be only slightly larger than males in the other species considered in this studied. Ebert (2005), who similarly did not find strong sexual dimorphism in the sizes of *B. interrupta*, by contrast did find males to be slightly larger in his study of this species in the EBS. Also, Ebert (2005) reported that TL in female *B. aleutica* was noticeably larger than in males, however the lengths of males in his study were well below the maximum observed size for this species.

In general skates tend to mature at 80 to 90% of their maximum TL (Dulvy et al. 2000, Ebert 2005). Although *B. aleutica* (81%), *B. interrupta* (80%) and *R. rhina* (82%) follow this trend, *R. binoculata* from the GOA fell well below this expected range (61%) (percentages based on female TL_{50}). While *B. aleutica*, *B. interrupta*, and *R. rhina* should be considered as late maturing species based on these relationships, maturity in *R. binoculata* appears to occur much earlier. This discrepancy may indicate a markedly different life history strategy for this species. Alternatively, overestimation of TL_{50} or the use of a maximum TL in this calculation that is not attainable within the GOA population would result in underestimates of this percentage. Despite this disparity, all estimates occurred within 60–90% of asymptotic length, which was suggested by Holden (1974) as the range of mean length of maturity for female elasmobranchs.

Visual assessments of maturity status may be unreliable or inconsistent, particularly during recovering phases of gonadal development (Gerristen and McGrath 2006, Vitale et al. 2006). Such errors may lead to systematic over- or underestimation of TL_{50}, skewing estimates of a population's reproductive potential. Although histological analysis of gonads was implemented, in part, as a secondary method of evaluating maturity status for a subset of samples, these analyses were only applied to males. Variability between TL, reproductive classification and/or gonad size was evident in each of the species examined in this study (e.g. Fig. 47). Because reproductive classifications were assigned by multiple field personnel, biases or differential interpretations may have influenced the observed variation. However, all personnel participating in field surveys received the same training. We note that the potential for misclassifying mature, but reproductively inactive specimens as immature was high given the criteria adopted for use in this study. Criteria for reproductive classifications frequently outline distinctions for maturing individuals or distinguish categories for mature, active individuals, but lack descriptions or separate stages for resting and post-partum conditions or the possibility of senescence (e.g. Stehmann 2002, Ebert 2005). Thus, specimens that did not clearly fit into the adult or gravid categories used in this study because of recrudescence of gonads or resorption of ova may have been inappropriately classified as immature. These errors would result in overestimates of TL_{50} and median ages at maturity. Further verification of reproductive condition through histological, hormonal, or a combination of these assays is needed to confirm gonadal characteristics during spent, recovering, and resting phases. Future studies should consider the potential for these conditions as well the possibility of senescence by expanding reproductive classification criteria.

Regional differences in size at maturity are often reported among skates (e.g. Templeman 1987). Total lengths at first and 50% maturity were slightly larger for female *B. interrupta* from the GOA as compared to those estimates by Ebert (2005) for *B. interrupta* from the EBS. The current estimates differ from those of Ebert (2005) primarily because of a larger maximum observed TL for females as well as smaller sizes at first maturity for both sexes from the GOA.

Size and age at maturity determined from logistic ogives were similar for both sexes of *B. aleutica*, though maturity occurred over a greater size range for females. Median size (and age) at maturity occurred at 124.1 cm (10.4 years) for females and 122.8 cm (10.2 years) for males. This corresponds to 80.9% and 81.9% of maximum observed length, and 61.2% and 63.8% of maximum observed age. Similar sizes at maturity were found in *Psammobatis extenta* (Braccini and Chiaramonte 2002). In a review of life history patterns, Cortés (2000) concluded that, on average, sharks reached maturity around 75% of their maximum size and 50% of maximum age, therefore *B. aleutica* seems to be a late maturing species.

Slight differences were exhibited from previous maturity estimates for *B. aleutica*. Females first matured at 111.6 cm TL, or 72.7% of maximum observed TL. This size is less than previously estimated by Ebert (2005), who found first maturity occurred at 119.0 cm TL, or 86.4% of maximum length. Additionally, in this study males first matured at 117.7 cm TL, corresponding 78.5% of maximum observed TL. Previous reports were similar, indicating males first mature at 119.0 cm TL, however Ebert (2005) corresponded this to 89.4% of maximum length. This was because no males were greater than 133.0 cm TL, although maximum observed size for males was 150 cm TL (Ishiyama 1958). Reported size (and age) at maturity for *B. aleutica* from Russian waters was similar for females, but lower for males. Estimates were between 112.0-133.2 cm TL (9-10 years) for females and 108.0-116.0 cm TL (8-9 years) for males (Shuntov 1998), corresponding to 72.7–86.5% and 72.0–77.3% of maximum length. Differences among studies may be attributed to discrepancies in methods for assessing maturity, differences between years, sampling locations, or a combination of these factors.

Previous details on the reproductive biology of *R. binoculata* are sparse, and comparisons with other studies of relatively low sample sizes provide differing perspectives on sizes at maturity. McFarlane and King (2006) reported first maturity and TL_{50} for females and males as 60.0 cm TL, 90.0 cm TL, 50.0 cm TL, and 72.0 cm TL, respectively, from British Columbia. In contrast, we found first maturity of females (125.8 cm TL) and males (124.0 cm TL) to occur at much greater sizes. Among females, notable increases in oviducal gland and uterus width did not occur until specimens attained total lengths in excess of 100.0 cm (Fig. 45). Similarly, a shift in clasper length and the presence of mature spermatocysts within the testes were not apparent in specimens less than 115 cm TL. However, few mature were obtained from the GOA, and the resulting estimate of TL_{50} was less than the size of the smallest mature male. In a study of *R. binoculata* from central California, Zeiner and Wolf (1993) reported sizes at first maturity of ~129.0 cm TL and 100.0 cm TL for females and males, respectively. The maturity estimates of Gburski et al. (2007) indicate maturity at much smaller sizes in British Columbia than off the central California coast or from the GOA, a trend that is opposite of most reported latitudinal differences in maturity (e.g. Templeman 1987, Frisk and Miller 2006). These inconsistencies may have arisen based on differing criteria for reproductive classifications or relatively small sample sizes, however, further research is required to clarify potential regional differences in maturation and improve our knowledge of the reproductive biology of this species.

Regional differences in TL_{50} and the size at first maturity were also evident for *R. rhina*. Off central California, the onset of maturity in male *R. rhina* is reported to occur at 61.5 cm TL and females greater than 130.0 cm TL are mature (Zeiner and Wolf 1993). McFarlane and King (2006) calculated TL_{50} as 83.0 cm TL for females and 65.0 cm for males. These estimates are considerably less than the TL_{50} of 113.1 cm TL for females and 102.0 cm TL for males determined in this study, but agrees with our

observation that female *R. rhina* mature at notably greater sizes than males (Fig. 49). Because maturity ogives were not calculated by Zeiner and Wolf (1993), TL_{50} cannot be compared between these regions. Sizes at first maturity and TL_{50} indicate greater sizes of maturity in general for *R. rhina* in the GOA. As observed for *R. binoculata*, these observed latitudinal differences in maturity may have been influenced by differing criteria for reproductive classifications, sample sizes, or the sample size range.

Histological analysis of gonads has been used to corroborate maturity stages determined by morphological examination in several species (Sulikowski et al. 2006, Sulikowski et al. 2007b). The increase in clasper size relative to TL corresponded with the increase in mature spermatocysts in males of all four species studied. A slight lag occurred as claspers developed more gradually than the spermatocysts. This observation is in agreement with those of Sulikowski et al. (2005b, 2006, 2007b).

Skates display three types of reproductive cycles: 1) reproductively active throughout the year, 2) a partially defined annual cycle with one or two peaks, and 3) a well-defined annual or biennial cycle. Some species appear to have defined annual cycles, for example, egg cases were found to be present only during summer months in *Sympterygia bonapartii* (Mabragaña et al. 2002). Species with a partially defined breeding cycle include *Raja clavata* (Holden 1975), *Leucoraja garmani (*McEachran 1970), and *Psammobatis normani* (Mabragaña and Cousseau 2004). Recently it has been suggested that many skates reproduce year-round with no apparent seasonal cycle. This includes several deeper water skates such as *B. trachura* (Davis et al. 2007), *B. parmifera* from the Bering Sea (Matta 2006) and *B. albomaculata* from the southwest Atlantic (Ruocco et al. 2006). Skates inhabiting deeper waters may experience little environmental variability, and thus may not require well-defined reproductive seasons.

It is likely that *B. interrupta* is reproductive throughout the year, whereas data for *B. aleutica* and *R. rhina* were less clear, suggesting at least an extended reproductive season, if not the occurrence of egg deposition throughout the year. Gravid *B. interrupta* were found throughout all six consecutive months examined. Changes in spermatogenesis indicated an increase in mature sperm production from June to August for *B. aleutica*, but data were inadequate to fully describe the seasonality of spermatogenesis in this, or any of the species examined in this study. Mature ova and sperm were found in the shallower water species *R. rhina* during all months sampled. The presence of peaks in reproductive activity could not be confirmed with the data available. Although Sulikowski et al. (2007b) did not find egg cases in all months, *Malacoraja senta* was considered reproductively capable year-round using the criteria of minimum ova diameter and oviducal weight, as well as synchronicity of mature sperm with percent gravid females per month. Additional sampling is needed to confirm these observed reproductive trends during the remainder of the year. Expanded histological analyses or hormonal assays may be necessary to further evaluate the reproductive cycles of each species (Parsons and Grier 1992, Tricas et al. 2000, Sulikowski et al. 2005b).

It is not possible with the present data for *B. interrupta* to tease apart whether differences in ova counts and size are due to a seasonal or geographical difference, since samples were taken at different locations in the Gulf each month. That said, a decline in the mean number of mature ova occurred in June and July. Sampling during June occurred along the Alaskan Peninsula in 2005 and in Marmot Bay in 2006. Sampling in July of 2005 occurred on the east side of Kodiak and part way up the Kenai Peninsula. Mean greatest ova diameter was lowest in August compared with all other months. Again, it is not possible with the current data to determine whether this is due to a seasonal difference or location difference, given that all samples from September were taken at a the same location in the GOA (Shelikof Straight).

The absence of gravid *R. binoculata* in our samples and limited number of mature specimens in general, restricts our ability to assess reproductive seasonality in this species. Segregation by size and sex is common among elasmobranchs, and the lack of gravid females within this study may be reflective of this segregation or indicate a broader movement pattern or differential habitat use by adults of this species.

In most skates, ovaries are paired and symmetrical, whereas other elasmobranchs often have one predominant and one rudimentary ovary (Lutton et al. 2005). The number of mature ova was not significantly different between left and right ovaries for either *B. aleutica* or *B. interrupta*, which is consistent with other studies (Braccini and Chiaramonte 2002, Ebert 2005, Ruocco et al. 2006).

There was no consistent pattern in the relationship between mature ova diameter or ovarian fecundity and maternal size among skates. Although Ebert (2005) found a relationship between number of mature ova and maternal size in *B. interrupta* from the EBS, this was not shown for the same species or for *R. rhina* in the present study with samples from the GOA. This finding is in agreement with the results for *B. aleutica* from this study, but Ebert (2005) found ova number increased with maternal size, then decreased for most individuals greater than 145 cm TL. However, Matta and Gunderson (2007) found a slight but significant relationship for *B. parmifera*. Additionally, there was no relationship between maximum ova diameter and maternal TL for *B. interrupta*. This was also true for the closely related *B. kincaidii* (Perez 2005). An increase in maximum oocyte diameter with increasing maternal TL was found for *B. aleutica*, however, and has been reported for *Psammobatis extenta* (Braccini and Chiaramonte 2002), *Dipturus laevis* (Gedamke et al. 2005), *D. chilensis* (Licandeo et al. 2006), and *B. parmifera* (Matta and Gunderson 2007).

Demographic analysis

Until recently, estimates of *M* applied to model the productivity of Bering Sea and GOA skate population were applied uniformly to each species as 0.10 yr^{-1} (S_x= 0.90 yr^{-1}) (Gaichas et al. 2003,

TenBrink et al. 2006). In the absence of direct estimates for these species and limited life history information from which to calculate indirect estimates of *M*, this strategy ensured a precautionary approach to management of these populations. Indirect approaches applied for estimating *M* in this study produced values of similar magnitude for *B. aleutica* and *R. binoculata* but were more broadly ranging in *B. interrupta* and *R. rhina*. These estimates were typically in excess of 0.10 yr^{-1}, however, two methods following Jensen (1996) indicated the possibility of markedly low *M* rates of 0.06 yr^{-1} for *R. rhina*. Recent indirect estimates of *M* for *B. parmifera* from the EBS produced values similar in range and magnitude to those obtained for *B. aleutica* in this study (Matta and Gunderson 2007). Our calculations of *M* for *R. binoculata* and *R. rhina* using the same method (Hoenig 1983) and data presented by Gburski et al. (2007) differ notably values generated by those authors, and from the our estimates based on other formulas. Gburski et al. (2007) reported *M* to be 0.26 yr^{-1} and 0.28 yr^{-1} for *R. binoculata* and *R. rhina*, respectively. Estimates of *M* for four *Bathyraja* species from the Falkland Islands of 0.21 yr^{-1} present values similar to those obtained in the present study (Agnew et al. 2000). Given the importance of this parameter to population models and fisheries management, conservative estimates should continue to be applied for these populations until direct estimates based on tag-recapture or catch curves can be obtained.

Typically, estimates of *M* represent the greatest source of uncertainty in stock assessments or demographic analyses (e.g. Vetter 1988, Cortés 2007). However, the lack of information on annual fecundity for Alaskan skates represents a significant and comparable source of uncertainty and variability in these demographic results. Although skates are frequently described as possessing low fecundities, this characterization is misleading. Indeed, in contrast to most teleosts, fecundity is quite low. However, as evidenced by annual fecundities frequently exceeding 140 (e.g. Koop 2005), skates are among the most fecund of all elasmobranchs. This reproductive potential, coupled with protracted periods of egg deposition provide a compensatory mechanism that is largely lacking among other elasmobranchs. The unusual production of multiple embryos in each egg case by *R. binoculata* confounds comparisons with other species and signifies a critical area of uncertainty in our projections of population growth potential. Directed research, including captive studies, on the fecundity of small- and large-bodied skates is critically needed to evaluate resiliency and improve models of population dynamics for these species.

Comparisons and interpretations of population growth projections among species are restricted by the quality of the input parameters, estimates of vital rates, corresponding distributions of probability density functions, and variation in the framework of model construction (Cailliet 1992, Cortés 2007). Previously published demographic analyses of skates presented incomplete demographic analyses (Walker and Hislop 1998) and stage- as opposed to age-based models (Frisk et al. 2002), thus restricting the comparative value of these studies. Although the models developed in this study were similarly constructed, differences in the amount of information available for each species required the use of

differing probability density functions for estimates of median age at first reproduction. Additionally, projections for *B. interrupta* were based on preliminary age and growth data. With these differences in mind, projections of demographic parameters provide a practical, albeit generalized, characterization of fundamental population growth potential and plasticity, particularly when data are lacking for more complex age-structured models.

In a review of life history traits among long-lived marine species, Musick (1999) concluded that populations with annual intrinsic growth rates less than 10% were particularly vulnerable to over-exploitation. Mean estimates of λ ranged between 20% (*R. rhina*) and 36% (*B. interrupta*), suggesting moderate growth potentials for the species examined in this study (Table 7). The mean rate of increase per generation (*rT*) for *B. aleutica* (3.33) was slightly less than that estimated for *R. rhina* (3.72) which was predicted to possess lower mean λ. Due in part to comparatively elevated mean R_0, population doubling times of each species ranged between 2 and 3 years. Although these skates do not rank among the most vulnerable elasmobranchs, high levels of fishing mortality have dramatically impacted the abundance, distribution and size composition of several skate species in the north Atlantic (Walker and Hislop 1998). Agnew et al. (2000) detected marked declines in the species composition and abundance of skates in the Falkland Islands over a period of only six years following the onset of a directed fishery. Given the late ages of maturity determined among these Alaskan skates, the magnitude of fishing effort within the GOA and Bering Sea, and susceptibility to fishing mortality during all life history stages, further, more detailed monitoring of these populations and precautionary management is warranted.

Studies of elasmobranch population dynamics have only recently incorporated Monte Carlo simulation to account for uncertainty and variability in life history parameters (e.g. Cortés 2002, Carlson et al. 2003). Mean projections of λ for *B. aleutica*, *B. interrupta*, *R. binoculata*, and *R. rhina* fall within the upper range of those estimated for other elasmobranchs using Monte Carlo procedures. The values calculated in this study are most similar to those of tiger (*Galeocerdo cuvier*, 1.25), bonnethead (*Sphyrna tiburo*, 1.30), and blue (*Prionace glauca*, 1.40) sharks (Cortés 2002).

Maximum body size has been suggested as an indicator of vulnerability in skates (Dulvy and Reynolds 2002, Frisk et al. 2002). Considering λ as a proxy for vulnerability, such a trend was not evidenced for body size in this study. Although the smallest species assessed in this study, *B. interrupta* (87 cm TL), generated the highest mean λ (1.36), projections for the largest species, *R. binoculata* (249 cm TL) produced comparatively similar estimates of λ (1.33). Despite differing depths of occurrence, demographic parameters of the two similarly sized, large bodied skates, *B. aleutica* and *R. rhina*, were comparable. The similarity between estimates for *B. interrupta* and *R. binoculata* may have arisen from difficulties in obtaining age estimates for these species. A growth study of *R. binoculata* from British Columbian waters (McFarlane and King 2006) indicated maximum ages almost 10 years greater than

reported for the GOA (Gburski et al. 2007) in addition to much lower growth coefficients. If the life history parameters incorporated into demographic models of *R. binoculata* using the GOA data represent underestimates of somatic growth and age at maturity, overestimates of λ may have resulted. Validation and verification of age estimates is currently lacking but needed for the four species examined in this study.

Elasticity patterns of *B. aleutica*, *B. interrupta*, *R. binoculata*, and *R. rhina* indicated that population growth rates are more strongly influenced by survival of juvenile and adult stages than survival of neonates or changes in fecundity (Table 8). This elasticity pattern conforms to the general trend observed among sharks and other long-lived vertebrates (Heppell et al. 2000, Mollet and Cailliet 2002). Heppell et al. (1999) applied elasticity ratios as measures of the density-dependent compensation necessary to return populations to a desired λ in response to fisheries exploitation. Elasticity ratios calculated in this study revealed that the extent of compensation required for fertility to offset even a 10% reduction in juvenile survival exceed 89% for each of these species. Despite the relatively greater levels of fecundity reported for skates, required levels of compensation through fertility and age 0 survivorship appear to be restricted or biologically unreasonable. Ratios estimated for adults and age 0 were less dramatic, indicating that conservation measures directed toward juvenile stages of these species may be particularly beneficial for improving or maintaining observed population growth rates.

Conclusions

Bathyraja aleutica

- Studies on the age, growth, and reproductive biology of *B. aleutica* are continuing. Additional samples of larger skates may help bring growth curves to a better asymptote, and older ages may be found. Further attempts at verification and validation are necessary. Vertebral samples from the remaining months of the year are needed, as are methods to better enhance and clarify the edge for MIR analyses. Future edge analyses may include MIR using caudal thorns.
- *Bathyraja aleutica* is a moderately slow growing species with longevity within the midrange of other skates. Although its life history is comparable to several other skate species, it highlights the need for species-specific life history data, as ages and growth parameters for larger and smaller species were not necessarily greater and lesser than that of *B. aleutica*.
- Assessing reproductive seasonality for *B. aleutica* requires reproductive data from all months, including gonad measurements and histology. Future work incorporating steroid hormones would further enhance our understanding of reproductive patterns. Details on the annual fecundity of this and other Alaskan skate species are unknown and represent a critical area for future research.

- Projected mean population growth rates indicate an annual growth potential of 25% for *B. aleutica* in the absence of fishing pressure. This growth potential is most strongly influenced by the survivorship of juvenile age classes.
- A study of the life history aspects of *B. aleutica* from the Gulf of Alaska is currently underway. Comparisons between these large marine ecosystems may reveal differential growth parameters, longevities, or maturation rates, which would support the need for species specific fisheries management.

Bathyraja interrupta

- Results of this study of the age and growth are preliminary. Several issues should be considered before a confident assessment of the age and growth of *B. interrupta* can be made. First, additional smaller individuals of both sexes and larger males will be included in the growth modeling. Secondly, ages of larger individuals with hazy growth bands will be adjusted for the approximate number of bands missing using the method employed by McFarlane and King (2006). This should not have much affect on the estimates of longevity, however this will allow for an increased sample size for the growth modeling. As with any age and growth estimates, the validation of the band pair deposition is vital. Samples from the winter (October to March) are necessary to complete the MIR analysis.
- This study shows that *B. interrupta* has a longevity and size at maturity similar to skates of a similar size (smaller-bodied).
- In order to understand the true nature of the reproductive cycle of *B. interrupta* future work should focus on the winter months that were not sampled in this study (October to March). This would clarify and complement the patterns shown in this study. In addition, steroid hormone analyses such as those conducted in Sulikowski et al. (2007c) in the Atlantic would potentially clarify many of the reproductive patterns of skate species in the Gulf of Alaska.
- Projections of population growth rates suggest moderate growth potentials for *B. interrupta*, which appears is likely to be the most resilient of the four species assessed to perturbations.
- Although *B. interrupta* is not taken in the directed skate fishery in the Gulf of Alaska it is a very common bycatch species and therefore these life history aspects should be considered when setting bycatch limits for fisheries management.

Raja binoculata

- As indicated by maturation near 60% of its maximum total length and a potential for comparatively greater fecundity, the life history of *R. binoculata* may differ markedly from that of other skates in the region.
- Details on the size at maturity and reproductive biology remain unclear. The lack of gravid females and limited number of mature males among the samples restricted our ability to evaluate maturity and reproductive seasonality for this species. Furthermore, comparisons with other studies provide conflicting results, indicating smaller sizes at maturity from British Columbia than observed off central California or in the Gulf of Alaska. Classifications that incorporate criteria for resting periods, senescence, and recrudescence should be considered in future reproductive studies of this and other skate species.
- Given the role of *R. binoculata* in directed fisheries and the likelihood of take as bycatch in trawl and longline fisheries throughout the Gulf of Alaska, expanded, coordinated studies on the reproductive biology and age and growth of this species are recommended.
- Although the largest species considered in this study, mean projections of annual population growth rates were similar to that of the smallest species assessed in the study. Directed studies on fecundity are required to refine demographic and stock-recruitment models for this and other species from Alaskan waters.

Raja rhina

- Females attain maturity at larger sizes than males and both mature relatively late in life. Median size at maturity and first observed maturity occur at greater sizes in the Gulf of Alaska than reported from British Columbia and central California. Female maturity occurs at approximately 82% of the maximum total length at an estimated median size of 113.1 cm total length.
- Reproductive activity and egg deposition appear to occur over a period of at least six months with no definitive peaks. The reproductive cycle of *R. rhina* may continue throughout the year, but data were not available from all months to assess this possibility. Annual female fecundity is unknown but represents a key area for future study so that an improved understanding of stock-recruitment relationships may be achieved for skates from Alaskan waters.
- Of the four species assessed in this study, *R. rhina* possessed the lowest potential average annual population growth rate. The projected mean growth potential of 20% suggests that the species has a moderate population growth rate in comparison to other elasmobranchs. Generation time and population doubling time were estimated to be greater for this species than in *B. aleutica*, *B. interrupta*, and *R. binoculata*.

Publications

Masters Thesis:

Ainsley, S.M. Age, growth, and reproduction of the Bering skate, *Bathyraja interrupta* (Gill and Townsend, 1897) in Alaskan waters. Expected date of completion 2008.

Haas, D.L. Age, growth, and reproduction of the Aleutian skate, *Bathyraja aleutica* (Gilbert, 1896) in Alaskan waters. Expected date of completion 2008.

Publications:

Ebert, D.A. 2007. Skates of Alaska. An identification guide produced for the North Pacific Research Board under project numbers 510 and 621.

Manuscripts in preparation:

[1, 2]Bizzarro, J.J. and M. Vaughn. First records of the whiteblotched skate, *Bathyraja maculata* Ishiyama and Ishihara, 1977 in the Gulf of Alaska. Northwestern Naturalist.

[1, 2]Haas, D.L. and D.A. Ebert. First record of hermaphroditism in the Bering skate, *Bathyraja interrupta* Gill and Townsend, 1897. Northwestern Naturalist.

[1, 2]Age and growth of the Aleutian skate *Bathyraja aleutica* (Gilbert, 1896) in Alaskan waters

[1, 2]Age and growth of the Bering skate *Bathyraja interrupta* (Gill and Townsend, 1897) in Alaskan waters

[1, 2]Reproduction of the Aleutian skate, *Bathyraja aleutica* (Gilbert, 1896) in Alaskan waters.

[1, 2]Reproduction of the Bering skate, *Bathyraja interrupta* (Gill and Townsend, 1897) in Alaskan waters.

[1, 2]Reproduction of two commercially exploited skates, *Raja binoculata* and *R. rhina*, in the western Gulf of Alaska.

[1, 2]Demography and longevity of four exploited Alaskan skates

[1] Working titles

[2] Anticipated submission in 2008

Outreach

Conference presentations:

American Elasmobranch Society (2007)

Ainsley, S.M., D.A. Ebert, and G.M. Cailliet

Age, growth, and reproduction of the Bering skate, *Bathyraja interrupta* (Gill and Townsend, 1897) from the Bering Sea and the Gulf of Alaska

Haas, D.L., D.A. Ebert, and G.M. Cailliet

Age, growth, and reproduction of the Aleutian skate, *Bathyraja aleutica* (Gilbert, 1896), in the eastern Bering Sea

American Fisheries Society (2007)

Ainsley, S.M., D.A. Ebert, and G.M. Cailliet

Age, growth, and reproduction of the Bering skate, *Bathyraja interrupta* (Gill and Townsend, 1897) from the Bering Sea and the Gulf of Alaska

Haas, D.L., D.A. Ebert, and G.M. Cailliet

Age, growth, and reproduction of the Aleutian skate, *Bathyraja aleutica* (Gilbert, 1896), in the eastern Bering Sea

Alaska Marine Science Symposium (2007)

Ebert, D.A., W.D. Smith, D.L. Haas, S.M. Ainsley, and G.M. Cailliet

Life History and Population Dynamics of Alaskan Skates: Providing Essential Biological Information for Effective Management of Bycatch and Target Species.

American Elasmobranch Society (2006)

Ebert, D.A., J.J. Bizzarro, D.L. Haas, A.L. Neway, S.M. Ainsley, W.D. Smith, and G.M. Cailliet

Age, growth, and reproduction of six Alaskan skates (Chondrichthyes: Rajiformes: *Bathyraja* and *Raja*)

Alaska Marine Science Symposium (2006)

Ebert, D.A., J.J. Bizzarro, D.L. Haas, A.L. Neway, S.M. Ainsley, W.D. Smith, and G.M. Cailliet

Age, growth, and reproduction of four Alaskan softnose skates (Chondrichthyes: Rajiformes: Arhynchobatidae: *Bathyraja*)

Ebert, D.A., J.J. Bizzarro, W.D. Smith, and G.M. Cailliet

Life history and population dynamics of Alaskan skates: providing essential biological information for effective management of bycatch and target species

Western Groundfish Conference (2006)

Ebert, D.A., J.J. Bizzarro, D.L. Haas, A.L. Neway, S.M. Ainsley, W.D. Smith, and G.M. Cailliet

Age, growth, and reproduction of four Alaskan softnose skates (Chondrichthyes: Rajiformes: Arhynchobatidae: *Bathyraja*)

American Fisheries Society (2005)

Ebert, D.A., W.D. Smith, J.J. Bizzarro, and G.M. Cailliet

Skate research in the eastern North Pacific

Media:

Santa Cruz Sentinel newspaper story 27 April 2005

San Francisco Chronicle newspaper story 8 April 2007

Acknowledgements

We would like to thank the many people from the National Marine Fisheries Service Alaska Fisheries Science Center (NMFS-AFSC) and Alaska Department of Fish and Game (ADF&G) in Homer and Kodiak who provided invaluable assistance on various portions of this study. In particular, we thank Jerry Berger, Eric Brown, Sarah Gaichas, Christopher Gburski, Jerry Hoff, Dan Kimura, Ned Laman, Bob Lauth, Beth Matta, Jay Orr, Frank Shaw, Jim Stark, and Duane Stevenson from NMFS-AFSC in Seattle for their input and cooperation in allowing us to participate on NMFS AFSC survey cruises in the eastern Bering Sea and Gulf of Alaska. Rob Swanson (NMFS-AFSC, Kodiak) provided valuable support for our port sampling efforts in Kodiak. Lynne Mattes and Kally Spalinger provided advice on port sampling and coordinated our participation in ADF&G surveys in the northern Gulf of Alaska. Ken Goldman (ADF&G, Homer) also secured sampling opportunities for our researchers onboard ADF&G survey vessels. Mike Byerly (ADF&G, Homer) and Tory O'Connell (ADF&G, Sitka) also provided valuable assistance with sampling surveys. James Sulikowski (University of New England) shared his knowledge on histological analysis. The help of students, alumni, and interns was of significant importance, and we thank the following individuals for their assistance: Joe Bizzarro, Lewis Barnett, Simon Brown, Chante Davis, Jasmine Fry, Ashley Neway, Heather Robinson (Pacific Shark Research Center/ Moss Landing Marine Laboratories), Priscilla Jimmeye (California State University Monterey Bay), and Josh Bauman (NMFS Southwest Fisheries Science Center).

Additional funding was provided by NOAA/NMFS to the National Shark Research Consortium and Pacific Shark Research Center, American Elasmobranch Society, Western Groundfish Conference, San Jose State University Lottery Funds, Earl and Ethel Myers Foundation Grant, and David and Lucille Packard Foundation.

Literature Cited

Abdel-Aziz, S.H. 1992. The use of vertebral rings of the brown ray *Raja miraletus* (Linnaeus, 1758) off Egyptian Mediterranean coast for estimation of age and growth. Cybium 16(2):121-132.

Agnew, D.J., Nolan, C.P., Beddington, J.R., and Baranowski, R. 2000. Approaches to the assessment and management of multispecies skate and ray fisheries using the Falkland Islands fishery as an example. Canadian Journal of Fisheries and Aquatic Sciences 57:429-440.

Beamish, R.J., and Fournier, D.A. 1981. A method for comparing the precision of a set of age determinations. Canadian Journal of Fisheries and Aquatic Sciences 38:982-983.

Beukema, J.J. 1989. Bias in estimates of maximum life span, with an example of the edible cockle, *Cerastoderma edule*. Netherlands Journal of Zoology 39(1-2):79-85.

Beverton, R.J.H., and Holt, S.J. 1957. On the dynamics of exploited fish populations. Fishery Investigations Series II. Vol. XIX, Her Majesty's Stationery Office, London, England. 533 pp.

Braccini, J.M., and Chiaramonte, G.E. 2002. Reproductive biology of *Psammobatis extenta.* Journal of Fish Biology 61:272–288

Brander, K. 1981. Disappearance of common skate *Raja batis* from the Irish Sea. Nature 5801:48-49.

Cailliet, G.M. 1992. Demography of the central California population of the leopard shark (*Triakis semifasicata*). Australian Journal of Marine and Freshwater Research 43:183-189.

Cailliet, G.M., and Goldman, K. 2004. Age determination and validation in chondrichthyan fishes. *In* J.C. Carrier, J.A. Musick, and M.R. Heithaus (Editors) Biology of sharks and their relatives, pp. 399-447. Boca Raton, FL: CRC Press LLC.

Cailliet, G.M., Martin, L.K., Kusher, D., Wolf, P., and Welden, B.A. 1983. Techniques for enhancing vertebral bands in age estimation of California elasmobranchs. NOAA Technical Reports NMFS 8:179-188.

Cailliet, G.M., Smith, W.D., Mollet, H.F., and Goldman, K.J. 2006. Age and growth studies of chondrichthyan fishes: the need for consistency in terminology, verification, validation, and growth function fitting. Environmental Biology of Fishes 77:211-228.

Camhi, M. 1999. Sharks on the Line II: an analysis of Pacific state shark fisheries. National Audubon Society, Living Oceans Program. Islip, NY. 116 pp.

Campana, S.E. 2001. Accuracy, precision, and quality control in age determination, including a review of the use and abuse of age validation methods. Journal of Fish Biology 59:197-242.

Campana, S.E., Annand, M.C., and McMillan, J.I. 1995. Graphical methods for determining the consistency of age determinations. Transactions of the American Fisheries Society 124:131-138.

Campana, S., Marks, L., Joyce, W., and Harley, S. 2001. Analytical assessment of the porbeagle shark (*Lamna nasus*) population in the Northwest Atlantic, with estimates of long-term sustainable yield. Canadian Stock Assessment, Research Document 2001/067, Ottawa, Ontario. 59 pp.

Carlson, J.K., and Baremore, I.E. 2005. Growth dynamics of the spinner shark (*Carcharhinus brevipinna*) off the United States southeast and Gulf of Mexico coasts: a comparison of methods. Fishery Bulletin 103:280-291.

Carlson, J.K., Cortés, E. and Bethea, D.M. 2003. Life history and population dynamics of the finetooth shark (*Carcharhinus isodon*) in the northeastern Gulf of Mexico. Fishery Bulletin 101:281-292.

Carpenter, S.R., and Kitchell, J.F. 1992. Trophic cascade and biomanipulation: interface of research and management. Limnology and Oceanography 37:208-213.

Casey, J.G., Pratt Jr., H.L. and Stillwell, C.E. 1985. Age and growth of the sandbar shark (*Carcharhinus plumbeus*) from the western North Atlantic. Canadian Journal of Fisheries and Aquatic Sciences 42:963-975.

Casey, J.M., and Myers, R.A. 1998. Near extinction of a large, widely distributed fish. Science 28:690-692.

Caswell, H. 2001. Matrix Population Models: Construction, Analysis, and Interpretation. 2nd edition. Sinauer Associates, Inc., Sunderland, MA. 722 pp.

Chang, W.Y.B. 1982. A statistical method for evaluating the reproducibility of age determination. Canadian Journal of Fisheries and Aquatic Sciences 39:1208-1210.

Chen, Y., Jackson, D.A., and Harvey, H.H. 1992. A comparison of von Bertalanffy and polynomial functions in modeling fish growth data. Canadian Journal of Fisheries and Aquatic Sciences 49:1228-1235.

Conrath, C.L. 2004. Reproductive biology. *In* J.A. Musick, R. Bonfil (Editors) Technical manual for the management of elasmobranchs, pp. 133-164. Asia Pacific Economic Cooperation and IUCN Shark Specialist Group Publication.

Conrath, C.L., Gelsleichter, J., and Musick, J.A. 2002. Age and growth of the smooth dogfish, *Mustelus canis*, in the northwest Atlantic. Fishery Bulletin 100:674-682.

Conrath, C.L, and Musick, J.A. 2002. Reproductive biology of the smooth dogfish. Environmental Biology of Fishes 64:367-377.

Cortés, E. 2000. Life history patterns and correlations in sharks. Reviews in Fisheries Science 8(4):299-344.

Cortés, E. 2002. Incorporating uncertainty into demographic modeling: Application to shark populations and their conservation. Conservation Biology 16(4):1048-1062.

Cortés, E. 2004. Life history patterns, demography, and population dynamics. *In* J.C. Carrier, J.A. Musick, M.R. Heithaus (Editors) Biology of Sharks and Their Relatives, pp. 449-469. Boca Raton, FL: CRC Press LLC.

Cortés, E. 2007. Chondrichthyan demographic modelling: an essay on its use, abuse, and future. Marine and Freshwater Research 58: 4-6.

Cox, D.L., and Koob, T.J. 1991. Predation on elasmobranch eggs. Environmental Biology of Fishes 38:117–125.

Cox, D.L., Walker, P., and Koob, T.J. 1999. Predation on eggs of the thorny skate. Transactions of the American Fisheries Society 128:380-384.

Davis, C.D., Cailliet, G.M. and Ebert, D.A. 2007. Age and growth of the roughtail skate *Bathyraja trachura* (Gilbert 1892) from the eastern North Pacific. Environmental Biology of Fishes (*in press*) DOI 10.1007/s10641-007-9224-7.

de Kroon, H., Plaisier, A., van Groenendael, J., and Caswell, H. 1986. Elasticity: The relative contribution of demographic parameters to population growth rate. Ecology 67(5):1427-1431.

Dulvy, N.K., Metcalfe, J.D., Flanville, J., Pawson, M.G., and Reynolds, J.D. 2000. Fishery stability, local extinctions, and shifts in community structure in skates. Conservation Biology 14(1):283-293.

Dulvy, N.K., and Reynolds, J.D. 2002. Predicting extinction vulnerability in skates. Conservation Biology 16(2):440-450.

Ebert, D.A. 2005. Reproductive biology of skates, *Bathyraja* (Ishiyama) along the eastern Bering Sea continental slope. Journal of Fish Biology 66:618-649.

Ebert, D.A., and Davis, C.D. 2007. Descriptions of skate egg cases (Chondrichthyes: Rajiformes: Rajoidei) from the eastern North Pacific. Zootaxa 1393: 1-18.

Ebert, T.A. 1999. Plant and Animal Populations: Lessons in Demography. Academic Press, San Diego, CA. 312 pp.

Ferreira, B.P., and Vooren, C.M. 1991. Age, growth, and structure of vertebra in the school shark *Galeorhinus galeus* (Linnaeus, 1758) from southern Brazil. Fishery Bulletin 89:19-31.

Ford, P. 1971. Differential growth rate in the tail of the Pacific big skate, *Raja binoculata*. Journal of the Fisheries Research Board of Canada 28:95-98.

Fowler, C.W. 1988. Population dynamics as related to rate of increase per generation. Evolutionary Ecology 2:197-204.

Frisk, M.G., Miller, T.J., and Fogarty, M.J. 2002. The population dynamics of the little skate *Leucoraja erinacea*, winter skate *Leucoraja ocellata*, and barndoor skate *Dipturus laevis*: predicting exploitation limits using matrix analyses. ICES Journal of Marine Science 59:576-586.

Frisk, M.G., and Miller, T.J. 2006. Age, growth, and latitudinal patterns of two Rajidae species in the northwestern Atlantic: little skate (*Leucoraja erinacea*) and winter skate (*Leucoraja ocellata*). Canadian Journal of Fisheries and Aquatic Sciences 53:1078-1091.

Gaichas, S., and Ianelli, J.N. 1999. An approach to analyzing multi-species complexes in data-limiting situations. *In* Stock assessment and fishery evaluation report to the groundfish resources of the Gulf of Alaska. Appendix E. North Pacific Fishery Management Council, 605 W. 4th Ave., Suite 306, Anchorage, AK 99501.

Gaichas, S., Fritz, L., and Ianelli, J.N. 1999. Other species considerations for the Gulf of Alaska. *In* Stock assessment and fishery evaluation report for the groundfish resources of the Gulf of Alaska. Appendix D. North Pacific Fishery Management Council, 605 W. 4th Ave., Suite 306, Anchorage, AK 99501.

Gaichas, S., Ruccio, M., Stevenson, D., and Swanson, R. 2003. Stock assessment and fishery evaluation of skate species (Rajidae) in the Gulf of Alaska. *In* Stock assessment and fishery evaluation report for the groundfish resources of the Gulf of Alaska for 2004. North Pacific Fishery Management Council, 605 W. 4th Ave., Suite 306, Anchorage, AK 99501.

Gaichas, S., Sagalkin, N., Gburski, C., Stevenson, D., & Swanson, R. 2005. Gulf of Alaska skates. *In* Stock assessment and fishery evaluation report for the groundfish resources of the Gulf of Alaska. North Pacific groundfish stock assessment and fishery evaluation reports for 2006. Appendix B, Chapter 16, pp. 881-926.

Gallagher, M.J., Green, M.J., and Nolan, C.P. 2006. The potential use of caudal thorns as a non-invasive ageing structure in the thorny skate (*Amblyraja radiata* Donovan, 1808). Environmental Biology of Fishes 77:265-272.

Gallagher, M., and Nolan, C.P. 1999. A novel method for the estimation of age and growth in rajids using caudal thorns. Canadian Journal of Fisheries and Aquatic Sciences 56(3-4):1590-1599.

Gamito, S. 1998. Growth models and their use in ecological modeling: an application to a fish population. Ecological Modeling 113:83-94.

Gburski, C.M., Gaichas, S.K., and Kimura, D.K. 2007. Age and growth of big skate (*Raja binoculata*) and longnose skate (*R. rhina*) in the Gulf of Alaska. Environmental Biology of Fishes (*in press*) DOI 10.1007/s10641-007-9231-8.

Gedamke, T., DuPaul, W.D., and Musick, J. A. 2005. Observations on the life history of the barndoor skate, *Dipturus laevis*, on Georges Bank (western North Atlantic). Journal of the Northwest Atlantic Fishery Science 35: 67-78.

Gerristen, H.D., and McGrath, D. 2006. Variability in the assignment of maturity stages of plaice (*Pleuronectes platessa* L.) and whiting (*Merlangius merlangus* L.) using macroscopic maturity criteria. Fisheries Research 77:72-77.

Heppell, S.S., Crowder, L.B., and Menzel, T.R. 1999. Life table analysis of long-lived marine species with implications for conservation and management. *In* J.A. Musick (Editor) Life in the slow lane: ecology and conservation of long-lived animals, pp. 137-148. Bethesda, MD: American Fisheries Society Symposium 23.

Heppell. S.S., Caswell, H., and Crowder, L.B. 2000. Life histories and elasticity patterns: perturbation analysis for species with minimal demographic data. Ecology 81(3):654-665.

Heupel, M.R., and Simpfendorfer, C.A. 2002. Estimation of mortality of juvenile blacktip sharks, *Carcharhinus limbatus*, within a nursery area using telemetry data. Canadian Journal of Fisheries and Aquatic Sciences 59:624-632.

Heupel, M.R., Whittier, J.M., and Bennett, M.B. 1999. Plasma steroid hormone profiles and reproductive biology of the epaulette shark, Hemiscyllium ocellatum. Journal of Experimental Zoology 284: 586-594.

Hitz, C.R. 1964. Observations on egg cases of the big skate (*Raja binoculata* Girard) found in Oregon coastal waters. Journal of the Fisheries Research Board of Canada 21(4):851-854.

Hoenig, J.M. 1983. Empirical use of longevity data to estimate mortality rates. Fishery Bulletin 82(1):898-903.

Hoenig, J.M., and Gruber, S.H. 1990. Life-history patterns in the elasmobranchs: implications for fisheries management. *In* H.L. Pratt, Jr., S.H. Gruber, T. Taniuchi (Editors) Elasmobranchs as living resources: Advances in the biology, ecology, systematics, and the status of the fisheries. NOAA Technical Report (90):1-16.

Holden, M.J. 1974. Problems in the rational exploitation of elasmobranch populations and some suggested solutions. *In* F.R. Harden Jones (Editor) Sea Fisheries Research, pp. 117-137. New York: John Wiley & Sons.

Holden, M.J. 1975. The fecundity of *Raja clavata* in British waters. Journal du Conseil International pour l'Exploration de la Mer 36(2):110-118.

Holden, M.J., and Vince, M.R. 1973. Age validation studies on the centra of *Raja clavata* using tetracycline. Journal du Conseil International pour l'Exploration de la Mer 35(1):13-17

Ishiyama, R. 1958. Studies on the Rajid fishes (Rajidae) found in the waters around Japan. Journal of Shimonoseki College of Fisheries 7(2/3):1-202.

Jensen, A.L. 1996. Beverton and Holt life history invariants result from optimal trade-off of reproduction and survival. Canadian Journal of Fisheries and Aquatic Sciences 54:987-989.

Johnson, A.G. 1979. A simple method for staining the centra of teleost vertebrae. Northeastern Gulf Science 3:113-115.

Knight, W. 1968. Asymptotic growth: an example of nonsense disguised as mathematics. Journal of the Fisheries Research Board of Canada 25(6):1303-1307.

Koop, J.H. 2005. Reproduction of captive *Raja* spp. in the Dolfinarium Harderwijk. Journal of the Marine Biological Association of the United Kingdom 85:1201-1202.

Krebs, C.J. 2001. Ecology: The Experimental Analysis of Distribution and Abundance. 5th edition. Benjamin Cummings, San Francisco. 695 pp.

LaMarca, M.J. 1966. A simple technique for demonstrating calcified annuli in the vertebrae of large elasmobranchs. Copeia 1966:351-352.

Laptikhovsky, V.V. 2004. Survival rates for rays discarded by the bottom trawl squid fishery off the Falkland Islands. Fishery Bulletin 102:757-759.

Licandeo, R.R., Lamilla, J.G., Rubilar, P.G., and Vega, R.M. 2006. Age, growth, and sexual maturity of the yellownose skate *Dipturus chilensis* in the south-eastern Pacific. Journal of Fish Biology 68:488-506.

Lucifora, L.O., and García, V.B. 2004. Gastropod predation on egg cases of skates (Chondrichthyes, Rajidae) in the southwestern Atlantic: quantification and life history implications. Marine Biology 145:917-922.

Lutton, B.V., St. George, J., Murrin, C.R., Fileti, L.A., and Callard, I.P. 2005. The elasmobranch ovary. *In* W.C. Hamlett (Editor) Reproductive biology and phylogeny of Chondrichthyes: sharks, batoids, and chimaeras, pp. 237-281. New Hampshire: Science Publishers, Inc.

Mabragaña, E., Lucifora, L.O., and Massa, A.M. 2002. The reproductive ecology and abundance of *Sympterygia bonapartii* endemic to the south-west Atlantic. Journal of Fish Biology 60:951-967.

Mabragaña, E., and Cousseau, M.B. 2004. Reproductive biology of two sympatric skates in the south-west Atlantic: *Psammobatis rudis* and *Psammobatis normani*. Journal of Fish Biology 65:559-573.

Maruska, K.P., Cowe, E.G., and Tricas, T.T. 1996. Periodic gonadal activity and protracted mating in elasmobranch fishes. Journal of Experimental Zoology 276:219-232.

Matta, M.E. 2006. Aspects of the life history of the Alaska skate, *Bathyraja parmifera*, in the eastern Bering Sea. MS Thesis, School of Aquatic and Fisheries Sciences, University of Washington, WA.

Matta, M.E., and Gunderson, D.R. 2007. Age, growth, maturity, and mortality of the Alaska skate, *Bathyraja parmifera*, in the eastern Bering Sea. Environmental Biology of Fishes (*in press*) DOI 10.1007/s10641-007-9223-8.

Matta, M.E., Gaichas, S., Lowe, S., Stevenson, D., Hoff, G., and Ebert, D. 2006. Bering Sea and Aleutian Islands skates. Stock assessment and fishery evaluation of skate species (Rajidae) in the Gulf of Alaska. *In* Stock assessment and fishery evaluation report for the groundfish resources of the Gulf of Alaska for 2007. North Pacific Fishery Management Council, 605 W. 4th Ave., Suite 306, Anchorage, AK 99501.

McEachran, J.D. 1970. Egg capsules and reproductive biology of the skate *Raja garmani* (Pisces: Rajidae). Copeia 1970(1):197-199.

McFarlane, G.A., and King, J.R. 2006. Age and growth of big skate (*Raja binoculata*) and longnose skate (*Raja rhina*) in British Columbia waters. Fisheries Research 78:169-178.

Mecklenburg, CW., Mecklenburg, T.A. and Thorsteinson, L.K. 2002. Fishes of Alaska. Bethesda, MD: American Fisheries Society. 104 pp.

Mollet, H.F., and Cailliet, G.M. 2002. Comparative demography of elasmobranchs using life history tables, Leslie matrices and stage-based matrix models. Marine and Freshwater Research 53:503-516.

Mollet, H.F., Ezcurra, J.M. and O'Sullivan, J.B. 2002. Captive biology of the pelagic stingray, *Dasyatis violacea* (Bonaparte, 1832). Marine and Freshwater Research 53:531-541.

Moreau, J. 1987. Mathematical and biological expression of growth in fishes: recent trends and further developments. *In* R.C. Summerfelt, G.E. Hall (Editors) Age and growth of fish, pp. 81-113. Iowa State University Press, Ames.

Musick, J. A. 1999. Ecology and conservation of long-lived marine animals. *In* J.A. Musick (Editor) Life in the slow lane: ecology and conservation of long-lived marine animals, American Fisheries Society Symposium 23, pp 1–10. Bethesda, MD: American Fisheries Society.

Natanson, L.J. 1993. Effect of temperature on band deposition in the little skate, *Raja erinacea*. Copeia, 1993: 199–206.

Natanson, L.J., and Cailliet, G.M. 1990. Vertebral growth zone deposition in Pacific angel sharks. Copeia 1990(4):1133-1145.

Natanson, L.J., Sulikowski, J.A., Kneebone, J.R., and Tsang, P.C. 2007. Age and growth estimates for the smooth skate, *Malacoraja senta*, in the Gulf of Maine. Environmental Biology of Fishes (*in press*) DOI 10.1007/s10641-007-9220-y.

Neer, J.A., and Cailliet, G.M. 2001. Aspects of the life history of the Pacific electric ray, *Torpedo californica* (Ayers). Copeia 2001:842-847.

Neer, J.A., and Thompson, B.A. 2005. Life history of the cownose ray, *Rhinoptera bonasus*, in the northern Gulf of Mexico, with comments on geographic variability in life history traits. Environmental Biology of Fishes 73:321-331.

North Pacific Fisheries Management Council. 1999. DRAFT. Environmental assessment/regulatory impact review/initial regulatory flexibility analysis for amendments 63/63 to the fishery management plans for the groundfish fisheries of the Bering Sea/Aleutian Islands and Gulf of Alaska to revise management of sharks and skates. Prepared April 2, 1999, by the North Pacific Fishery Management Council and Alaska Department of Fish and Game, Juneau, AK. 72 pp.

Officer, R.A., Gason, A.S., Walker, T.I., and Clement, J.G. 1996. Sources of variation in counts of growth increments in vertebrae from the gummy shark, *Mustelus antarticus*, and school shark, *Galeorhinus galeus*: implications for age determination. Canadian Journal of Fisheries and Aquatic Sciences 53:1765-1777.

Orlov, A.M. 1998. The diets and feeding habits of some deep-water benthic skates (Rajidae) in the Pacific Waters off the northern Kuril Islands and southeastern Kamchatka. Alaska Fishery Research Bulletin 5(1):1-17.

Orlov, A.M. 1999. Trophic relationships of commercial fishes in the Pacific waters off southeastern Kamchatka and the northern Kuril Islands. *In* Ecosystem approaches for fishery management, pp. 231-263. Alaska Sea Grant College Program (AK-SG-99-01), University of Alaska Fairbanks.

Parsons, T.R. 1992. The removal of marine predators by fisheries and the impact of trophic structure. Marine Fisheries Bulletin 25(1-4):51-53.

Parsons, G.R., and Grier, H. 1992. Seasonal changes in shark testicular structure and spermatogenesis. Journal of Experimental Zoology 261: 173–184.

Panfili, J., Troadec, H., de Pontual, H., and Wright. P.J. (Editors). 2002. Manual of fish sclerochronology, pp.138-142. France: Brest.

Perez, C.R. 2005. Age, growth and reproduction of the sandpaper skate, *Bathyraja kincaidii* (Garman, 1908) in the Eastern North Pacific. MS Thesis, California State University, Monterey Bay, CA.

Probert, P.K. 1984. Disturbance, sediment stability, and trophic structure of soft-bottom communities. Journal of Marine Research 42: 893-921.

Richards, F.J. 1959. A flexible growth function for empirical use. Journal of Experimental Botany 10(29):290-300.

Ricker, W.E. 1979. Growth rates and models. *In* W.S. Hoar, D.J. Randall, J.R. Brett (Editors) Fish Physiology, Volume III, pp. 677-743. New York: Academic Press.

Roff, D.A. 1980. A motion to retire the von Bertalanffy function. Canadian Journal of Fisheries and Aquatic Sciences 37:127-129.

Ruocco, N.L., Lucifora, L.O., Diaz de Astarloa, J.M., and Wöhler, O. 2006. Reproductive biology and abundance of the white-dotted skate, *Bathyraja albomaculata*, in the Southwest Atlantic. ICES Journal of Marine Science 63:105-116.

Ryland, J.S., and Ajayi, T.O. 1984. Growth and population dynamics of three *Raja* species (Batoidei) in Carmarthen Bay, British Isles. Journal du Conseil International pour l'Exploration de la Mer 41:111-120.

Shuntov, V.P. 1998. Biology and ecosystem interrelationships of commercial hydrobionts in the Russian far-eastern seas. Izvestiya of the Pacific Research Fisheries Centre 124:425-428.

Simpfendorfer, C.A., Chidlow, J., McAuley, R., and Unsworth, P. 2000. Age and growth of the whiskery shark, *Furgaleus macki*, from southwestern Australia. Environmental Biology of Fishes 58: 335-343.

Smith, C., and Griffiths, C. 1997. Shark and skate egg cases cast up on two South African beaches and their rates of hatching success, or causes of death. South African Journal of Zoology 32(4):112-117.

Smith, W.D. 2005. Life history aspects and population dynamics of a commercially exploited stingray, *Dasyatis dipterura*. MS Thesis, San Francisco State University, CA.

Smith, W.D., Cailliet, G.M., and Melendez, E.M. 2007. Maturity and growth characteristics of a commercially exploited stingray, *Dasyatis dipterura*. Marine and Freshwater Research 58:54–66.

Stehmann, M.F. 2002. Proposal of a maturity stages scale for oviparous and viviparous cartilaginous fishes (Pisces, Chondrichthyes). Archive of Fishery and Marine Research 50(1): 23-48.

Stobutzki, I.C., Miller, M.J., Heales, D.S., and Brewer, D.T. 2002. Sustainability of elasmobranchs caught as bycatch in a tropical prawn (shrimp) trawl fishery. Fishery Bulletin 100(4):800-821.

Sulikowski, J.A., Driggers, W.B. III., Ingram, G.W. Jr., Kneebone, J., Ferguson, D.E., and Tsang, P.C.W. 2007c. Profiling plasma steroid hormones: a non-lethal approach for the study of skate reproductive biology and its potential use in conservation management. Environmental Biology of Fishes (*in press*) DOI 10.1007/s10641-007-9257-y.

Sulikowski, J.A., Elzey, S., Kneebone, J., Jurek, J., Howell, W.H., and Tsang, P.C.W. 2007b. The reproductive cycle of the smooth skate, Malacoraja senta, in the Gulf of Maine. Marine and Freshwater Research 58: 98-103.

Sulikowski, J.A., Irvine, S.B., DaValerio, K.C., and Carlson, J.K. 2007a. Age, growth and maturity of the roundel skate, *Raja texana*, from the Gulf of Mexico, USA. Marine and Freshwater Research 58:41-53.

Sulikowski, J.A., Kneebone, J., Elzey, S., Jurek, J., Danley, P.D., Howell, W.H., and Tsang, P.C.W. 2005a. Age and growth estimates of the thorny skate (*Amblyraja radiata*) in the western Gulf of Maine. Fishery Bulletin 103:161-168.

Sulikowski, J.A., Kneebone, J., Elzey, S., Jurek, J., Danley, P.D., Howell, W.H., and Tsang, P.C.W. 2006. Using the composite variables of reproductive morphology, histology and steroid hormones to determine age and size at sexual maturity for the thorny skate *Amblyraja radiata* in the western Gulf of Maine. Journal of Fish Biology 69:1449-1465.

Sulikowski, J.A., Morin, M.D., Suk, S.H., and Howell, W.H. 2003. Age and growth of the winter skate, *Leucoraja ocellata*, in the Gulf of Maine. Fishery Bulletin 101:405-413.

Sulikowski, J.A., Tsang, P.C.W., and Howell, W.H. 2004. An annual cycle of steroid hormone concentrations and gonad development in the winter skate, *Leucoraja ocellata*, from the western Gulf of Maine. Marine Biology 144:845-853.

Sulikowski, J.A., Tsang, P.C.W., and Howell, W.H. 2005b. Age and size at sexual maturity for the winter skate, *Leucoraja ocellata*, in the western Gulf of Maine based on morphological, histological and steroid hormone analyses. Environmental Biology of Fishes 72:429-441.

Tanaka, S. and Mizue, K. 1979. Age and growth of Japanese dogfish, *Mustelus manazo* Bleeker in the East China Sea. Bulletin of the Japanese Society of Scientific Fisheries 45(1):43-50.

Templeman, W. 1987. Differences in sexual maturity and related characteristics between populations of thorny skate (*Raja radiata*) in the Northwest Atlantic. Journal of Northwest Atlantic Fishery Science 7:155-167.

TenBrink, T., Gaichas, S., Sagalkin, N., Gburski, C., Stevenson, D., Swanson, R., and Lowe, S. 2006. Gulf of Alaska skates (executive summary). Stock assessment and fishery evaluation of skate species (Rajidae) in the Gulf of Alaska. *In* Stock assessment and fishery evaluation report for the groundfish resources of the Gulf of Alaska for 2007. North Pacific Fishery Management Council, 605 W. 4th Ave., Suite 306, Anchorage, AK 99501.

Teshima, K. and Tomonaga, S. 1986. Reproduction of Aleutian skate, *Bathyraja aleutica,* with comments on embryonic development. *In* T. Uyeno, R. Arai, T. Taniuchi, K. Matsuura (Editors) Indo-Pacific Fish Biology: Proceedings of the Second International Conference on Indo-Pacific Fishes, pp. 303–309. Tokyo: Ichthyological Society of Japan.

Tricas, T.C., Maruska, K.P., and Rasmussen, E. 2000. Annual cycles of steroid hormone production, gonad development, and reproductive behavior in the Atlantic stingray. General and Comparative Endocrinology 118(2):209-225.

Vetter, E.F. 1988. Estimation of natural mortality in fish stocks: a review. Fishery Bulletin 86:25-43.

Vitale, F., Svedäng, H., and Cardinale, M. 2006. Histological analysis invalidates macroscopically determined maturity ogives of the Kattegat cod *(Gadus morhua*) and suggests new proxies for estimating maturity status of individual fish. ICES Journal of Marine Science 63: 485-492.

von Bertalanffy, L. 1960. Principles and theory of growth. *In* W.W. Wowinski (Editor) Fundamental aspects of normal and malignant growth, pp.137-259. New York, NY: Elsevier Publishing Company,.

Walker, P.A., and Hislop, G. 1998. Sensitive skates or resilient rays? Spatial and temporal shifts in ray species composition in the central and north-western North Sea between 1930 and the present day. ICES Journal of Marine Science 55: 392-402.

Walmsley-Hart, S.A., Sauer, W.H.H., and Buxton, C.D. 1999. The biology of the skates *Raja wallacei* and *R. pullopunctata* (Batoidea: Rajidae) on the Agulhas Bank, South Africa. South African Journal of Marine Science 21:165-179.

Waring, G.T. 1984. Age, growth and mortality of the little skate off the northeast coast of the United States. Transactions of the American Fisheries Society 113:314-321.

Zar, J.H. 1999. Biostatistical Analysis. 4th Edition. Prentice Hall, Upper Saddle River, N.J. 663 pp.

Zeiner, S.J., and Wolf, P.G. 1993. Growth characteristics and estimates of age at maturity of two species of skates (*Raja binoculata* and *Raja rhina*) from Monterey Bay, California. *In* S. Branstetter (Editor) Conservation biology of elasmobranchs, pp. 87-90. NOAA Technical Report, NMFS 115.

Zenger, H.H., Jr. 2004. Data report: 2002 Aleutian Islands bottom trawl survey. NOAA Technical Memorandum, NMFS-AFSC-143.